# FATE OF NITROGEN FERTILIZER IN RAINFED MAIZE SYSTEMS OF TROPICAL HIGHLANDS OF KENYA

**KEVIN CHURCHIL OLUOCH**

**A THESIS SUBMITTED TO THE SCHOOL OF AGRICULTURE AND BIOTECHNOLOGY IN PARTIAL FULFILMENT OF THE REQUIREMENTS FOR THE AWARD OF DEGREE OF MASTER OF SCIENCE IN SOIL SCIENCE, UNIVERSITY OF ELDORET, KENYA**

**2025**

# DECLARATION

**Declaration by the Student**

This thesis is my original work and has never been presented for the award of an academic degree in any other university and should not be copied, or reproduced in any format without written authority from the author and/or University of Eldoret.

**KEVIN CHURCHIL OLUOCH**

______________________________ Date: **01/08/2025**

**SAGR/SOS/M/001/22**

**Approval by the Supervisors**

This thesis is submitted with our approval as the University Supervisors.

**ABIGAEL OTINGA** **Date: 04/08/2025**

**Department of Soil Science**

**University of Eldoret, Kenya**

**RUTH NJOROGE** **Date: 04/ 08/2025**

**Department of Soil Science**

**University of Eldoret, Kenya**

**ELIZA HARRIS** **Date: 11/08/2025**

**Climate and Environmental Physics**

**University of Bern, Switzerland**

# DEDICATION

To my dad, mom, siblings and everyone who has contributed to this significant milestone.

## ACKNOWLEDGEMENT

First, I would like to give thanks to the Almighty God for His mercy and good health while pursuing my Master's degree.

I sincerely wish to extend my gratitude to my academic advisors (Dr. Abigael Otinga, Dr. Ruth Njoroge (Department of Soil Science, University of Eldoret) and Prof. Eliza Harris (Climate and Environmental Physics, University of Bern)) for their guidance, comments, encouragement and constructive suggestions. I'm also truly indebted to Mr. Harrison Churu for his continuous support and commitment.

I acknowledge the Swiss National Science Foundation (SNSF) through the Swiss Data Science (SDSC) for offering me a scholarship to pursue my Master's degree through the N2O-SSA project. I am grateful to other members of the N2O-SSA project, Prof. Six, Dr. Matti, Dr. Leitner, Dr. Agredazywczuk, Dr. Tufail, Mr. Oduor, Mrs. Ouma and Mr. Oyugi for their constant support, insights, inputs and contributions towards my abstract and posters. I also wish to thank the International Livestock Research Institute (ILRI) for facilitating the field work by providing chambers and a GHG analyser. My sincere gratitude to the Outreach and International Student Centre (OISC) for providing the research field.

Special thanks to the University of Bern and ETH Zurich for hosting me during my visit to Switzerland. I sincerely appreciate Dr. Matti, Mr. Frank and Miss Sonja for taking their time to take me through the laboratory operations during the lab visits at ETH Zurich, University of Bern and High Altitude Research Stations Jungfraujoch, respectively.

I want to thank the University of Eldoret, Department of Soil Science and Department of Environmental Science for the opportunity and technical support afforded to me. I'm grateful to Miss Scholastica and Mary for their support and assistance with the lab work.

I also wish to thank my fellow students and friends, Churu, Tamba, Dishon, Chege, Irine, Godfrey, Denis and Suzzette for their encouragement during the study period.

## ABSTRACT

Crop production in sub-Sahara Africa (SSA) is often constrained by declining soil fertility associated with negative nutrient balances as a result of continuous cropping with little or no replenishment of nutrients. To offset the negative nutrient balance, especially nitrogen (N), in SSA agroecosystems and meet the ever-increasing food demand, it is paramount to intensify N fertilizer use. However, this could prove deleterious to ecosystem functioning since increased N fertilizer is associated with elevated reactive nitrogen (Nr) loading in the environment. Therefore, a study comprising increasing N fertilizer rates, 0, 25, 50, 75, 100 and 125 kg N $ha^{-1}$ was conducted in the highland tropics of the Rift Valley, Kenya. The objective was to evaluate fertilizer-induced soil mineral N (Nmin) changes within the soil profile and nitrous oxide ($N_2O$) emissions in maize monoculture systems. On average, the N application of 125 kg N $ha^{-1}$ exhibited the largest $NO_3^-$ (14.8 mg $kg^{-1}$) and $NH_4^+$ (11.85 mg $kg^{-1}$) concentration across depth and different N rates. The annual $N_2O$ fluxes ranged from 0.33 to 0.77 kg $N_2O$-N $ha^{-1}$ across the different N rates. Additionally, yield-scaled emissions ranged from 0.07 to 0.14 g $N_2O$-N $kg^{-1}$ grain yield across different N rates. Increasing N fertiliser rates increased grain yield by 7, 14, 24, 37 and 46 % while applying 25, 50, 75, 100 and 125 kg N $ha^{-1}$, respectively. Application of 25 kg N $ha^{-1}$ gave indications of soil N mining, with a nitrogen use efficiency ($NUE_{grain}$) value of > 1, whereas the rest of the N rates had an $NUE_{grain}$ value of < 1. The optimum physiological efficiency and partial-factor productivity were realised when N was supplied at 75 kg N $ha^{-1}$. Overall, the results suggest that increasing N application to 75 kg N $ha^{-1}$ would not only improve grain yield but also increase soil N intensity, $N_2O$ emissions and optimise NUE. Therefore, matching crop demands through judicious N use will be critical to ensure efficient use of fertiliser N and reduce losses to the ecosystem.

# TABLE OF CONTENTS

## LIST OF TABLES

# LIST OF FIGURES

## LIST OF APPENDICES

# LIST OF ABREVIATIONS AND ACRONYMS

| | |
|---|---|
| **AEZs** | Agro-ecological Zones |
| **ANOVA** | Analysis of Variance |
| **d** | day |
| **DAP** | Days after planting |
| **DAP** | Di-ammonium Phosphate |
| **EFs** | Emission Factors |
| **FAO** | Food and Agriculture Organization |
| **GHG** | Greenhouse gas |
| **HPMZ** | High Potential Maize Zone |
| **IPCC** | Intergovernmental Panel on Climate Change |
| **N** | Nitrogen |
| **$N_2O$** | Nitrous Oxide |
| **NDCs** | Nationally Determined Contributions |
| **$NH_3$** | Ammonia |
| **Nmin** | mineral N |
| **NO** | Nitric Oxide |
| **$NO_3^-$** | Nitrate |
| **$NO_x$** | Nitrogen Oxides |
| **Nr** | Reactive Nitrogen |
| **NUE** | Nitrogen Use Efficiency |
| **ppb** | parts per billion |
| **RCBD** | Randomized Complete Block Design |
| **SOC** | Soil Organic Carbon |
| **SSA** | Sub-Sahara Africa |
| **UNFCCC** | United Nations Framework Convention on Climate Change |

# CHAPTER ONE

# INTRODUCTION

## 1.1 Background Information

According to FAO (1996), food security exists when all people, at all times, have physical, social and economic access to sufficient, safe and nutritious food which meets their dietary needs and food preferences for an active and healthy life. However, this situation is far from being achieved in Sub-Saharan Africa (SSA), where the prevalence of undernourishment accounts for 22.3% of the population in the region (FAO *et al*., 2025). This is expected to be aggravated by the rising food demand attributed to the rapidly growing population, estimated to reach 2.1 billion by 2050 (Ezeh *et al*., 2020). Cereals are the most vital source of food and nutrition in the region, and ultimately, their demand is projected to double by 2050 (Alimagham *et al*., 2024). Additionally, they also serve as a crucial raw material for the manufacture of livestock feeds and alcohol products (das Graças Costa & de Souza, 2023).

In Kenya, maize is the staple food and contributes significantly to the population's protein and calorie intake (Jena *et al*., 2021), therefore acting as an important indicator of food security (Ngeno, 2024). Additionally, it is the most widely cultivated crop in the country, occupying over two million hectares (ha) across various agroecological zones (AEZs) (Ouma & De Groote, 2011; FAOSTAT, 2024). Its production is primarily by smallholder farmers, who account for about 75% of the national output. However, maize production in Kenya has stagnated way below the optimal yields achievable under rain-fed agriculture (Njeru *et al*., 2023), significantly contributing to food insecurity despite the region having the potential of being maize-sufficient. This further jeopardizes efforts to achieve the second Sustainable Development Goal (SDG) of ending hunger by 2030.

Low maize production has been attributed to, among other factors, declining soil fertility (Giller, 2020), especially of major elements such as potassium (K), phosphorus (P) and most importantly, nitrogen (N). Nitrogen (N) is an essential nutrient in plant growth (Anas *et al*., 2020) and is also a key determinant of grain yield. There has been continuous N mining in SSA, resulting in cumulative negative N balances of approximately 700 kg N over the last three decades (Dimkpa *et al*., 2023), which has led to soil degradation and ultimately threatens food security.

Notably, maize consumes the highest amount of fertilizer in the country, applied to roughly 70% of the total maize-growing area (Kirimi *et al*., 2023). Despite this, the average N use intensity (40 kg $ha^{-1}$) – **Table 1** - is still below the recommended application rate of between 100 and 120 kg $ha^{-1}$ for optimal maize grain production. Indeed, the average grain yield has stagnated below 2 t $ha^{-1}$ for the past few decades (FAOSTAT, 2024), resulting in low cereal sufficiency (<1) (Van Ittersum *et al*., 2025) and an increase in grain imports (Abodi *et al*., 2021). Therefore, there is an urgent need to intensify fertilizer use, particularly nitrogen (N), in the country to improve yields, meet the crop's nutrient requirements, and reverse the decline in soil fertility (Pasley *et al*., 2020).

**Table 1: Average N use intensity for maize production in Kenya**

| | Volume of N used in maize production fields (tonnes) in Kenya | | | | |
|---|---|---|---|---|---|
| **Fertilizer** | **2013** | **2014** | **2015** | **2016** | **2017** |
| Diammonium Phosphate (DAP) | 26,159 | 15,284 | 14,605 | 20,518 | 29,446 |
| NPK (23:23:0) | 3,857 | 3,473 | 9,761 | 7,188 | 4,502 |
| Calcium Ammonium Nitrate (CAN) | 20,690 | 18,625 | 18,346 | 19,236 | 24,550 |
| Urea | 7,259 | 6,523 | 9,344 | 12,583 | 8,071 |
| Mavuno top dressing | 631 | 567 | 587 | 693 | |
| Yara Mila (23:10:5) | 262 | | | | |
| **Total N use in maize fields** | **58,858** | **44,472** | **52,643** | **60,218** | **66,569** |
| Harvested Area (ha) | | 2,116,000 | 2,267,152 | 2,337,587 | |
| Area fertilized (ha) | | 1,362,832 | 1,423,244 | 1,476,524 | |
| **N-fertilizer rate (kg ha$^{-1}$)** | | **32.6** | **37.0** | **40.8** | |

**Source:** (AFO, 2018)

Several studies have confirmed that increasing N-fertilizer in maize cropping systems improves grain yields (Winnie *et al.*, 2022; Breure *et al.*, 2023; Aramburu-Merlos *et al.*, 2024). Despite its importance in improving grain yields, its increased use in maize cropping systems could concomitantly accelerate N loss, considering that < 50% is recovered in the final harvested product (Scheer *et al.*, 2023). Meanwhile, the rest of N is lost, ultimately, leading to loading of reactive N (Nr) in the ecosystem, as witnessed in other intensively cultivated regions of the world (H. Zhao *et al.*, 2022). Further, threatening the existence of life on the planet (Erisman *et al.*, 2013), as elevated Nr contributes to air pollution, aquatic eutrophication, biodiversity loss, acidification and eventually, climate change (Gong *et al.*, 2024). In intensified agricultural systems, the interactions among climate, soil and plant strongly influence the internal N cycle, thereby regulating the fate of N input by urea or ammonical fertiliser. During this process, some N is lost from the system in the form of ammonia ($NH_3$), nitrates ($NO_3^-$), and nitrogen oxides ($NO_x$, including NO and $N_2O$) (Strenge *et al.*, 2023). These inorganic forms of N are lost through runoff, leaching, volatilization and gaseous emission (Rashmi *et al*., 2017), and can be deposited over large distances, even reaching pristine ecosystems through wet or dry deposition.

Nitrogen loss pathways are largely controlled by microbial action on different nitrogen substrates (Kuypers *et al*., 2018), which is primarily influenced by meteorological conditions, soil properties, and management practices. Runoff, for instance, is exacerbated by heavy rainfall, poor soil structure, slope, and a lack of soil cover. Meanwhile, leaching is dependent on the soil texture, the amount and intensity of rainfall (Hess *et al*., 2020), tillage (Wang *et al*., 2015), management practices, and the quantity of nitrogen fertilizer applied (Wang *et al*., 2019). Nitrous oxide ($N_2O$), a potent greenhouse gas (GHG), emissions from agricultural lands are influenced by several interacting factors, including edaphic, meteorological and soil management (Signor & Cerri, 2013). Therefore, achieving a balance in N use is imperative to meet crop production needs while minimising N losses to the ecosystem.

Fertilizer-induced Nr losses in intensified cropping system are inevitable. However, there is a paucity of information on the amount of N lost through leaching and $N_2O$ emissions, especially in the highland tropics of the Rift Valley of Kenya, a key agricultural region contributing significantly to the national food production. This is because studies have rarely focused on the soil N dynamics in this region, despite its huge potential as an $N_2O$ source. Therefore, regular and up-to-date information on soil N dynamics in maize mono-cropping systems is vital for developing sound mitigation policies and improving the reporting of GHGs in our national inventory.

### 1.2 Problem Statement

The success of the Asian Green Revolution from the 1970s to the 1990s demonstrates the impact of increased fertilizer use on crop production in the SSA region, especially nitrogen (N). However, as observed in other intensively cultivated areas worldwide, higher N use is often results in low nutrient use efficiency (NUE) and greater Nr losses. These losses contribute to air pollution, acidification of land and water systems, eutrophication, crop and biodiversity loss, and the greenhouse effect. In Kenya's high-potential maize zones, high rainfall received throughout the year coupled with increased N inputs, are likely to intensify these losses in the region. Yet, uncertainties in these losses remain due to limited spatial measurements of Nr losses from soils in this area leading to incomplete understanding of the processes controlling these losses. Without precise and localized N loss data, scaling estimates from farms to national or regional levels remains challenging, limiting our ability to develop effective ecosystem mitigation strategies related to N fertilizer use.

### 1.3 Justification of the Study

Under the 2015 Paris Agreement, 195 member states, including Kenya, committed to submit their Nationally Determined Contributions (NDCs) to the United Nations Framework Convention on Climate Change (UNFCCC) biennially (Rosenstock & Wilkes, 2021). Agriculture was identified as a vital intervention in reducing GHG emissions and ensuring that the temperature rise is maintained below 2 °C (Gyanchandani, 2016; van Loon *et al*., 2019). However, most SSA countries find it challenging to report soil $N_2O$ emissions, since they lack a national $N_2O$ emissions inventory and thus, use the Intergovernmental Panel on Climate Change (IPCC) Tier 1 guidelines to report emission levels (Ogle *et al*., 2013). This is, conversely, subject to an overestimation of the quantity of nitrous oxide emitted from agricultural soils, especially since the response is non-linear (Hickman *et al*., 2014; Macharia *et al*., 2020; Albanito *et al*., 2017).

However, in recent years, $N_2O$ emissions in SSA have garnered considerable attention, particularly the fertilizer-induced $N_2O$ emissions from agricultural lands. This topic has been examined by several scientists who are eager to address the lack of information on $N_2O$ emissions in SSA (Hickman *et al*., 2011, 2014a, 2014b, 2015; Sommer *et al*., 2015; Pelster *et al*., 2017; Leitner *et al*., 2020; Macharia *et al*., 2020; Musafiri *et al*., 2020; Lemarpe *et al*., 2021; Githongo *et al*., 2022; Tully *et al*., 2023). However, studies measuring $N_2O$ in SSA remain scarce compared to other regions of the world. For example, Rosenstock & Wilkes (2021) reported that in 2016, less than 100 site-years of $N_2O$ emission data were collected across SSA, whereas in China alone, about 6000 site-years of data collected were recorded from maize fields during the same period. This limited dataset contributes to siginficant uncertainties and constrains the accurate estimation of emission factors (EFs) at both national and regional scales.

Several models have been used to estimate both current and future $N_2O$ emissions from agricultural lands in SSA (Hickman *et al*., 2011; Albanito *et al*., 2017; Leitner *et al*., 2020). These models have also been used to estimate emissions under different fertilizer scenarios (Huddell *et al*., 2020; Leitner *et al*., 2020). However, their accuracy is often limited by insufficient information on key input datasets such as fertilizer type and amount, soil properties and climate factors, which are critical for reliable model development. This data gap poses a major challenge in validating and testing these models to estimate soil $N_2O$ emissions across spatially diverse croplands at national and regional scales.

In Kenya, few studies have attempted to link $N_2O$ emissions to soil and climatic factors that influence microbial activities and drive emissions. Therefore, it is essential to conduct comprehensive measurements and provide information on soil $N_2O$ fluxes, soil properties, agricultural land management and climatic conditions during the measurement period. Such information would provide a basis for developing accurate $N_2O$ Emission Factors (EFs) models capable of estimating emissions at different production scales, both nationally and regionally. Against this background, this study seeks to investigate N pathways in maize monocrop systems in Uasin Gishu County, focusing on how increased N fertilizer application influences $N_2O$ emissions.

## 1.4 Objectives

### 1.4.1 Broad Objective

To contribute to data on fertilizer-induced greenhouse gas (GHG) emissions in cropping systems for sustainable agricultural productivity

### 1.4.2 Specific Objectives

1. To evaluate the effect of inorganic nitrogen fertilizer application on soil nitrogen dynamics
2. To evaluate the effect of inorganic nitrogen fertilizer application on maize grain yield and nitrogen use efficiency.

## 1.5 Research Questions

1. Does increasing inorganic nitrogen fertilizer application rates influence soil nitrogen availability and losses in maize monocrop production systems?
2. Does increasing inorganic nitrogen fertilizer application rates increase maize grain yield and nitrogen use efficiency?

# CHAPTER TWO

# LITERATURE REVIEW

## 2.1 Nitrogen and its significance in crop production

Nitrogen (N) is an essential nutrient necessary for crop production, and its availability is one of the primary factors limiting yield (Zou *et al*., 2018). Besides its role in providing nutrition to plants, it forms the fundamental structure of most organic molecules, including chlorophyll, proteins, nucleic acids, alkaloids, amino acids, and vitamins, all of which play vital roles in plant growth, development, and the quality of the harvestable produce (Wang *et al*., 2024). In crop production, nitrogen is sourced from both organic and inorganic sources. However, in recent years, the use of inorganic nitrogen has increased exponentially to meet the ever-growing demand for food (Adalibieke *et al*., 2023).

Its use has increased sevenfold over the last four decades (Maheswari *et al*., 2017; Zayed *et al*., 2023) and it is estimated that since the start of the 21st century, about half of the human population has directly depended on N fertilizer for food (Fowler *et al*., 2013). According to FAO (2024), N fertilizers are among the most widely used for crop production worldwide, accounting for 66%, 62%, 49%, 56%, and 61% of the total fertilizer use in Europe, Asia, the Americas, Oceania, and Africa, respectively. Globally, cereal crops (maize, wheat and rice) dominate N fertiliser use by crop, receiving half of the produced synthetic N (16, 18 and 16%, respectively) (Ladha *et al*., 2020) and their use in the production of cereals has increased 9-fold, from 6.9 to 65.2 Mt. Furthermore, cereal production increased by 340% between 1961 and 2019, from 876.9 to 3,279 Mt, and during the same period, maize production rose approximately six times (FAO, 2021).

## 2.2 Current fertilizer use in Africa for crop production

In contrast, fertilizer use on the continent is markedly low (22 kg $ha^{-1}$) compared to the global average (113 kg $ha^{-1}$) and other intensively cultivated regions, such as Asia (177 kg $ha^{-1}$) (FAO, 2024). This corresponds to an average N use of about 14 kg $ha^{-1}$, far below the optimal N requirement and the 50 kg nutrient $ha^{-1}$ target set in the 2006 *Abuja declaration on Fertilizer for an African Green Revolution*. As a result, this has proven detrimental to the continent's food security, resulting in low crop production due to insufficient N supply and accelerating soil degradation through nutrient mining, estimated at 660 to 700 kg N $ha^{-1}$ (Dimkpa *et al*., 2023). Nitrogen mining has been identified as the single most important factor limiting crop production (Giller, 2020), ultimately, constraining the productivity of agricultural soils, as reflected by the low crop production gains of 2% (Edmonds *et al*., 2009).

Maize is the principal staple food across SSA and although significant efforts have been made in recent decades to improve its production through the development of new and improved varieties, average annual yield remain low, ~ 2 t $ha^{-1}$. Demand for maize, however, continues to grow and by 2050, it is expected to increase by 233%, driven by rapid population growth in the region (Aramburu-Merlos *et al*., 2024). This rising demand is expected to increase pressure on already nutrient-depleted soils, potentially encouraging the exploitation of other volatile ecosystems, such as the encroachment of forests to expand the cultivated area. Nevertheless, there remains a considerable opportunity for SSA to increase maize production on existing agricultural land to narrow the large yield gap. Several studies have also echoed similar views, highlighting the need for increased fertilizer use in crop production systems, especially N, to enhance yields and reverse soil fertility decline linked to low N inputs (Hickman *et al*., 2015; ten Berge *et al*., 2019).

## 2.3 Prospects of increasing fertilizer use in crop production

The renewed focus on increasing fertilizer use, referred to as the 'Second Green Revolution', is based on the success of the Asian Green Revolution, which took place between 1965 and 1990 (Hazell, 2009). The Green Revolution in Asia resulted in higher grain production, which was due to a combination of improved seed varieties and increased fertilizer use per hectare of farmland, rising from 23.6 to 102 kg $ha^{-1}$ in 1970 and 1995, respectively. This initiative boosted grain yields by 178%, making countries in the region cereal sufficient (Pathak *et al*., 2024). To achieve similar agricultural success in SSA, several initiatives have been introduced, including the implementation of input subsidy programs.

Until recently, input subsidy programs (ISPs) have been implemented in 12 SSA countries, including Nigeria, Zambia, Malawi, Kenya, Rwanda, Tanzania, Senegal, Mali, Ghana, Burkina Faso, Burundi and Mozambique (Jayne *et al*., 2018). Although these programs have been influenced by various socio-political factors, they have contributed to increased fertilizer use and ultimately improved maize yields. For instance, in Kenya, ISPs have elevated maize production by 361 kg grain per 100 kg of subsidised fertilizer, while in Malawi and Zambia, it increased by 165-188 kg grain per 100 kg of fertilizer, respectively (Nhlengethwa *et al*., 2023). Despite these gains, production still fall short of meeting the increasing food demand accelerated by rapid population growth. Consequently, Ricker-Gilbert *et al*. (2024) recommended that the private sector should lead the government-led initiative and focus more given to smallholder farmers to truly benefit from the program.

A recent study by Aramburu-Merlos *et al*. (2024) on maize production in different climatic zones in SSA reported that proper management practices should be carried out to close the maize yield gap in SSA. For instance, planting hybrid seeds coupled with application of N fertilizer rates of 50 kg N $ha^{-1}$ would result in a 61% increase in the average attainable yield from 1.8 to 2.9 t $ha^{-1}$. Further, early planting of hybrid seeds with N fertilizer at increased planting density would improve the attainable yield 2.4-fold, from 1.8 to 4.3 t $ha^{-1}$. This would subsequently narrow the yield gap by 30%. Moreover, the study also reported that integrating good agronomic practices coupled with doubling the N fertilizer application rate to 100 kg N $ha^{-1}$ would increase the attainable yield to 70% of the potential yield. However, increasing N fertilizer use in SSA cropping systems would pose a challenge in enhancing yield while simultaneously maintaining high use efficiency due to losses associated with increased N fertilizer use.

## 2.4 Nitrogen Use Efficiency (NUE)

Nitrogen use efficiency (NUE) is a crucial index in crop production systems, as the efficient use of N fertilizer in crop production is vital in improving yields and reducing ecosystem degradation.  It encompasses the crop’s ability to uptake N vis-à-vis the N input (N uptake efficiency) and to convert the acquired N into the final harvested product (yield), as well as N utilization efficiency (Hanif, 2023). Other indices of NUE in crop production include nitrogen recovery efficiency (RE), agronomic efficiency (AE), partial factor productivity (PFP), nitrogen uptake efficiency (NUpE), physiological efficiency (PE) and partial nitrogen balance (PNB) (Congreves *et al.*, 2021). The NUE are further categorised into fertiliser-, soil- and plant-based indices. Fertilizer-based NUE indices express the amount of fertilizer applied relative to plant aboveground biomass, yield, or tissue N-content; they include RE, AE, PFP, and PNB. On the other hand, NUpE and PE are soil- and plant-based indices, respectively. NUpE expresses plant N-uptake relative to N applied, whereas PE is the ratio of plant tissue N converted to grain.

A wide body of literature exists on the NUE of crops in different production systems (Dobermann, 2005; Fageria & Baligar, 2005; Lassaletta *et al*., 2014; Omara *et al*., 2019; Govindasamy *et al*., 2023). A meta-analysis study by Lassaletta *et al*. (2014) reported that the current global N recovered in the final harvest is about 47% of the total N inputs. As mentioned earlier, cereals account for half of the synthetic N used globally in crop production; however, the global cereal N recovery ranges between 35% and 65% (Herrera *et al*., 2016). Therefore, approximately 35 to 65% of reactive nitrogen is either lost through various pathways or retained by the soil.

Additionally, plant N uptake and losses are a function of several environmental and management factors, including soil texture, mineralogy, crop type, tillage method, meteorological conditions and N fertilizer source, application, timing, rate and placement method. Low-input systems often have high NUE, which signifies N exploitation and further leads to negative N balances. This is mainly due to the overreliance on the mineralization of the organic pool and N-fixation. In contrast, NUE is reduced under high N fertilization due to the crops' inability to utilize N efficiently.

### 2.5 N loss from agricultural soils

Since more than half of the N fertilizer applied is unintentionally lost to the environment, agriculture is a significant source of anthropogenic reactive nitrogen (Nr), particularly from synthetic N fertilizers. Nr includes all the biologically, photochemically and/or radioatively active forms of N, such as the organic compounds, inorganic N and chemically active gases in the troposphere ($NH_3$, $N_2O$ and $NO_x$) (De Vries, 2021). Synthetic N fertilizers account for 63% of all anthropogenic sources of reactive N (Dobermann, 2005), considering that less than 50% of N used for crop production is recovered in the final harvest. However, some of the N is recovered in the soil, while the rest is lost to the environment through various process, including nitrate leaching, ammonia volatilization and nitrous oxide emission (Elrys *et al*., 2021).

### 2.5.1 Nitrous oxide ($N_2O$) emissions

The global atmospheric nitrous oxide ($N_2O$) concentrations have increased significantly by 20%, from 270 ppb in 1750 (preindustrial period) to 331 ppb, currently (Tian *et al*., 2020). It is a potent greenhouse gas (GHG) with a 6% radiative forcing and a global warming potential 300 times that of carbon (iv) oxide, over 100-year period, contributing significantly to climate change (Hong *et al*., 2023). Once in the atmosphere, $N_2O$ reacts with high-energy oxygen atoms to form nitric oxide (NO), which depletes the stratospheric ozone layer (Portmann *et al*., 2012). It is estimated that its atmospheric concentration is increasing at an average rate of 0.73 ppb per year (Tian *et al*., 2019), and in 2021, $N_2O$ levels reached a record high of 2.97 billion metric tons of carbon (iv) oxide equivalent ($GtCO_2e$).

Nitrous oxide emissions primarily result from microbial-mediated biochemical processes of nitrification and denitrification (Butterbach-Bahl *et al*., 2013). Its increased accumulation in the atmosphere is mainly attributed to agriculture, which contributes to ca. 60% to 70% of the global $N_2O$ emissions from N fertilizer (Zhou *et al*., 2012; Zhao *et al*., 2025). Over the past four decades, fertilizer-induced annual global nitrous oxide emissions have increased by 30% to 6.7-7.3 Tg $N_2O$ $yr^{-1,}$ and this is expected to rise by 30-65 % by 2030 (Ezui *et al*., 2022). In contrast, $N_2O$ emissions from SSA agricultural soils are low, contributing between 6 and 19 % of the global anthropogenic $N_2O$ emissions (Kim *et al*., 2016; Lemarpe *et al*., 2021). This is largely because agricultural systems in SSA are associated with low inputs (Richards *et al*., 2016) and a significant proportion of emissions results from the expansion of agricultural areas, which mostly involves the use of fire for clearing vegetation.

However, with the recent emphasis on increased N fertilizer use to enhance crop production in the region, it is expected that $N_2O$ emissions will be altered.

Due to its significant role in climate change, $N_2O$ has gained prominence in recent years. As such, it has been studied across different ecosystems within the SSA region (Hickman *et al*., 2011, 2014a, 2014b, 2015; Sommer *et al*., 2015; Pelster *et al*., 2017; Zheng *et al*., 2019a; Van Loon *et al*., 2019; Leitner *et al*., 2020; Macharia *et al*., 2020; Musafiri *et al*., 2020; Bigaignon *et al*., 2020; Wachiye *et al*., 2020; Lemarpe *et al*., 2021; Tesfaye *et al*., 2021a; Ntinyari & Gweyi-Onyango, 2021; Githongo *et al*., 2022; Tully *et al*., 2023; Bougma *et al*., 2025). When quantifying $N_2O$ emissions from soils in situ measurements using either manual static or automatic chambers, micrometeorological and laboratory incubation methods presents the most reliable and standard approaches. Unfortunately, the experimental complexity and costs of specialist equipment and analyses have limited the use these $N_2O$ emission measurement techniques. Therefore, several studies have tried to use either empirical or process-based methods to estimate $N_2O$ emissions in SSA (Grace *et al*., 2016; Albanito *et al*., 2017; Tian *et al*., 2020; Tesfaye *et al*., 2021b). Nevertheless, using these methods to estimate $N_2O$ emissions from agricultural lands in SSA is highly uncertain due to various constraints, such as limited spatial studies on fertilizer-induced $N_2O$ emissions from croplands and the lack of documentation of input data, including the type of fertilizer used, its quantity, and the initial soil properties (Ogle *et al*., 2013; Albanito *et al*., 2017).

For this reason, the majority of developing countries use the Intergovernmental Panel on Climate Change (IPCC) Tier 1 default emission factor (EF) of 1% to measure nitrous oxide emissions from their respective agricultural lands, i.e., the IPCC Tier 1 guidelines assume that 1% of N fertilizer applied is directly emitted as $N_2O$ (Bougma *et al*., 2025).

However, this is not usually the case, as the reported figure is usually less than 1 kg $N_2O$- N $ha^{-1}$ and thus, might result in the reporting of inaccurate and unreliable data due to overestimation, as evidenced by numerous studies measuring $N_2O$ emissions from arable soils that reported a non-linear relationship between increasing N fertilizer rate and nitrous oxide emissions (Hickman *et al*., 2014, 2015).

These studies are, however, limited in scope when compared to other regions or even globally in terms of spatial coverage and the length of the measurement period, which are usually <200 days, which exacerbates the uncertainty in reporting $N_2O$ emissions at a regional scale since $N_2O$ fluxes are a highly spatiotemporal variable. This is further supported by findings by Smith *et al*. (1997), who reviewed the relationship between the period of measuring $N_2O$ fluxes from agricultural lands to estimate the emissions, and discovered that $N_2O$ emissions from > 30, > 100 and > 200 days were 0.6%, 1.1% and 1.9% respectively. Bouwman *et al*. (2002) also reported that N-fertilizers have longer-lasting effects on $N_2O$ emissions past the growing period of the crop. Therefore, it is important to increase the length of measurement of in-situ $N_2O$ measurements in croplands, using automated chamber systems, to effectively determine the fertilizer-induced $N_2O$ emissions and improve reporting in national inventories.

### 2.5.2 Nitrate ($NO_3^-$) leaching

Leaching forms one of the most significant pathways for nitrogen (N) loss in agricultural systems, making the process a prominent contributor of nitrate ($NO_3^-$) to the hydrosphere and leading to water contamination (Bijay-Singh & Craswell, 2021). In agricultural soils, $NO_3^-$ ion is formed through the nitrification of ammonium ions ($NH_4^-$) derived from synthetic fertilizers. Nitrification is a two-step biochemical process involving the oxidation of ammonia in the membrane site of the nitrifying or archaea microorganism in the presence of ammonia monooxygenase enzyme (amoA) to nitrite

($NO_2$) (Cameron *et al*., 2013). This step is aided by the hydroxylamine oxidoreductase (HAO) enzyme, which catalyses the reaction between the hydroxylamine ($NH_2OH$) and water. The nitrite is further oxidised to nitrate ($NO_3$) by the nitrite-oxidising bacteria (Ayiti & Babalola, 2022). However, the produced $NO_3^-$ ion is highly water-soluble, allowing it to move easily with water that percolates through the soil. This movement down the soil profile is facilitated by repulsion from the negatively charged surface of clay minerals (Padilla *et al*., 2018).

Fertilizer use in agricultural soils is a major source of nitrate leaching worldwide, accounting for 30% (0.3 kg N $kg^{-1}$ N applied) of the total N input, default emission factor as used by the Intergovernmental Panel on Climate Change (IPCC) (Eysholdt *et al*., 2022). However, other studies have reported various estimates, 19% (Lin *et al*., 2001), 6.7-19% (Zhou *et al*., 2012), 22% and 15% in wheat and maize systems, respectively (Zhou & Butterbach-Bahl, 2014), 14.6% (Wang *et al*., 2018) and 6-12% (Wang *et al*., 2019). Zhou & Butterbach-Bahl (2014) in their global synthesis, reported that $NO_3^-$ leaching increased linearly with increasing N application rates and is consistent with the IPCC emission factor. However, Wang *et al*. (2019) found the relationship to be non-linear.

Generally, nitrate leaching varies considerably across agricultural systems due to differences in the underlying factors. They include tillage systems, climatic factors (precipitation and temperature), N fertilizer management, irrigation, edaphic factors (soil structure and texture) and land use systems (forest, agricultural land and grasslands) (Cameron *et al*., 2013; Boy-Roura *et al*., 2016). A study by Wang *et al*. (2018) on nitrate leaching from vegetable systems across 18 field and greenhouse studies in China found a high $NO_3^-$ leaching of 79.1 kg N $ha^{-1}$ from N fertilizer input of 423 kg N $ha^{-1}$, with 98 and 59.8 kg N $ha^{-1}$ in the greenhouse and open-field systems.

Further, there was a positive linear response of leaching with increasing N rates, irrigation water and the number of growing days, 200%, 121 and 165%, respectively. Another meta-analysis in Europe reported $NO_3^-$ leaching values of between 3 and 99 kg N $ha^{-1}$ in Denmark and 1 to 124 kg N $ha^{-1}$ across other European countries. These values were considerably higher than those reported by Zhou & Butterbach-Bahl (2014) across 32 studies, 20 (57.4 kg N $ha^{-1}$) and 12 ( 29 kg N $ha^{-1}$) in maize and wheat production systems, respectively. However, almost similar $NO_3^-$ leaching values were observed by Russo *et al*. (2017) in a maize system in Kenya, which ranged between 40 and 81 kg N $ha^{-1}$ when increasing the N application rate to 200 kg N $ha^{-1}$ plots.

Furthermore, $NO_3^-$ concentration in agricultural soils is a key indicator of microbial-driven processes since it acts as a precursor during denitrification. Several studies have found a positive relationship between soil $NO_3^-$-N intensity (the time-weighted concentration of $NO_3^-$available for microbial action) and cumulative $N_2O$ emissions. This further suggests that $NO_3^-$ intensity could be used as a proxy to estimate $N_2O$ emissions from agricultural soils (Yao *et al*., 2020). To measure soil $NO_3^-$ concentration in agricultural systems, several methods have been adopted, including the use of lysimeters, passive sampler techniques, and soil extraction. However, these methods are not without their disadvantages. For instance, it is difficult to measure soil $NO_3^-$ concentration from a single point over time, as it may measure $NO_3^-$ bound to the soil matrix and not in solution (Russo *et al*., 2017). Meanwhile, lysimeters are subject to underestimation, especially when the pore spaces are disconnected. Further, in situations with large pores, the use of lysimeters may overestimate the pore-water $NO_3^-$ concentration relative to the bulk soil (Russo *et al*., 2017).

Nonetheless, Wey *et al*. (2021) found a positive relationship when determining autumn Nmin using soil extraction and leaching fluxes using suction cups or self-integrating accumulators. Therefore, suggesting that determining Nmin concentration via the extraction method could be considered in $NO_3^-$ leaching studies, but warns that it is not an absolute indicator for nitrate leaching.

### 2.5.3 Ammonia ($NH_3$) volatilization

Agriculture is a major source of ammonia ($NH_3$) volatilisation, contributing 80-95% of the total $NH_3$ volatilisation. Global estimates report an average loss of between 10% and 19% of the total N applied in agricultural lands and grasslands (Cameron *et al*., 2013; Pan *et al*., 2016; Schwenke *et al*., 2016; Wu *et al*., 2021; Hurtado *et al*., 2024). With N fertilizer use increasing across agricultural lands worldwide, $NH_3$ volatilization has also increased, by 78% between 1980 and 2018 (Hurtado *et al*., 2024). In agricultural systems, the process could result from either animal urine or ammonium fertilizers, in the presence of a urease enzyme, which catalyses the reaction, as shown in equations 1 to 3 (Freney *et al*., 1981):

$$\boldsymbol{H_2N - CO - NH_2 + 2\,H_2O \rightarrow (NH_4)_2CO_3} \quad \textbf{(1)}$$

$$\boldsymbol{(NH_4)_2CO_3 + 2\,H^+ \rightarrow 2\,NH_4^+ + CO_2 + H_2O} \quad \textbf{(2)}$$

$$\boldsymbol{NH_4^+ + OH^- \rightarrow NH_3 + H_2O} \quad \textbf{(3)}$$

Once in the atmosphere, $NH_3$ acts as a precursor to atmospheric fine particulates ($PM_{2.5}$) by neutralizing acids such as sulphuric acid, hydrochloric acid, and nitric acid (Ramalingappa *et al*., 2023). In this process, ammonium salts are formed, which contribute to air pollution. Ammonia gas can also re-enter the ecosystem as dry or wet deposits, leading to eutrophication of inland and coastal waters, soil acidification, and ultimately, biodiversity loss. The re-entry of $NH_3$ into the ecosystem is a significant source of indirect $N_2O$ emissions from terrestrial ecosystems, accounting for annual indirect $N_2O$ emissions ranging from 0.1 to 0.16 million tons (Wu *et al*., 2021). The interplay between meteorological conditions, edaphic factors, sources of ammonia, and fertilizer management strategies governs the volatilization process. A global study by Pan *et al*. (2016) reported that $NH_3$ volatilization was positively related to increasing N application rates (180.7%), but negatively related to deep placement of fertilizer (54.7%), irrigation (34.5%), residue retention (25.5%), and urease inhibitors (53.7%).

Additionally, ammonia ($NH_3$) volatilization can occur through plants during gaseous exchange via the stomata. Plants consistently emit $NH_3$ throughout their growth cycle, driven by the higher partial pressure of $NH_3$ in the apoplast relative to the surrounding air (Hayashi *et al*., 2011). However, this process is regulated by the atmospheric $NH_3$ concentration and the ammonia compensation point (ACP), point at which $NH_3$ uptake or emission reaches equilibrium. For instance, when the ACP exceeds the ambient $NH_3$ concentration, $NH_3$ emission occurs; conversely, when it is lower, $NH_3$ is absorbed by plants.

In agricultural fields, the atmospheric $NH_3$ concentration typically ranges from 1 to 14 µg $m^{-3}$, but this value can increase after urea application, while the ACP values vary between 0.7 and 4.2 µg $m^{-3}$ $NH_3$. The ACP is regulated by light intensity, crop growth stage, N nutrition status of the crop, internal $CO_2$ concentration and air temperature (Schoninger *et al*., 2018). A study by Hayashi *et al*. (2011) attempted to quantify $NH_3$ emission from the flag leaf of rice in Japan and reported emission ranges of 25 to 38 ng N $cm^{-2}$ $ha^{-1}$ and 22 ng N $cm^{-2}$ $ha^{-1}$ during the day and at night, respectively. Although it was expected that leaf senescence would accelerate the $NH_3$ emission, the study reported no variations as the flag leaf senesced from heading to maturity stages.

### 2.5.4 Denitrification

Denitrification is an anaerobic multi-stepwise microbial reduction of either $NO_3^-$ or $NO_2^-$ to dinitrogen ($N_2$) in the presence of four different enzymes (de Sousa & Bhosle, 2012). The four enzymes include (i) the nitrate reductase (NaR), which reduces $NO_3^-$ to nitrite ($NO_2^-$) and its production is induced by the availability of $NO_3^-$ under reduced $O_2$ concentration; (ii) nitrite reductase (NiR) reduces $NO_2^-$ to NO; (iii) nitric oxide reductase (NOR) reduces NO to $N_2O$ and (iv) nitrous oxide reductase reduces $N_2O$ to $N_2$ as shown in equation 4.

$$\boldsymbol{NO_3^- \rightarrow NO_2^- \rightarrow NO \rightarrow N_2O \rightarrow N_2} \quad \textbf{(4)}$$

Globally, it is estimated that coastal and marine, terrestrial, and freshwater ecosystems account for 58%, 22%, and 20% of total denitrification, respectively (de Sousa & Bhosle, 2012). In terrestrial ecosystems, soil denitrification converts 30-60% of reactive nitrogen (Nr) into inert nitrogen gas ($N_2$), making it a key process in the global N cycle (Wang *et al.*, 2018). However, this also represents a major pathway of N loss that could otherwise support crop production or if excessive, contribute to ecosystem degradation. Globally, it is estimated that 20-87 Tg N is lost from arable soils annually and approximately 85% of this loss occurring as $N_2$ (Battye *et al.*, 2017; Pan *et al.*, 2022). Despite its significance, our understanding of $N_2$ emissions and their extent globally remains limited, partly due to the high background concentration of atmospheric $N_2$, which makes constrains measurements. Although several studies have attempted to quantify soil denitrification, surprisingly very few studies have been conducted in Africa.

Several edaphic, environmental and management factors strongly influence the rate of soil denitrification (Luo *et al.*, 1999; Hofstra & Bouwman, 2005; Clark *et al.*, 2020;

Pan *et al*., 2022). A global study by Pan *et al*. (2022) on 3367 observations from 225 studies globally reported an average daily loss of 0.25 kg N $ha^{-1}$ across 648 field observations through soil denitrification, with an overall emission factor ($EF_D$) of 4.8% across different agricultural soils. The study further reported of increase in soil denitrification with increasing soil water-filled pore spaces, $NO_3^-$ and mineral N content and soil temperature. Similarly, the $N_2$ emissions were positively related to soil mineral N and water-filled pore spaces. Additionally, increasing N application rates enhanced the soil denitrification rate and $N_2$ emissions by 219% and 204%, respectively. $NO_3^-$-based fertilizers particularly enhanced the soil denitrification rate (199%), while the $NH_4^+$-based fertilizers reduced $N_2$ emissions (56%). Soil management practices such as the addition of lime, irrigation and retention of residues increased the denitrification rate by 52%, 75% and 144%, respectively. On the other hand, applying biochar and the use of nitrification inhibitors reduced denitrification rates by 38% and 41%, respectively.

Similar findings were also reported by Wang *et al*. (2018), who observed that increasing N application rates elevated soil denitrification by 174%; however, this increase was exponential with increasing N rates of < 250 kg $ha^{-1}$ in both agricultural and grasslands. Overall, the global synthesis found that denitrification was higher in grasslands than in agricultural lands, 271% and 147%, respectively.

**2.6 Consequences of reactive nitrogen (Nr) losses in the ecosystem**

The N cycle has been significantly altered in the past century by human activities, especially since the discovery of the Haber-Bosch process (Li *et al*., 2025), which artificially fixes nitrogen under high temperatures and pressures to produce ammonia ($NH_3$). This process is a major source of synthetic nitrogen and generates about 210 Tg of Nr annually, compared to 203 Tg produced through natural processes. As a result, doubling the global N cycle (Fowler *et al*., 2013) and the Nr loading to the ecosystem has surpassed the 'planetary boundary' as illustrated in Figure 1. The planetary boundary framework was adopted in 2009 and its main aim was to define 'a safe operating space for the human population to thrive based on our evolving understanding of the functioning and resilience of the Earth System (ES) (Steffen *et al*., 2015). This was done by setting the planetary boundary at 25% of the total amount of newly generated reactive N (Razon, 2018).

Studies have placed the current geological period as the Anthropocene, where anthropogenic activities have rapidly deviated the Earth System from the stable Holocene state of the past 12,000 years (Steffen *et al*., 2015; Rockström *et al*., 2023). When there is increased Nr loss into the environment, it cascades through the atmosphere, aquatic and terrestrial ecosystems (Erisman *et al*., 2013), consequently leading to air pollution, acidification of terrestrial and aquatic systems, eutrophication, biodiversity loss and the greenhouse effect (Gong *et al*., 2024) as shown in Figure 2. This makes Nr one of the top five emerging threats to humanity and the planet as a whole. Specifically, increased NOx emissions can lead to the accumulation of ozone ($O_3$) in the troposphere (Nguyen *et al*., 2023). Ozone in the troposphere acts as a powerful oxidant and a primary constituent of photochemical smog, which causes respiratory diseases in humans (Donzelli & Suarez-Varela, 2024). Increased $O_3$ in the atmosphere can also lead to crop loss, especially when taken in by plants during gaseous exchange. Global estimates have reported yield losses ranging between 3 and 16% in wheat, rice and maize (De Vries, 2021). Furthermore, the elevated N deposition as a result of increased Nr in the atmosphere is also responsible for biodiversity loss, as N deposition levels exceeding 5-10 kg N $ha^{-1}$ $yr^{-1}$ reduce plant species diversity since more nitrophillic species thrive under such conditions.

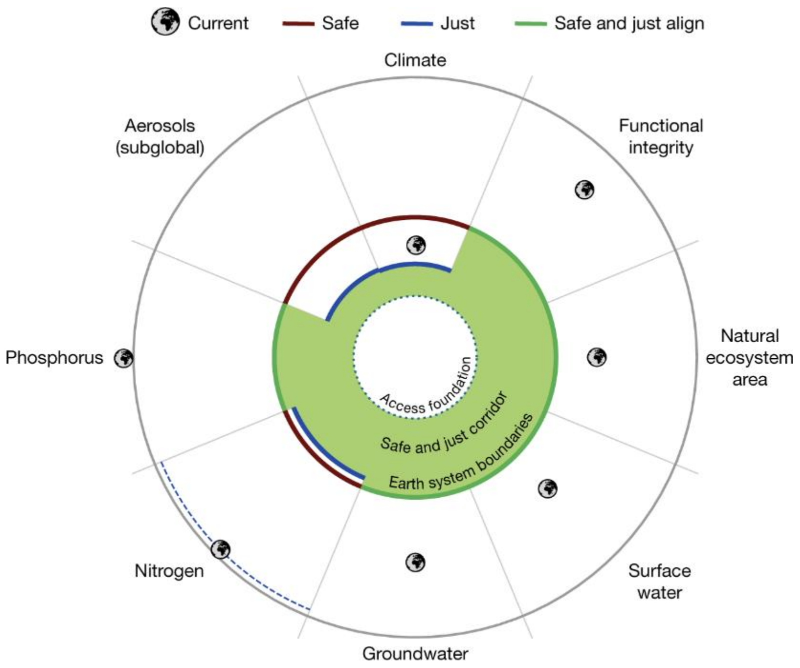


**Figure 1: Estimates of the safe Earth Systems Boundaries (illustrated by the dark red colour), just Earth Systems Boundaries (blue), where safe and just ESBs align (green) and the current global estimates (denoted by the Earth icons). Source: (Rockström *et al*., 2023)**

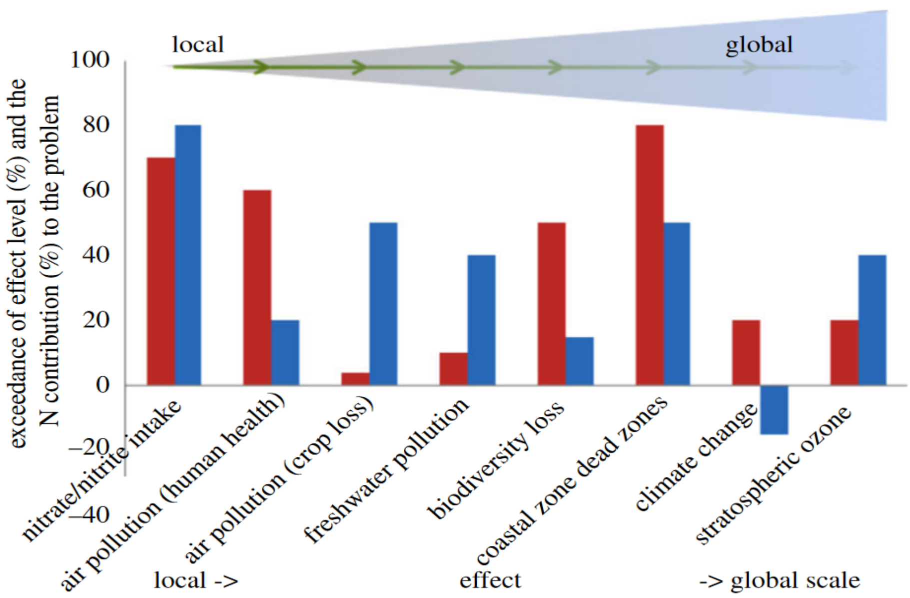


**Figure 2: Nr effects on the ecosystem, the red bar indicates the exceedance of the effects of reactive nitrogen (Nr) for the ecosystem or human population, while the blue bar shows the Nr contribution to the total effect relative to other causes of the problem. Adopted from (Erisman *et al*., 2013)**

# CHAPTER THREE

# METHODOLOGY

## 3.1 Study Site Description

The experiment was laid out at the Outreach and International Students Centre (OISC) agricultural research field at the University of Eldoret, Uasin Gishu County. The county is located between latitudes 0° 03" S and 0° 55" N and longitudes 34° 50" E and 35° 37" E (**Figure 3**). and is 2100 m above sea level in the highlands of the Rift Valley. The county consists of three main agroecological zones (AEZs), which are further subdivided into seven distinct sub-zones. The AEZs in the county include the Upper Highland zones (UH1 and UH2) and the Lower Highland zones (LH1 and LH2 in the southern areas; Upper Midland zone (UM4) in the western and northwestern areas; and the Lower Highland 3 zone, which extends across most parts of the county, including the study site (Jaetzold & Schmidt, 1983).

Uasin Gishu County has a subtropical highland climate, with an average annual temperature of 19.2 °C and an average rainfall of about 2027 mm over the past decade (FAO, 2023). Rainfall distribution in the county follows a unimodal pattern, featuring two distinct peaks occurring between March and September and between May and August, while the dry period extends from November to February. This rainfall pattern supports only one cereal cropping season yearly. The main annual crops grown in the county include maize, Irish potato, wheat, barley and sunflower, while perennial crops, such as coffee and various fruit trees, including avocados, are also cultivated.

The county’s soils are predominantly Ferralsols and Nitisols, which have developed from tertiary intermediate volcanic and basement rock systems. However, Ferralsols dominate the study area and are characterized by a red-brown colour and ferralic B horizon (whose clay fraction constitutes low-activity clays and sesquioxides (oxides and hydroxides of Aluminium and Iron). These soils have weak to strong angular blocky structures and are well-drained. However, they also possess low fertility resulting from low nutrient adsorption capacity (IUSS Working Group WRB, 2022). Despite this, the county plays a significant role in food production in Kenya because of its contribution to the dairy sector and high production of maize and wheat, with an average production of 364,102.3 and 34,662 MT, respectively (Agriculture and Food Authority, 2021; Kenya National Bureau of Statistics, 2023). Therefore, contributing immensely to the economy of the county, which is mainly agro-based with varying farming systems consisting of both small-holder and highly mechanized large-scale farmers.

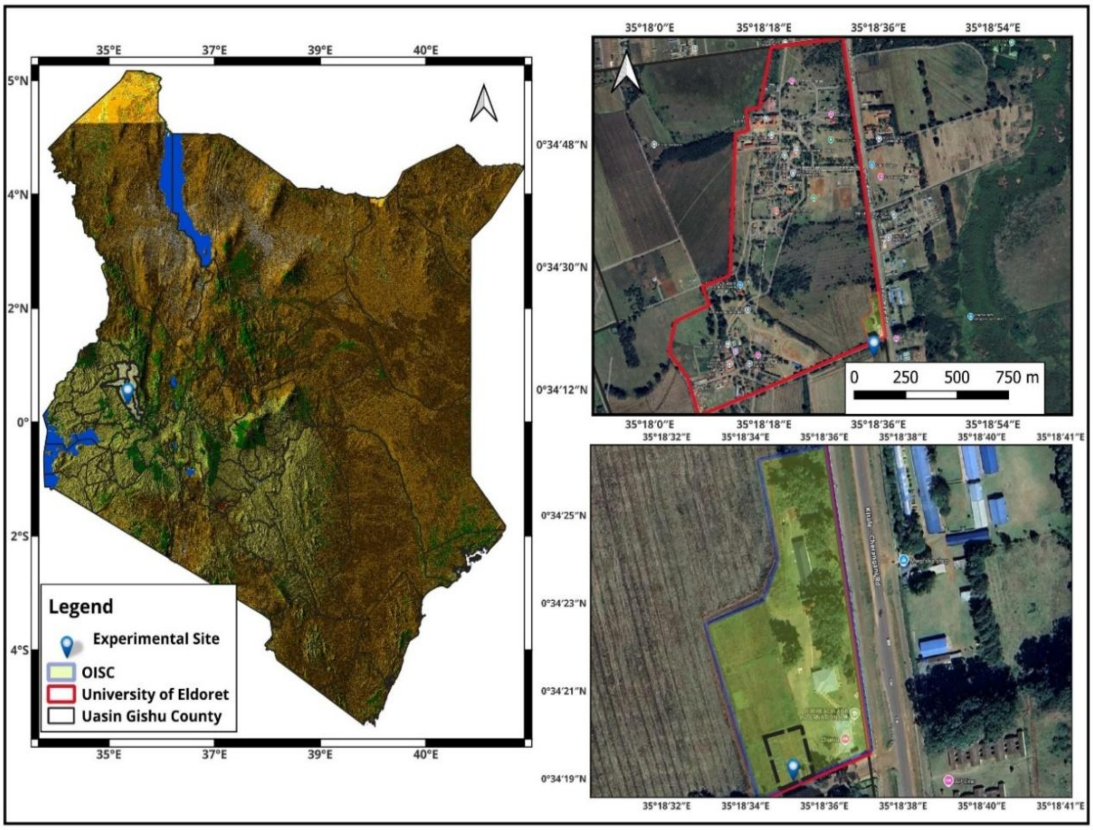


**Figure 3: Study location at the Outreach and International Student Centre (OISC), University of Eldoret, Kenya**

### 3.2 Experimental design and layout

**Figure 4** shows the experimental design and layout of the units. The experiment was an on-station field experiment consisting of six (6) nitrogen fertilizer rates arranged in a Randomized Complete Block Design (RCBD) and replicated thrice, thus, a total of 18 experimental units (**Figure 4**). The rates included 0, 25, 50, 75, 100 and 125 kg N ha$^{-1}$. The experimental units measured 3 m by 4 m (each plot having a total area of 12 m$^2$ and an effective sampling area of 6m$^2$ (2 by 3 m), separated by 1 m and 1 m buffers between blocks and plots, respectively.

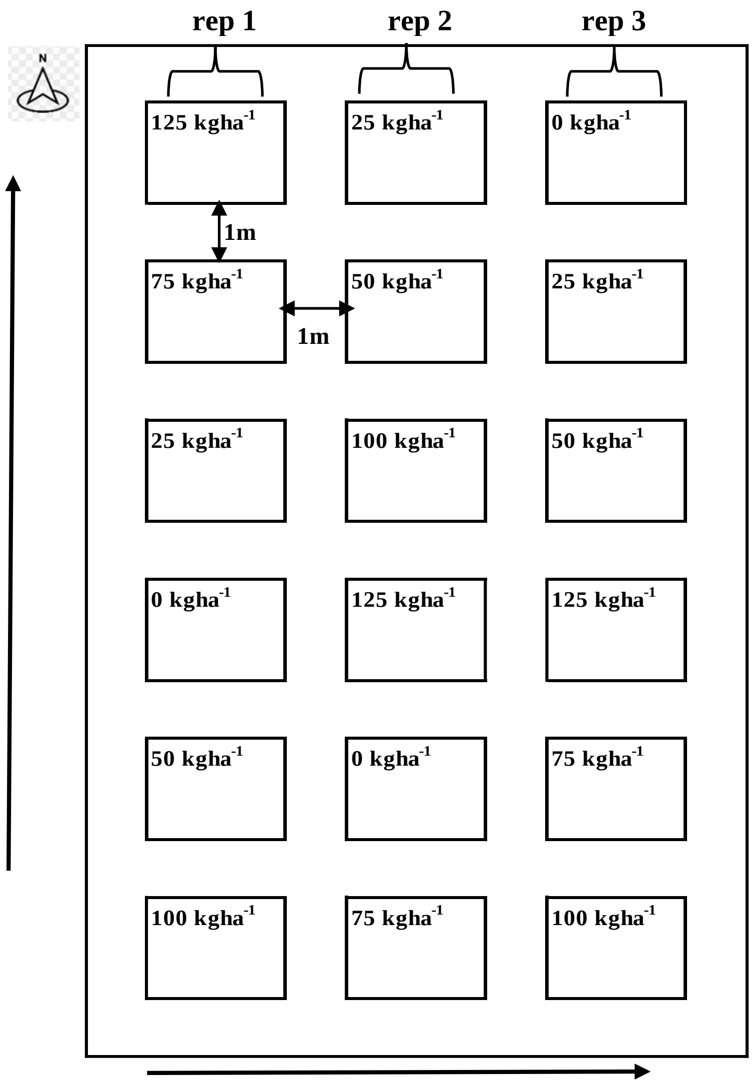


**Figure 4: Experimental design and layout of treatments 0, 25, 50, 75, 100 and 125 kg N ha$^{-1}$ replicated thrice**

### 3.3 Experiment set-up and agronomic practices

Maize seeds (two) of variety H6213 were sown at the beginning of the rainy season (April 2024) at a depth of 5 cm on tilled plots. They were spaced at intervals of 0.25 m within the rows and 0.75 m between rows. During planting, in the fertilized plots, one-third of the N nutrient was applied in the form of urea (46% N), with the remaining two-thirds split and applied later. The first split was applied during the 6th week after planting (WAP), while the second was applied during the silking stage (13$^{th}$ WAP, except for the control, and this was done through spot application. Additionally, all plots, except the control, received the recommended application rate of 30 kg P planting.

### 3.4 Data Collection

#### 3.4.1 Soil sampling for monitoring of $NH_4^+$-N and $NO_3^-$-N

The initial soil sampling was carried out before setting up the experiment for initial soil characterization. In each plot, a series of nine soil cores was sampled randomly, using an auger of diameter 5 cm, to a depth of 60 cm, at an increment of 0 – 20 cm, 20 – 40 cm and 40 – 60 cm, and later composited to form one representative sample for each depth. The subsequent soil sampling regime was carried out in every experimental unit from two points along the two inner rows. Sampling was done within the effective sampling area of 6 $m^2$ (2 m by 3 m) at varying depths of 0-20 cm, 20-40 cm and 40-60 cm. The samples were collected at varying frequencies of 14, 21, 42, 56, 70, 95, 112, 127, 165, 195, 224, 238, 287, 301 and 329 days after planting (DAP). The surface layer (0-20 cm) was sampled throughout the stated times, while the subsequent depths were only sampled on some dates due to the complexities involved in obtaining the sample and the need to preserve the integrity of the plots.

### 3.4.2 $N_2O$ Measurement

#### i. Chamber Design and Deployment

The $N_2O$ fluxes were measured using an automated static non-steady state flow-through chamber system for 329 days. Before planting, chambers were placed between rows **Figure 5** on stainless steel bases (0.5 by 0.5 m) initially driven into the soil to a depth of 10 cm. The chambers and bases were sealed tightly using a rubber gasket and remained in place for the whole evaluation period. The chamber design and specifications were as described by Clough *et al*. (2020). For example, lids were insulated with a reflective foil tape to preserve and maintain the air temperature within the headspace during flux measurements. The inside of each chamber was fitted with two fans to constantly mix the air and eliminate possible bias from vertical gas concentration gradient when the lids were closed during gas sampling. Moreover, the chambers were equipped with a vent to prevent a pressure gradient between the interior and the exterior of the chambers during $N_2O$ flux measurement. An additional temperature sensor was fitted to the side of each chamber and used to take temperature readings within the headspace of the chambers. **Figure 5** gives an illustration of the chamber deployment in an experimental plot.

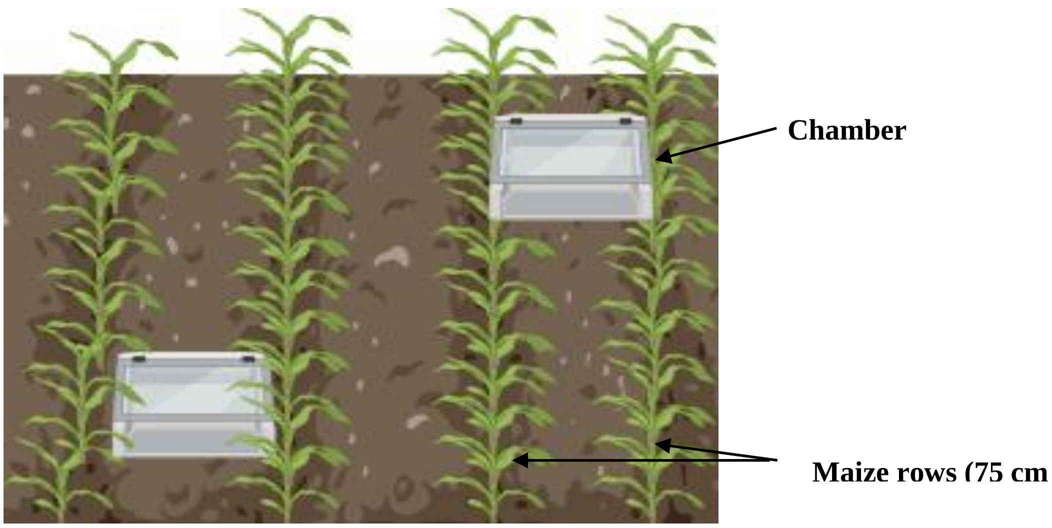


**Figure 5: An illustration of chamber deployment within an experimental unit**

### ii. Actual $N_2O$ flux measurement

The sampling regime was weekly (during the weekends, starting from Friday evening to Monday morning) and 47 measurements were made throughout the whole evaluation period on five N fertilizer levels, 0, 25, 50, 100 and 125 kg N $ha^{-1}$. For individual measurement from each chamber, a tube connected to the outside of a sampling port was used to sample the gas within the headspace to the PICARRO gas analyser past a solenoid valve **Figure 6**. The PICARRO gas analyser employs the cavity ring-down spectroscopy (CRDS) principle to determine $N_2O$ concentration in parts per billion (ppb). Furthermore, the analyser had to always be connected to a vacuum pump (A2000), which maintained the cavity pressure inside the analyser.

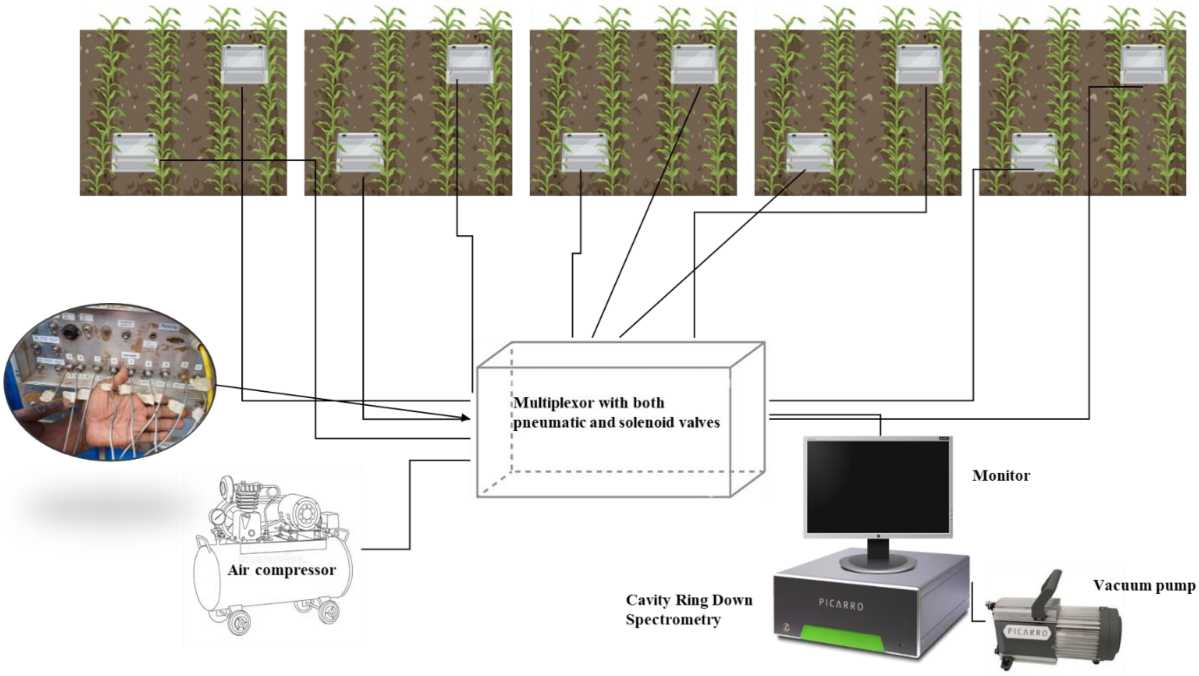


**Figure 6: An automated chamber system schematic**

### iii. Estimation of $N_2O$ fluxes for missing data

During $N_2O$ data collections, there were extended periods with data gaps due to faulty instrumentation. To fill these data gaps, separate imputations were carried out for each chamber using a random forest model in Python to estimate the weekly fluxes during this period. The predictor variables included data on rainfall (mm), soil temperature (°C), moisture content (%), oxygen concentration and fertiliser decay (an exponential decay model with a half-life of ~1 year, accounting for initial application and restart dates). Various measures were used to analyse the performance of the model, which consisted of the determination coefficient (R2), root mean square error (RMSE) and mean absolute error (MAE). The model outputs are shown in **Appendix XVI** to **XX**

**iv. Determination of Daily, Cumulative and Yield-scaled $N_2O$ emissions and the Emission factors**

**a. Determination of $N_2O$ fluxes**

The $N_2O$ fluxes were estimated according to the following equation (Zheng *et al*., 2019b):

$$\boldsymbol{F} = (\Delta \boldsymbol{c} \times \boldsymbol{V_{ch}} \times \boldsymbol{P} \times \boldsymbol{MW_{N_2O}} \times \mathbf{10^{-2}} / \boldsymbol{R} \times \boldsymbol{T} \times \boldsymbol{A_{ch}}) \qquad \textbf{(5)}$$

Where $F$ is the $N_2O$ flux (µg $N_2O$-N $m^{-2}$ $h^{-1}$); $\Delta c$ is the rate of change in the mixing ratio of $N_2O$ in the chamber air ($ppb_v$ $h^{-1}$); $V_{ch}$ is the volume of the chamber ($cm^{-3}$); $P$ is the pressure (atm); $MW$ is the molecular weight of $N_2O$ (28.0134 g $mol^{-1}$); $R$ is the gas constant (0.08206 L atm $mol^{-1}$ $K^{-1}$); $T$ is the temperature (K); and $A_{ch}$ is the base area of the chamber ($cm^2$)

The hourly fluxes (µg $N_2O$-N $m^{-2}$ $h^{-1}$) were then upscaled to daily fluxes (g $N_2O$-N $ha^{-1}$ $d^{-1}$) by multiplying the chamber fluxes by 0.24.

**b. Annual Cumulative $N_2O$ emissions**

The measured and estimated fluxes were used to compute the cumulative annual $N_2O$ emissions for each N application rate using the trapezoidal integration with linear interpolation of fluxes between two sampling times (Zebarth *et al*., 2012). The total summation was then divided by the total number of days of the measurement period and multiplied by 365 (the number of days in a year).

**c. Yield-scaled $N_2O$ emissions (YSE)**

YSE reflects the amount of $N_2O$ emitted per unit of grain yield produced and was calculated as follows:

$$\boldsymbol{YSE = Cum\ N_2O\ fluxes/grain\ yield} \quad \textbf{(6)}$$

Where, *YSE* = yield-scaled $N_2O$ emissions (g $N_2O$ $kg^{-1}$ grain yield; *Cum $N_2O$ fluxes* = annual $N_2O$ fluxes (kg $N_2O$-N $ha^{-1}$ $yr^{-1}$); and *grain yield* (kg $ha^{-1}$)

**d. Emission factors (EF)**

EF represents the proportion of N fertilizer lost as $N_2O$ compared to the background, of each N fertilization level and was estimated using equation **7** (de Klein *et al*., 2020):

$$\boldsymbol{EF}\ (\%) = \left(\frac{\boldsymbol{N_2O_f - N_2O_o}}{\boldsymbol{N_{app}}}\right) \times \boldsymbol{100} \quad \textbf{(7)}$$

Where *EF* = emission factor (%); $N_2O_f$ = annual cumulative $N_2O$ fluxes in the N-fertilised plot (kg $N_2O$-N $ha^{-1}$ $yr^{-1}$); $N_2O_o$ = annual cumulative fluxes in the non-fertilised plot (kg $N_2O$-N $ha^{-1}$ $yr^{-1}$); and $N_{app}$ = amount of N applied in the respective plot (kg N $ha^{-1}$).

### 3.4.3 Meteorological Measurement

Daily atmospheric conditions were measured using two *ATMOS 41 - Meter Group* all-in-one weather stations for the duration of the study. The stations have 12 embedded sensors that measure solar radiation, precipitation, air temperature, relative humidity, atmospheric pressure and wind speed and direction. The weather stations are connected to two ZL6 pro data loggers (METER Group, Inc.-Pullman, WA, USA), which possess a built-in solar panel for extended deployments and offer 15-minute real-time data uploads with automatic cloud data backup. Furthermore, the ATMOS 41 was also connected with soil moisture/temperature (TEROS 11) and oxygen concentration (SO-411) sensors, which extend 15 cm into the soil.

### 3.4.4 Maize harvesting: Grain yield, biomass and dry matter estimation

To estimate the biological yield, the number of plants and maize cobs within the effective sampling area (ESA) of 6 $m^2$ (2 m by 3 m) in each plot was recorded at physiological maturity (195 DAP). The stalks were then cut and weighed in the field, and this weight was used to estimate the aboveground biomass. A subsample was then collected from each plot by chopping two randomly selected stovers and recording their weights (fresh). This was followed by drying in the greenhouse for two weeks to reduce the moisture content before determining the dry weight. The fresh and dry weights were then used to calculate the moisture fraction, which was factored into the dry matter estimation.

Maize cobs from the sampling area were harvested and weighed, then randomly selected subsamples of six cobs (from the largest to the smallest) were collected, and their fresh weight was measured within 24 hours of harvesting. The subsamples were then dried in the greenhouse for three weeks to reach a moisture content of less than 15%. Afterwards, the cobs were shelled, and the grain weight was determined. The yield estimation was calculated using equation **8** (Murrell & Chivenge, 2023):

$$\boldsymbol{Yield\ of the\ ESA\ (kg) = \frac{total\ fresh\ weight\ of\ cobs}{fresh\ weight\ of\ the\ subsamples\ cobs} \times dry\ weight\ of\ grains}$$

$$\boldsymbol{Yield\ (t\ ha^{-1}) = [\left(Yield\ of\ the\ ESA\ area\ \times\ {10000\ m^2}/{6m^2}\right) \div 1000\ kg]} \qquad \textbf{(8)}$$

## 3.5 Laboratory Analysis

### 3.5.1 Sample Preparation

The samples (soil and plant) were air-dried in the greenhouse for two weeks, except for the mineral N soil samples. The air-dried soil was passed through 2 mm and 60 mesh sieves, whereas the dried plant samples were ground to pass through a sieve.

### 3.5.2 Soil Analysis

**a. Chemical Analysis**

The air-dried soil samples underwent chemical analysis for soil pH (in a 1:2.5 soil-water suspension), available phosphorus, organic carbon, and total nitrogen using standard procedures described by Okalebo *et al*. (2002).

**i. Soil pH**

The soil pH was determined on a 2.5:1 soil water suspension ratio (50 ml of distilled water to 20 g air-dry soil). First, the suspension of each sample was stirred for 10 minutes, left to stand for 30 minutes, before shaking again for 2 minutes. The pH of the suspension was then measured using a soil pH meter equipped with a glass electrode.

**ii. Available phosphorus**

The available phosphorus (P) content was measured using extraction followed by colorimetric determination. 50 ml of sodium hydrogen carbonate ($NaHCO_3$) adjusted to pH 8.5 was added to 2.5 g air-dry soil at a ratio of 20:1 soil to extractant solution. The mixture was then stirred for 30 minutes before filtering the suspension. This was followed by a colorimetric determination of soil P in the filtrate by adding 5 ml and 10 ml of 0.8M Boric acid and ascorbic acid, respectively, before topping to the 50 ml mark using distilled water. The final solution was left to stand for an hour before measuring the absorbance at 880 nm using a UV spectrometer. The available P was calculated using the following equation **9**.

$$\boldsymbol{P}\ (\boldsymbol{mg\ kg^{-1}}) = \frac{(\boldsymbol{a}-\boldsymbol{b})\times\boldsymbol{v}\times\boldsymbol{f}\times\mathbf{1000}}{\mathbf{1000}\times\boldsymbol{w}} \quad \textbf{(9)}$$

Where *a* is the P concentration in the sample, *b* is the P concentration in the blank, *v* is the extractant solution volume, *f* is the dilution factor and *w* is the sample weight (2.5 g).

### iii. Soil organic carbon

The soil organic carbon was determined using oxidation and titration methods. A mixture of 0.1 g of air-dried soil (passed through a 0.25 mm sieve), 5 ml of potassium dichromate, and 7.5 ml of concentrated sulfuric acid was placed on a pre-heated block at 155 °C for 30 minutes. The digest sample was then quantitatively transferred to a conical flask with distilled water. Three drops of 1, 10-phenanthroline monohydrate – ferrous sulfate solution (indicator) were added. The solution was titrated against ferrous ammonium sulfate solution, with the endpoint marked by a colour change from green to brown. The soil organic carbon was calculated as shown in equation **10**.

$$\boldsymbol{OC}\ (\%) = \frac{\boldsymbol{T}\times\mathbf{0.2}\times\mathbf{0.3}}{\boldsymbol{w}} \quad \textbf{(10)}$$

Where *T* is the titration volume, given by the difference between the sample and blank titres and *w* is the sample weight

### iv. Soil total nitrogen

Total soil N was determined using the Kjeldahl method, which involves the complete oxidation and subsequent spectrometric analysis. Briefly, 0.3 g of air-dried soil was mixed with 4.4 ml of digestion solution and digested in a block digester at 360 °C for two hours until the solution became clear. The digest was then transferred qualitatively to a 50 ml volumetric flask and topped distilled water up to the mark. The total N content in the aliquot was quantified colorimetrically after adding 5 ml of N1 and N2 reagents to 0.2 ml of the digest sample and absorbance reading at 650 nm using a UV spectrophotometer.

### v. Soil mineral N ($NH_4^+$ and $NO_3^-$)

Ammonium ($NH_4^+$) and nitrate ($NO_3^-$) concentrations in fresh soil samples collected from depths of 0-20, 20-40 and 40-60 cm were determined by extracting the samples with 0.5 M $K_2SO_4$ and subsequent colorimetric analysis at 655 and 419 nm, respectively. The concentration of $NH_4^+$ and $NO_3^-$-N was computed as shown in equation **11**:

$$NH_4^+/NO_3^- - N\ (mg\ kg^{-1}) = \frac{(a-b)\times v\times MCF\times 1000}{w} \quad \textbf{(11)}$$

Where a is the concentration of either $NH_4^+$- and $NO_3^-$-N in the sample solution; b is the concentration of $NH_4^+$- and $NO_3^-$ -N in the blank solution; v is the volume of the extract; MCF is the Moisture Correction Factor; f is the multiplication factor; and w is the weight of the fresh soil.

### vi. Mineral N Intensity

To estimate the magnitude of mineral N accumulated during the entire length of the measurement period, a temporal linear interpolation equation was used (Burton *et al.*, 2008), as shown in equation **12**:

$$NI = \frac{\sum_{i=0}^{n}\{([N]_{i+1}+[N]_i)/2\ \times(t_{i+1}-t_i)\}}{t_n-t_o} \quad \textbf{(12)}$$

Where $NI$ = N intensity (mg d kg$^{-1}$); $N$ = mineral N concentration (mg kg$^{-1}$); $i$ = previous sampling day; $n$ = number of days during the measurement period; $t_i$ = previous sampling day; and $t_{i+1}$ = subsequent sampling day.

### a. Physical analysis

**i. Soil bulk density**

A metal core ring of diameter 5 cm and height 5 cm was driven into the soil surface after initially scraping off 2 cm. The sample was then dried at 105 °C for 48 hours in an oven and recorded the dry weight. The soil bulk density was then calculated using equation **13**:

$$\rho_s(g\ cm^{-3}) = \frac{M_s}{V_t} \quad \textbf{(13)}$$

Where $M_w$ is the Mass of water (g), given by the difference between the mass of the core ring + fresh soil and mass of the core ring + dry soil; $M_s$ is the mass of the dry soil (g); $\rho_s$ is the soil bulk density and $V_t$ is the total volume of the soil.

**ii. Soil particle size analysis**

The proportion of sand, silt and clay was determined using the hydrometer method, where 50 g of soil saturated with water was dispersed using 10 ml of 10% sodium hexametaphosphate solution and left to stand for 10 minutes. This was followed by transferring the solution into a dispersing cup and stirring for 2 minutes using an electric stirrer. The suspension was thereafter transferred into a 1000 ml measuring cylinder and topped up to 1130 ml using water after inserting the hydrometer. Further, the suspension was mixed by inverting the cylinder 10 times before recording the hydrometer and temperature readings at 40 seconds (H1 and T2, respectively). A repeat of inverting the cylinder 10 times was done and the cylinder was left to stand for two hours undisturbed before recording the hydrometer and temperature readings (H2 and T2, respectively). The temperature readings were used in correcting the hydrometer readings at both times, 40 seconds and two hours. The proportions of individual particles were calculated as follows:

$$\boldsymbol{Sand}\ \% = \frac{(a-b)}{a} \times \mathbf{100} \quad \textbf{(14)}$$

$$\boldsymbol{Clay}\ \% = \frac{c}{a} \times \mathbf{100} \quad \textbf{(15)}$$

$$\boldsymbol{Silt}\ \% = \mathbf{100} - (\boldsymbol{sand}\ \% + \boldsymbol{clay}\ \%) \quad \textbf{(16)}$$

Where a is the weight of the soil (50 g), b is the hydrometer reading at 40 seconds, c is the hydrometer reading at two hours.

**iii. Soil moisture content**

The soil moisture content was determined gravimetrically by weighing 20 g of a fresh soil sample and drying in an oven at 105 °C for 24 hours. The soil moisture content was then used to calculate the moisture correction factor for estimating soil mineral N concentration. The calculation was as follows:

$$\boldsymbol{\omega} = \frac{\boldsymbol{M_w}}{\boldsymbol{M_s}} \quad \textbf{(17)}$$

$$\boldsymbol{MCF} = \frac{\mathbf{1} - \boldsymbol{\omega}}{\mathbf{1}} \quad \textbf{(18)}$$

Where ω is the gravimetric water content; $M_w$ is the mass of water, g (computed by the difference between the mass of fresh soil and dry soil; $M_s$ is the mass of dry soil, g and *MCF* is the moisture correction factor

### 3.5.3 Plant tissue analysis

Dried tissue samples of leaves, grain and stover were ground to pass through a 60-mesh sieve, followed by N content analysis. The N content analysis employs the principles of the Kjeldahl method, which involves oxidation followed by colorimetric determination. The ear leaf, grain and stover samples were digested at 360 °C for 2 hours with concentrated sulphuric acid in the presence of lithium sulfate, a catalyst (selenium powder), and hydrogen peroxide, which oxidizes the organic matter. The concentration of N in the digest was then determined colorimetrically using a UV spectrophotometer at a wavelength of 650 nm (Okalebo *et al*., 2002).

The N content was then used to calculate N uptake by the grain and the whole plant, as illustrated below:

$$\boldsymbol{GNU} = \boldsymbol{Y} \times \boldsymbol{N}\ (\%) \quad \textbf{(19)}$$

$$\boldsymbol{TNU} = \boldsymbol{DM} \times \boldsymbol{N}(\%) \quad \textbf{(20)}$$

Where *GNU* = Grain N uptake (kg ha$^{-1}$); *Y* = Grain yield (kg ha$^{-1}$); *N* = N content (%); *TNU* = Total plant N uptake (kg ha$^{-1}$); and *DM* = Dry matter (stover + grain weight, kg ha$^{-1}$).

### 3.6 Nitrogen Use Efficiency (NUE)

The N concentration in maize tissues was used to calculate different aspects of nutrient use efficiencies (NUE) according to the equations shown below (Dobermann, 2007; Congreves *et al*., 2021; Govindasamy *et al*., 2023):

**i. Recovery efficiency**

This is the relative increase in N uptake by the plant per unit of N applied, with acceptable ranges of 0.30 and 0.50 kg kg$^{-1}$ N.

$$\boldsymbol{RE_{FertN}} = \frac{\boldsymbol{TNU_N - TNU_o}}{\boldsymbol{N_{app}}} \quad \textbf{(21)}$$

**ii. $\mathbf{NUE_{grain}}$**

This is the proportion of N fertilizer allocated to yield, in this case. $NUE_{crop}$ values of > 1 and < 1 denote net removal and surplus, respectively.

$$\boldsymbol{NUE_{grain}} = \frac{\boldsymbol{GNU}}{\boldsymbol{N_{app}}} \quad \textbf{(22)}$$

**iii. Physiological efficiency**

This is the fraction of plant N that is converted to yield, while also accounting for yield and uptake in the non-fertilised plot. The optimum ranges lie between 30 and 60 kg kg$^{-1}$

$$\boldsymbol{PE} = \frac{\boldsymbol{Y_N - Y_O}}{\boldsymbol{TNU_N - TNU_O}} \quad \textbf{(23)}$$

**iv. Agronomic efficiency**

This is the relative yield increase per unit of N applied and ranges between 10 and 30 kg grain yield kg$^{-1}$ N

$$AE = \frac{Y_N - Y_O}{N_{app}} \quad \textbf{(24)}$$

**v. Partial factor productivity**

This is the expression of yield per unit of N fertiliser applied

$$PFP = Y/F \ or \ (Y_o/F) + AE \quad \textbf{(25)}$$

**vi. Partial N balance**

This is the ratio of plant N content to the amount of N fertiliser applied. A value of > 1 indicates N mining, while < 1 shows surplus N supply.

$$PNB = TNU/N_{app} \quad \textbf{(26)}$$

Where $RE_{FertN}$ is the recovery efficiency of the N fertilizer applied (kg kg$^{-1}$ N; $TNU_N$ is the total plant N uptake in the fertilized plot (kg kg$^{-1}$); and $TNU_O$ is the total N uptake in the control plot (kg kg$^{-1}$); $NUE_{crop}$ is the nitrogen use efficiency; *PE* is the physiological efficiency (kg grain yield kg$^{-1}$ N); $Y_N$ is the yield of the N fertilized plot; $Y_O$ is the yield of the non-fertilized plot; *AE* is the agronomic efficiency and *PFP* is the partial factor productivity.

**3.7 Statistical Analysis**

Data were analysed using R statistical software version 4.5.0 (R Core Team, 2025). A Linear mixed effects model (*lme)* (Bates *et al*., 2015) was adopted to evaluate the effects of N application rates on the Nmin variables at each depth during the growing and fallow periods. Where N rates and depth were fixed effects, whereas replicates and sampling time were treated as random effects to get the random intercept and slope of each plot due to the seasonal effect of sampling time. A one-way ANOVA was used to determine the effects of N application rate on grain and biomass yield, grain N, grain and biomass N uptake, N harvest index and the NUE indices. Thereafter, the means were separated at 5% level of significance. To better capture the relationship between Nmin (variables) and environmental factors, Pearson correlation coefficients were determined to identify the regulating factors.

# CHAPTER FOUR

# RESULTS

## 4.1 Initial soil characteristics

The initial soil characteristics of the experimental site are presented in Table . In general, the upper soil layer (0-20 cm) exhibited higher nutrient concentrations compared to the subsequent depths, except for the soil pH, which increased with increasing depth. The soil pH was strongly acidic (4.84) with adequate organic carbon (1.92%), sufficient available phosphorus and $NO_3^-$ - (17.38 and 22.41 mg $kg^{-1}$, respectively) and low total N (0.1%) and Ammonium-N (1.55 mg $kg^{-1}$).

At the 20-40 cm depth, a similar trend to the surface horizon was observed, with the soil pH being strongly acidic (4.91), moderate organic carbon (1.9%), and sufficient available phosphorus (10.29 mg kg-1) and Nitrate-N (14.83 mg $kg^{-1}$). A low concentration of $NH_4^+$-N (1.1 mg $kg^{-1}$) and total N (0.08%) was also exhibited at this depth. In contrast to the soil pH in the preceding depths, soil pH in the deeper layer, 40-60 cm, was moderately acidic (5.14), with inadequate organic C (1.45%) and sufficient $NO_3^-$ -N (10.54 mg $kg^{-1}$). Whereas, total N, available P and $NH_4^+$-N concentrations were all insufficient, 0.07%, 5.39 and 1.36 mg $kg^{-1}$, respectively. The soil textural class across the three depths was classified as Sandy clay loam, Sandy clay and Clay for 0-20, 20-40 and 40-60 cm, respectively.

**Table 2: Initial soil characterization; selected physical and chemical properties of soils at 0-20, 20-40 and 40-60 cm depths**

| | Soil Depth | | |
|---|---|---|---|
| **Soil parameter** | **0-20 cm** | **20-40 cm** | **40-60 cm** |
| **pH (1:2.5 water)** | 4.84 | 4.91 | 5.14 |
| **Organic C (%)** | 1.92 | 1.9 | 1.45 |
| **Total N (%)** | 0.1 | 0.08 | 0.07 |
| **Available P (Olsen) (mg $kg^{-1}$)** | 17.38 | 10.29 | 5.39 |
| **$NO_3^-$-N (mg $kg^{-1}$)** | 22.41 | 14.83 | 10.54 |
| **$NH_4^+$-N (mg $kg^{-1}$)** | 1.55 | 1.1 | 1.36 |
| **Texture** | | | |
| **Sand (%)** | 54 | 46 | 40 |
| **Clay (%)** | 28 | 40 | 40 |
| **Silt (%)** | 18 | 14 | 20 |
| **Textural class** | **Sandy clay loam** | **Sandy clay** | **Clay** |

**4.2 Meteorological data**

Figure 7 shows the precipitation and soil moisture and temperature data obtained during the study period. The total rainfall received during the evaluation period amounted to 1131.1 mm, with 843.3 mm during the maize growing season and 287.9 mm in the fallow period. The highest cumulative rainfall was received during the initial growing stages (42 DAP), which accounted for 38.7% (326.2 mm) of the total growing season rainfall. This data was further subset into cumulative and average values between each consecutive sampling time for correlation analysis with select soil chemical properties variables.

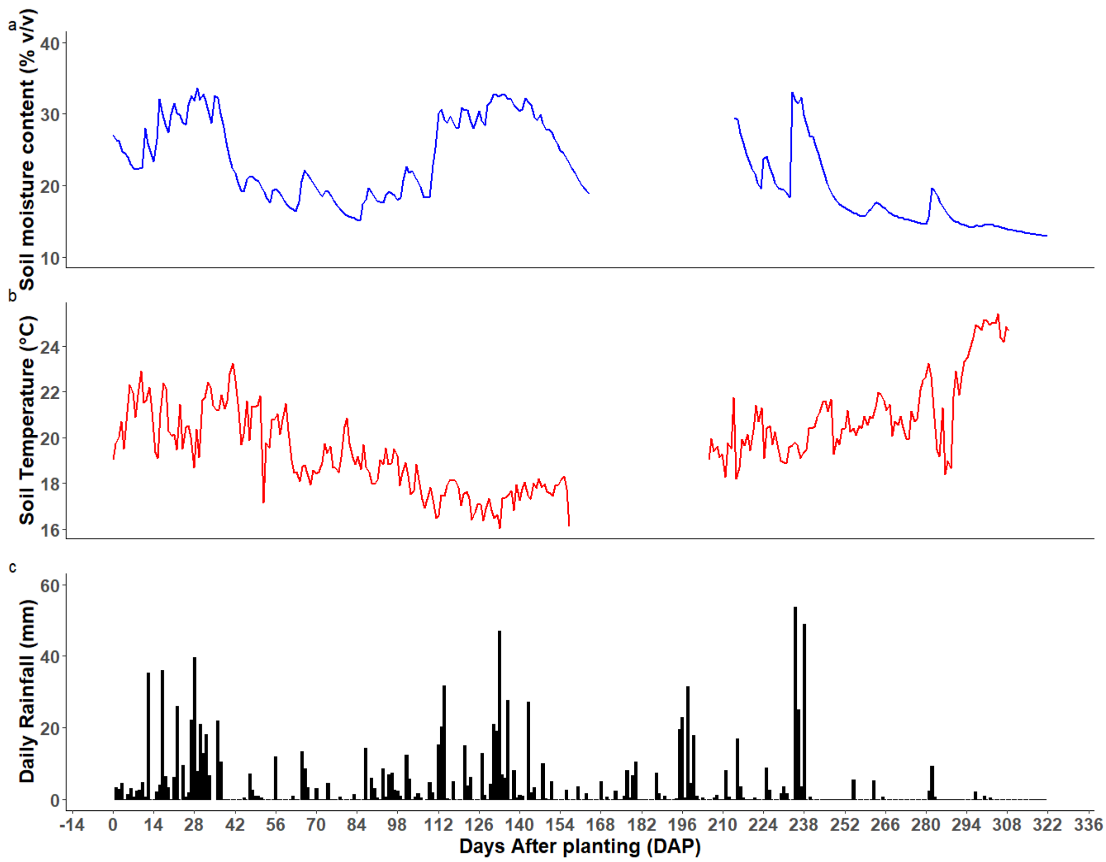


**Figure 7: Daily rainfall distribution, mean soil moisture content (volumetric) and temperature (0-15 cm) of the study site measured from 4 Apr. 2024 to 27 Feb. 2025**

### 4.3 The effect of inorganic nitrogen fertilizer application on soil N dynamics

#### 4.3.1 Soil Mineral N pool

**a. Soil $NO_3^-$-N concentration**

The overall trend of $NO_3^-$-N concentration and its vertical distribution along the soil profile is shown in **Figure 8**. Generally, the $NO_3^-$-N levels increased after the initial fertiliser application at planting, with a sharp rise and peaked at 14 days after planting (DAP). Meanwhile, the increase in the 20–40 cm depth was more gradual and later peaked at 42 DAP. However, no increase was observed at 40–60 cm during early growth stages, though it surprisingly peaked at 127 DAP, which was isolated. These peaks were mostly short-lived and were followed by rapid declines, consistent across all the depths as the crop-growing season progressed. A convergence of $NO_3^-$-N levels among the N rates was observed at harvest across all depths (195 DAP). In contrast, concentrations in the 0–20 cm and 20–40 cm layers were lower than the initial levels before planting, with no notable difference observed in the 40–60 cm depth.

On average, $NO_3^-$-N concentrations in the lower depths for both N-fertilized and control plots remained low during the growing season, indicating minimal downward movement. After harvest, notable spikes in $NO_3^-$-N concentrations were evident, especially in plots with 100 and 125 kg N $ha^{-1}$, and this pattern was consistent across all depths.

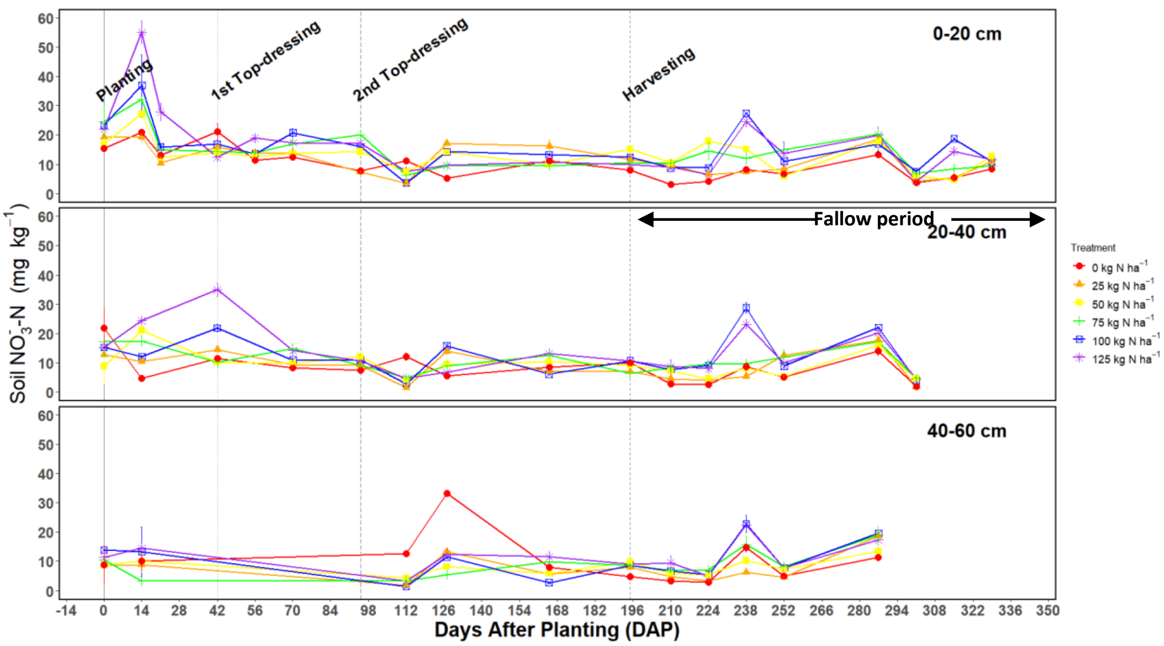


**Figure 8: Temporal distribution of soil $NO_3^-$-N along the soil profile, as influenced by N application rates throughout the maize-growing and fallow periods. Each point represents an average of the three replicates for each given treatment, and the error bars are the standard error of means (n = 3)**

**b. Soil $NH_4^+$ -N concentration**

Soil $NH_4^+$-N exhibited high variability across all depths, particularly during the initial stages of maize growth, with multiple peaks observed following each N application

(**Figure 9**). At the surface layer, the increase in soil $NH_4^+$ concentration was gradual, before later peaking at 21 DAP (24.8 mg $NH_4^+$-N $kg^{-1}$) and was immediately followed by a drop in concentration. The subsequent and final peaks were observed at 70 and 112 DAP in the 125 kg N $ha^{-1}$ plot (30.24 and 26.61 mg $NH_4^+$-N $kg^{-1}$, respectively). Generally, the peaks alternated between 100 and 125 kg N $ha^{-1}$ N application, particularly in the 0 – 20 cm depth. This was followed immediately by a sharp decrease in the $NH_4^+$-N concentration, consistent among all N fertilizer rates and remained below 12 mg $NH_4^+$-N $kg^{-1}$ for the remainder of the cropping season. Eventually, the observed $NH_4^+$-N concentrations converged during harvesting.

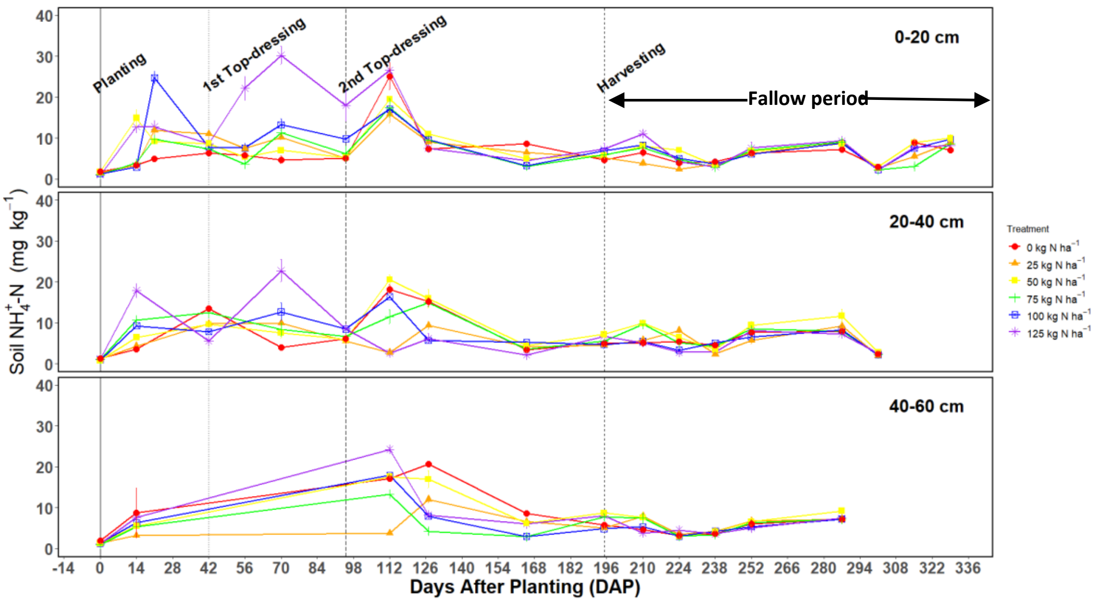


**Figure 9: Temporal distribution of soil $NH_4^+$-N along the soil profile, as influenced by N application rates throughout the maize-growing and fallow periods. Each point represents an average of the three replicates for each given treatment, and the error bars are the standard error of means (n = 3)**

In the 20 – 40 cm depth, an identical pattern to the upper layer was observed, with multiple peaks observed at 14 (17.96 mg $kg^{-1}$), 70 (22.78 mg $kg^{-1}$) and 112 DAP (20.59 mg $kg^{-1}$), which corresponded with N fertilizer application events and alternated between 50 and 125 kg N $ha^{-1}$. Meanwhile, in the 40 – 60 cm depth, the increase was gradual, with delayed peaks observed at 112 and 127 DAP. However, the highest concentration (24.27 mg $kg^{-1}$) was observed in the 125 kg N $ha^{-1}$ plot at 112 DAP. At harvesting, there was no disparity in the $NH_4^+$-N content among the N-fertilised and non-fertilised plots, which varied from 4.57 to 7.23 mg $kg^{-1}$. During the fallow period, the $NH_4^+$-N concentrations mostly converged and showed no differences between the observations.

### c. Soil mineral N intensity

The influences of different N application rates on the time-weighted annual soil Nmin variables are shown in **Figure 10**. The soil Nmin annual intensities ($NO_3^-$, $NH_4^+$ and the sum of $NH_4^+ + NO_3^-$) down the soil profile increased with N application rates ($p < 0.05$). The $NO_3^-$-N intensity varied considerably across the three depths, from 10.87 to 16.88, 10.04 to 18.06 and 8.99 to 14.26 mg $NO_3^-$-N d $kg^{-1}$ in the 0 – 20, 20 – 40 and 40 – 60 cm, respectively.

The $NH_4^+$-N intensity increased linearly in the surface layer across the N rates, ranging from 7.65 to 12.03 mg $NH_4^+$-N d $kg^{-1}$. Whereas, in the 20 – 40 and 40 – 60 cm depths, the increase was polynomial, with values ranging between 7.67 and 10.58 and 6.93 and 12.75 mg $NH_4^+$-N d $kg^{-1}$, respectively, across the different N rates. The plot with a 125 kg N ha-1 application rate exhibited the largest magnitude of N (sum of $NH_4^+ + NO_3^-$) intensity across the 0–20 cm (28.91 mg N d kg-1) and 20–40 cm (27.36 mg N d kg-1) depths, in contrast to the other N rates. Surprisingly, the non-fertilised plot had the highest intensity in the deeper depth (27.01 mg N d $kg^{-1}$) compared to the rest of the fertilizer plots, which averaged 20.51 mg N d $kg^{-1}$.

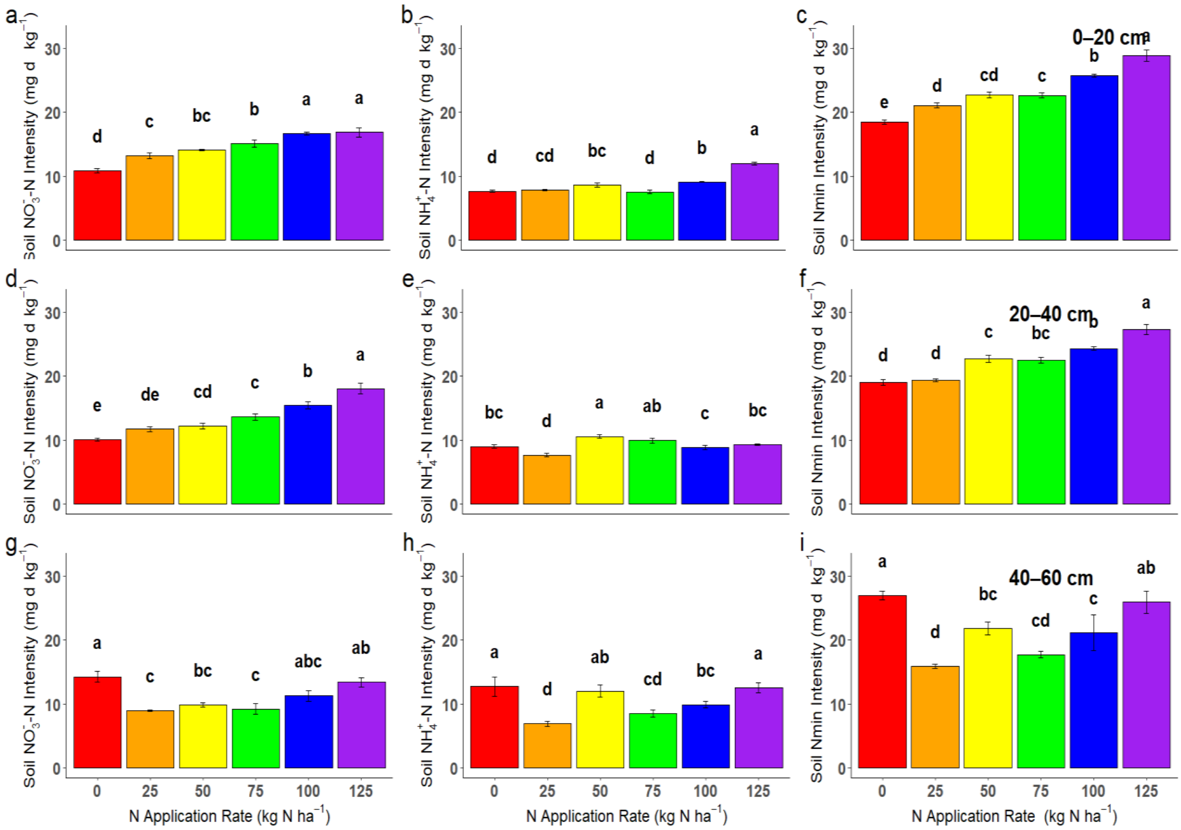


**Figure 10: Time-weighted soil Nmin intensities ($NO_3^-$-, $NH_4^+$-N and sum ($NO_3^-$ + $NH_4^+$) across 0-20 cm (a to c), 20-40 cm (d to f) and 40-60 cm (g to i) as influenced by N application rates. Different letters indicate significant differences (p<0.05) based on the LSD test after a one-way ANOVA. The error bars are the standard error of means, n = 3**

### 4.3.2 Increasing N application rates effect on $N_2O$ Emissions

#### i. $N_2O$ fluxes

Temporal $N_2O$ fluxes across different N application rates are shown in **Figure 11**. The $N_2O$ fluxes ranged from 2 to 20.65 µg $N_2O$-N m$^{-2}$ h$^{-1}$ throughout the entire period. Consistently lower $N_2O$ fluxes were observed at 50 kg N ha$^{-1}$ application level. In contrast, the 100 kg N ha$^{-1}$ level showed higher fluxes early in the season, peaking four weeks after the initial fertilizer application (**Figure 11**). These fluxes then decreased as the season progressed into the late vegetative growth stage. Immediately after the second top dressing, $N_2O$ fluxes spiked, with the highest levels in the 100 and 125 kg

N ha$^{-1}$ plots compared to lower fertilization levels. By the end of the growing season, the high $N_2O$ fluxes in the 125 kg N ha$^{-1}$ had returned to background level. During the fallow period, a resurgence in the fluxes was observed, especially in plots receiving higher N rates; meanwhile, the plots with lower fertilization maintained significantly lower fluxes.

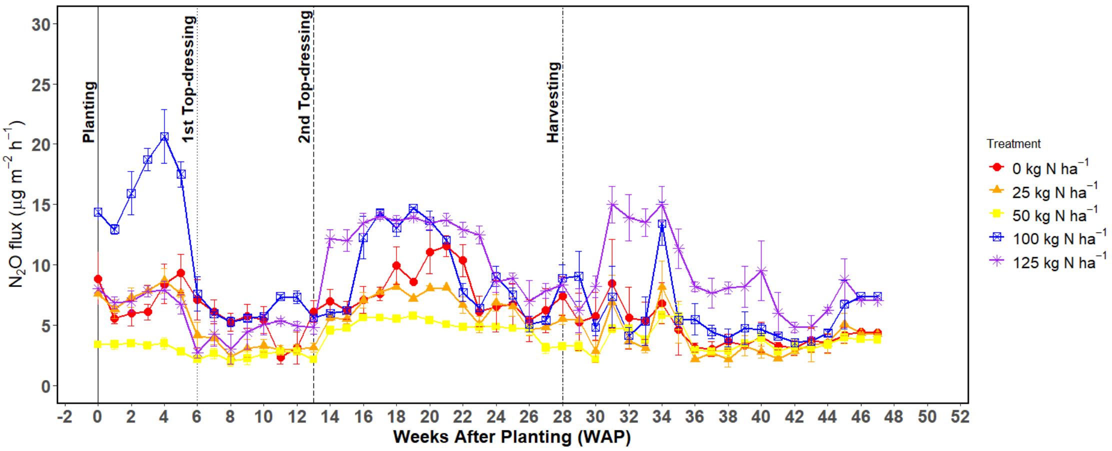


**Figure 111: Temporal $N_2O$ fluxes as influenced by N application rates from 04 Apr. 2024 to 27 Feb. 2025**

### ii. Daily and annual $N_2O$ fluxes, Emission factors and yield-scale emissions

The annual fluxes ranged between 0.33 and 0.77 kg $N_2O$-N ha$^{-1}$ across the different N application rates, with an average of 0.56 kg $N_2O$-N ha$^{-1}$. Negative emission factors were observed in the N application rates of 25 and 50 kg N ha$^{-1}$; meanwhile, the EFs in both 100 and 125 kg N ha$^{-1}$ did not show any difference (0.2%). Similar observations were also made in the yield-scaled emissions, with a minimum-maximum of 0.07 to 0.14 g $N_2O$-N kg$^{-1}$ grain yield.

**Table 3: Mean and annual $N_2O$ fluxes, Emission factors and yield-scale emissions as influenced by N application rate**

| N application rate (kg N $ha^{-1}$) | Mean flux (g $N_2O$-N $ha^{-1}$) | Annual fluxes (kg $N_2O$-N $ha^{-1}$) | Emission factors (%) | Yield-scaled emission (g $N_2O$-N $kg^{-1}$ grain yield) |
|---|---|---|---|---|
| 0 | 1.44 | 0.53 | - | 0.14 |
| 25 | 1.21 | 0.44 | -0.34 | 0.1 |
| 50 | 0.91 | 0.33 | -0.39 | 0.07 |
| 100 | 2.00 | 0.73 | 0.2 | 0.14 |
| 125 | 2.11 | 0.77 | 0.2 | 0.14 |

### 4.3.3 Relationship between soil Nmin variables, meteorological factors and other soil properties

**Figure 12** presents the magnitude and direction of correlation among soil variables (soil moisture, temperature, and pH), precipitation variables (cumulative rainfall and average rainfall), and soil Nmin variables ($NO_3^-$ and $NH_4^+$-N) during the maize growing season, analysed using Pearson correlation analysis at each depth. At the surface depth, precipitation variations significantly influenced soil moisture content and temperature. For instance, robust positive relationships were observed between the average precipitation and average soil moisture content ($r = 0.95$, $p < 0.001$) as well as between the mean soil temperature and $NO_3^-$-N concentration across all treatments ($r = 0.45$, $p < 0.001$). Conversely, $NH_4^+$-N showed a non-significant weak negative correlation with the average soil temperature ($r = -0.11$, $p > 0.05$) and soil pH ($r = -0.14$, $p > 0.05$), across all N application rates. In the 20-40 cm depth, $NO_3^-$-N was positively correlated with the average precipitation ($r = 0.37$, $p < 0.01$), soil moisture content ($r = 0.36$, $p = 0.01$) and negatively with soil pH ($r = 0.19$, $p < 0.05$), across all N application rates. Meanwhile, $NH_4^+$-N was negatively correlated with the soil moisture content and pH ($r = -0.33$, $p < 0.05$; $r = 0.3$, $p < 0.05$, respectively) across all N application rates. Furthermore, the magnitude of the relationship between $NH_4^+$-N and average precipitation was weaker ($r = -0.12$, $p < 0.01$). In the deepest layer, 40-60 cm, a similar trend of a positive relationship between the average precipitation and $NO_3^-$-N concentration was observed ($r = 0.41$, $p < 0.05$), along with a negative correlation between soil pH and $NH_4^+$-N ($r = 0.40$, $p < 0.05$). In this depth, the correlation between soil $NO_3^-$ -N and soil pH was more pronounced ($r = -0.47$, $p < 0.05$).

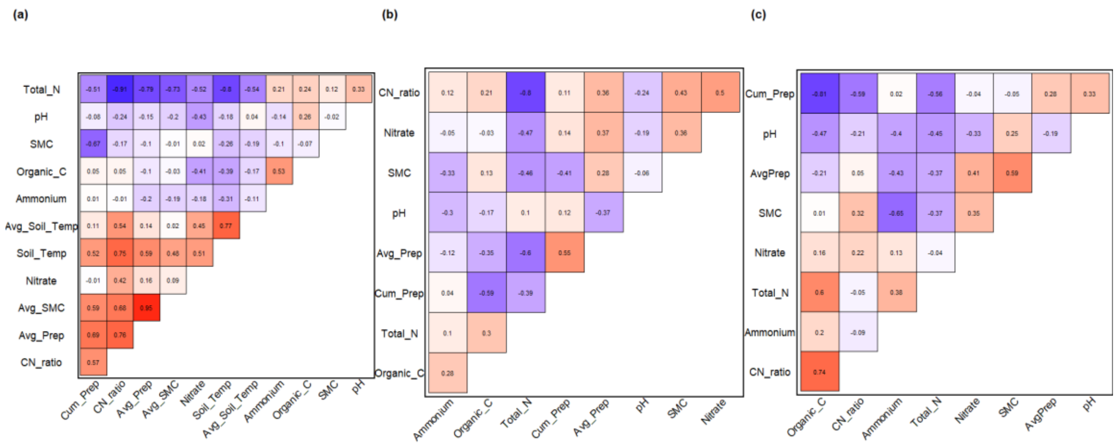


**Figure 12: Relationship between soil variables and micrometeorological factors across different N application rates and depth ((a) 0-20 cm, (b) 20-40 cm and (c) 40-60 cm). Cum_Prep, cumulative precipitation between each sampling (mm); AvgPrep, average precipitation between each sampling (mm); Avg_Soil_Temp, the average soil temperature between each sampling (°c); Soil_Temp, soil temperature of each sampling day (°C); SMC, gravimetric soil moisture content at each sampling day (%); Avg_SMC, average volumetric soil moisture content between consecutive sampling (%); $NO_3^-$ -N, soil nitrate-N (mg $kg^{-1}$); $NH_4^+$-N, soil ammonium-N (mg $kg^{-1}$)**

### 4.3.4 Relationship between soil N intensity and $N_2O$ emission

The relationship between annual cumulative $N_2O$ fluxes and mineral N intensity were examined across all the N application rates (**Figure 13**). The $N_2O$ fluxes increased exponentially with increase in $NO_3^-$ intensity ($r^2 = 0.94$) and total mineral N intensity ($r^2 = 0.69$), meanwhile, the fluxes increased linearly with increasing $NH_4^+$ concentration.

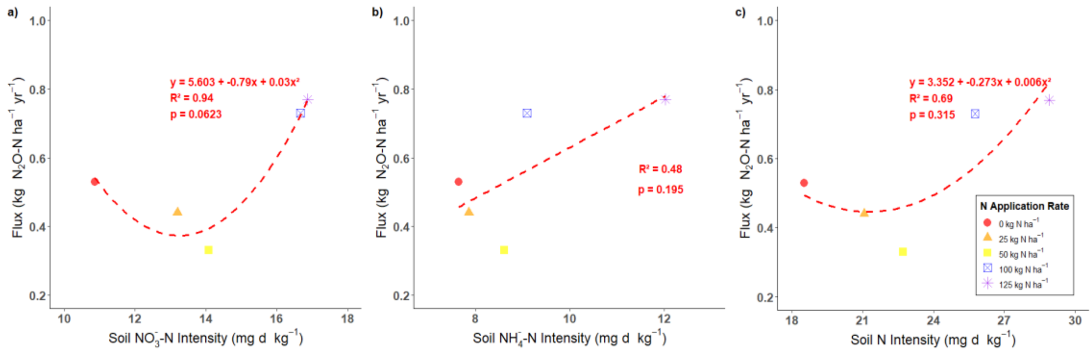


**Figure 13: Relationship between cumulative $N_2O$ fluxes and mineral N intensity**

### 4.4 Effect of inorganic nitrogen fertilizer application on maize grain yield and nitrogen use efficiency

#### 4.4.1 Maize grain yield, and above-ground dry matter, grain N content and N uptake

Maize grain yield and dry matter responded positively to increased N application rate ($p < 0.05$, Figure 14). An N application rate of 125 kg N ha$^{-1}$ exhibited the highest grain yield (5.4 t ha$^{-1}$), while the lowest grain yield was recorded in the 0 kg N ha$^{-1}$ (3.69 t ha$^{-1}$), which represented a 50% increase. However, there was no significant difference between 100 and 125 kg N ha$^{-1}$, indicating that the grain yield peaked at the former application rate and plateaued. Therefore, increases in N fertilizer beyond 100 kg N ha-1 do not significantly improve the grain yield. This trend was also consistent in the above-ground biomass, where 100 kg N ha$^{-1}$ exhibited the largest biomass yield (10.85 t ha$^{-1}$), with no significant difference between 75, 100 and 125 kg N ha$^{-1}$. Additionally, maize grain yield responded positively with increasing dry matter ($r^2 = 0.62$, $p < 0.05$), illustrated in **Figure 15**.

The N uptake was higher for N-fertilized plants relative to the non-fertilized plants, with uptake ranging between 58 and 92 kg ha$^{-1}$ in the non-fertilized and 125 kg N ha$^{-1}$, respectively. Nevertheless, increasing the N application rate did not affect the average harvest index (HI) ($p > 0.05$), which ranged between 0.31 and 0.34 and averaged 0.33 kg grain $kg^{-1}$ dry matter.

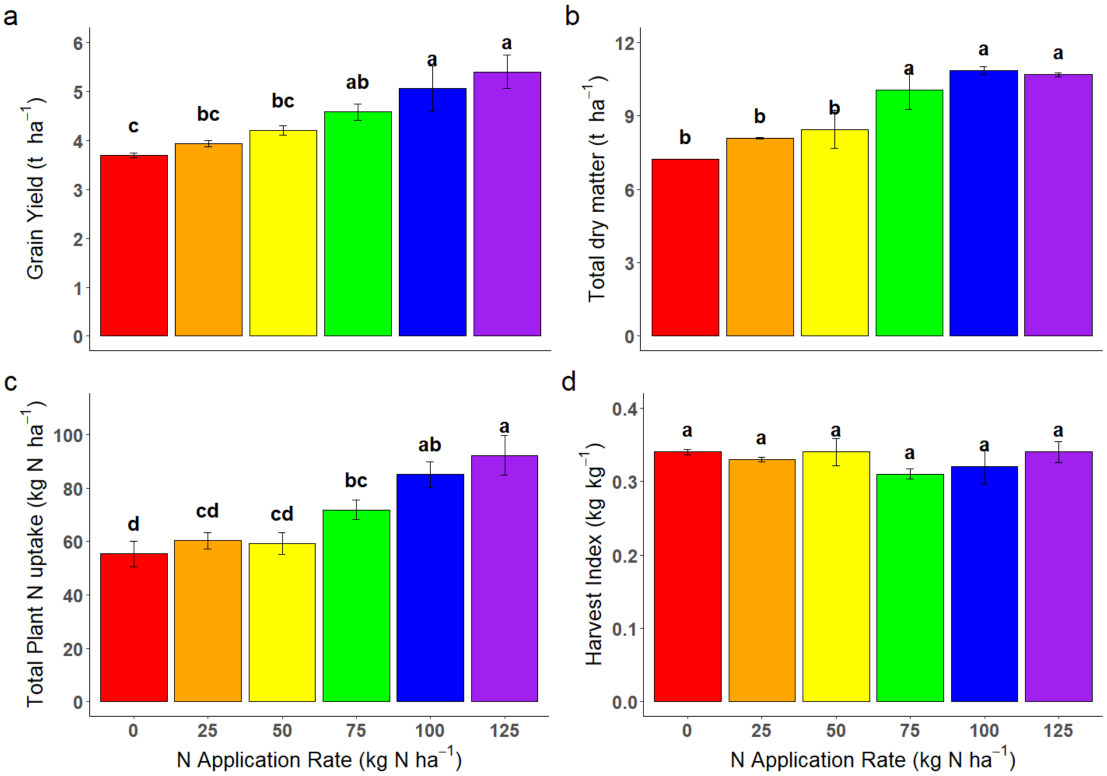


**Figure 14: The effects of N application rates on various plant responses at physiological maturity (195 days after planting): a) Grain yield (t $ha^{-1}$); b) Total above-ground dry matter (t $ha^{-1}$); c) Total above-ground N uptake (kg N $ha^{-1}$); and d) N harvest index (%). Standard errors of the mean and letters refer to statistical differences ($p < 0.05$) among the N-fertilizer (n=3)**

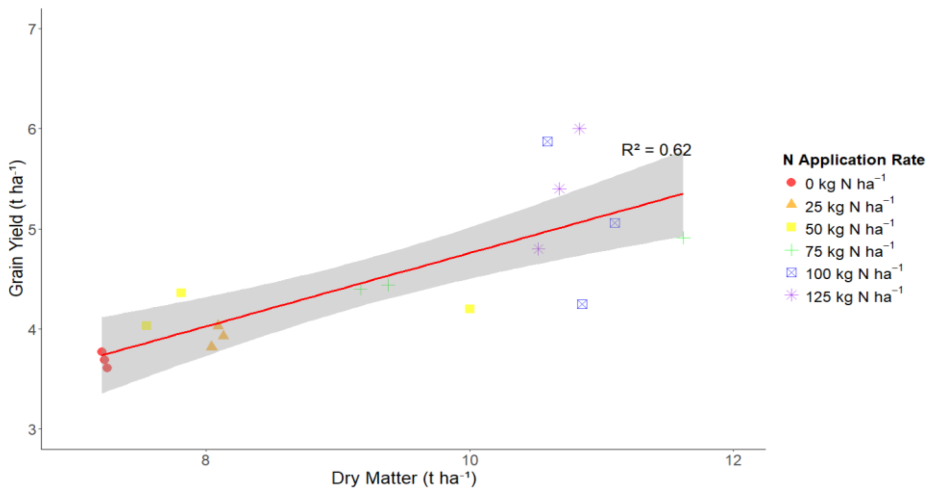


**Figure 15: Relationship between dry matter and grain yield**

### 4.4.2 Nitrogen use efficiency indices

Table shows the various nitrogen use efficiency (NUE) indices at harvesting. Increasing N application significantly influenced $NUE_{grain}$, partial factor productivity (PFP), partial N balance (PNB), and physiological efficiency (PE) ($p < 0.05$) but not the agronomic efficiency (AE) and recovery efficiency (RE). The NUE was highest in the 25 kg N $ha^{-1}$ treatment (1.20) and decreased linearly with increasing N application rates to 0.37 in the 125 kg N $ha^{-1}$ treatment. A similar trend was also observed for PFP and PNB. Meanwhile, the PE increased with N application rate, and peaked at 75 kg N $ha^{-1}$ (55.94 kg $kg^{-1}$) before slightly reducing as N application rate increased to 125 kg N $ha^{-1}$. Moreover, no effect of N application rate was observed on RE ($p > 0.05$).

**Table 4: NUE indices at harvest as influenced by N application rates. (Matching lowercase letters indicate non-significant differences at p < 0.05)**

| N application rate | $NUE_{grain}$ | PFP | PNB | PE | AE | RE |
|---|---|---|---|---|---|---|
| | | (kg $kg^{-1}$) | | | | |
| 25 kg N $ha^{-1}$ | 1.20[a] | 157.07[a] | 2.41[a] | 29.23[b] | 9.47[a] | 0.31[a] |
| 50 kg N $ha^{-1}$ | **0.64[b]** | **83.93[b]** | 1.18[b] | 29.06[b] | 10.13[a] | 0.23[a] |
| 75 kg N $ha^{-1}$ | **0.50[b]** | 61.11[c] | **0.96[c]** | **55.94[a]** | 11.91[a] | 0.22[a] |
| 100 kg N $ha^{-1}$ | 0.43[cd] | 50.60[d] | 0.85[cd] | 43.26[ab] | **13.70[a]** | 0.30[a] |
| 125 kg N $ha^{-1}$ | 0.37[d] | 43.20[d] | 0.74[d] | 46.58[ab] | 13.68[a] | 0.30[a] |
| **LSD (0.05)** | 0.12 | 10.16 | 0.22 | 18.74 | 10.16 | 0.17 |
| **$SE_m$ (±)** | 0.016 | 1.39 | 0.03 | 2.57 | 1.39 | 0.02 |
| **F-probability** | <0.001 | <0.001 | <0.001 | 0.04 | 0.81 | 0.64 |
| **Overall mean** | **0.63** | **79.18** | **1.12** | **40.82** | **11.78** | **0.27** |

# CHAPTER FIVE

# DISCUSSION

## 5.1 N application effect on soil mineral N variables

The soil Nmin pool in terrestrial ecosystems is highly dynamic, as the interplay between N inputs, biogeochemical processes, and meteorological factors majorly influences it (Ferraz-Almeida, 2024). In this study, a rapid increase in soil Nmin ($NO_3^-$ and $NH_4^+$) was observed shortly after the application of N fertilizer. These results are consistent with findings from other studies that reported a similar trend in Nmin increase shortly after fertilizer application (Gentile *et al*., 2009; Mucheru-Muna *et al*., 2009; Mugwe *et al*., 2011; Tully *et al*., 2016). Urea, the source of N, undergoes hydrolysis within the first seven days after application (Motasim *et al*., 2024) upon contact with water, and is quickly transformed into $(NH_4)_2CO_3$ in the presence of the urease enzyme. The $(NH_4)_2CO_3$ further dissociates to form $NH_4^+$ and $CO_3^{2-}$ ions, as shown in the equation below:

$$(\mathbf{NH_2})_2\mathbf{CO} + \mathbf{2H_2O} \rightarrow (\mathbf{NH_4})_2\mathbf{CO_3} \rightarrow \mathbf{2NH_4^+} + \mathbf{CO_3^{2-}} \quad \mathbf{(27)}$$

In soils, the $NH_4^+$ ion is either absorbed by plants or quickly oxidized to $NO_3^-$ through a two-step microbial process known as nitrification (Govindasamy *et al*., 2023). Although nitrification rates were not measured in the current study, a higher $NO_3^-$ -N concentration relative to the $NH_4^+$ in the surface layer demonstrates rapid nitrification. This was also illustrated by $NO_3^-/NH_4^+$ ratio of > 1 (**Appendix XI**), indicating an open N cycle and potential risk of $NO_3^-$ loss down the soil profile (Soilueang *et al*., 2023).

The enhanced N availability earlier in the season, especially in plots where 125 kg N ha$^{-1}$ was applied, elevated the potential for N loss from the topsoil, as indicated by increased $NO_3^-$-N content in the subsequent depth of 20-40 cm, 42 DAP (**Figure 8**). The higher $NO_3^-$-N concentration in the 20-40 cm depth could have resulted from the downward movement of NO3-, which was facilitated by the high soil moisture content resulting from increased rainfall during the early growing period. The increased soil $NO_3^-$-N concentration at this depth (20-40 cm) signifies an asynchrony between N supply and crop uptake, especially during the early growing period when the N demand is less compared to the latter stages of maize growth (Sinclair & Rufty, 2012). This was well captured in the study, as illustrated by the constant concentration of Nmin content for the remainder of the growing season (**Figure 8**).

Unlike $NO_3^-$, $NH_4^+$ is immobile in the soil; however, a sharp increase in the lower depths after each N fertilizer application was observed in the present study. This may be attributed to the increased soil moisture due to precipitation and the shading effect provided by the maize canopy, which likely reduced moisture loss via evaporation. The percolating water and high soil moisture might have aided in diffusing urea down the soil profile, facilitating hydrolysis and the subsequent dissociation of $(NH_4)_2CO$, resulting in greater $NH_4^+$ concentration (Motasim *et al*., 2024), particularly after application. During the latter stages of the crop growing season, no significant variations in both $NO_3^-$- and $NH_4^+$-N content were observed among the N rates across the three soil depths. This could have resulted from Nmin exhaustion by the maize crop and the Nmin returning to background concentration. Despite this, notable spikes in Nmin were observed during the fallow period and this could be attributed to decomposition and mineralisation of soil organic carbon.

Generally, the topsoil exhibited higher Nmin ($NO_3^-$ and $NH_4^+$) content than the lower depths. This was further illustrated by low Nmin concentration in N-fertilized plots during the reproductive stage to the end of the growing period, which was consistent with that observed in the control. This suggests that N loss from the maize cropping system in the Rift Valley highlands is mitigated even with increased N fertilizer use.

However, the $N_{min}$ loss, especially $NO_3^-$-N, does not preclude leaching events under specific conditions, as the system is susceptible to episodic N loss events, particularly following heavy rainfall, as observed in **Figure 8**. This could be attributed to the 1:1 kaolinite clays, which dominate the highly weathered Ferralsols in the region. These clays tend to develop a net anion exchange capacity, especially at low pH, enhancing $NO_3^-$ adsorption and thus, reducing its movement down the soil profile with the percolating water (Harmand *et al*., 2010). The low Nmin content in the lower depths could also be due to the split application of the N fertilizer. Split N application in agricultural systems improves synchrony between N supply and crop N demand, thereby aiding in the avoidance of unnecessary losses (Mutegi *et al*., 2012). Furthermore, the long growing period of the maize crop could have resulted in maximum N uptake for grain filling, which is why there was low Nmin availability in the surface layer at harvest

**5.2 $N_2O$ emissions under different N application rates**

The magnitude of $N_2O$ emissions reported in this study (0.33 to 0.77 kg $N_2O$-N $ha^{-1}$ $yr^{-1}$) is more or less consistent with those reported in other similar studies in SSA (0.13 to 1.43 kg $N_2O$ $ha^{-1}$) (Mapanda *et al*., 2011; Hickman *et al*., 2014; Macharia *et al*., 2020; Zheng *et al*., 2019; Musafiri *et al*., 2020; Githongo *et al*., 2022; Kibet *et al*., 2022). The average daily and cumulative fluxes increased with increasing N rates, which corroborates findings from previous studies involving multiple N application rates in SSA (Hickman *et al*., 2014; Hickman *et al*., 2015; Mapanda *et al*., 2011; Zheng *et al*., 2019). Increased N rates enhanced Nmin concentration ($NO_3^-$ and $NH_4^+$), which act as substrates for $N_2O$ production. Further illustrated by the positive interaction between N intensities and cumulative $N_2O$ fluxes, which was consistent with other studies (Burton *et al*., 2008; Zebarth *et al*., 2012; Macharia *et al*., 2020). N intensity is an important index in soil N management as it reflects the size and duration of mineral N in the soil, which influences microbial processes, thereby increasing the risk of Nr loss to the ecosystem. This finding further supports reports by Yao *et al*.(2020), who proved that N intensity could be used as a proxy to estimate $N_2O$ emissions in terrestrial ecosystems. This could be a reprieve, especially to policymakers and scientists in SSA who are constrained by limited spatial $N_2O$ measurements, which hinder their efforts in accounting for the nationally determined contributions (NDCs) and providing mitigating measures. In contrast, the annual flux observed in the non-fertilized plot in this study (0.53 kg $N_2O$-N $ha^{-1}$) was markedly higher than values reported in similar conditions in maize systems across the region, which ranged between 0.104 and 0.324 kg $N_2O$-N $ha^{-1}$ (Mapanda *et al*., 2011; Macharia *et al*., 2020; Musafiri *et al*., 2020; Hickman *et al*., 2015; Githongo *et al*., 2022). However, Hickman *et al*. (2014) observed higher fluxes of 0.71 kg $N_2O$-N $ha^{-1}$, which was surprisingly higher than those of the plots receiving 50, 75 and 100 kg N $ha^{-}$1. A similar observation was also recorded in the current study, where the non-fertilized plot exhibited higher average daily and annual fluxes in contrast to the 25 and 50 kg N $ha^{-1}$ plots.

The emission factors (EFs) observed in this study (0.2%) were within the ranges reported in maize systems in Kenya. For instance, Githongo *et al*. (2022), while determining the GHG fluxes as influenced by different inorganic and organic N source combinations in the upper Eastern Kenya, observed EFs varying between 0.02 and 0.14%. Similarly, Musafiri *et al*.( 2020) reported consistent ranges of between 0.05 and 0.14 in the manure and inorganic fertilizer treatments, respectively, both supplying 120 kg N $ha^{-1}$. However, Macharia *et al*.( 2020) reported a considerably higher range of 0.2 to 0.9% in the Central highland of Kenya. This proves that the use of IPCC Tier 1, emission factor of 1%, in estimating $N_2O$ emissions from agricultural soils in Kenya is subject to overestimation. The yield-scaled emission, which reflects the $N_2O$ emissions vis` the unit of grain yield, were low (averaging 0.12, with a minimum and maximum of 0.07 - 0.14 g $N_2O$-N $kg^{-1}$ grain yield, respectively). This could be attributed be enhanced grain yields as N rates increased to 125 kg N $ha^{-1}$. Similar observations were made by Leitner *et al.*(2020), who projected a ~97% reduction in yield-scaled $N_2O$ emissions from 4.55 to 0.14 g $N_2O$-N $kg^{-1}$ grain yield when closing the yield gaps in SSA by 25%.

## 5.3 Regulatory factors influencing soil Nmin pools and select soil chemical properties

The dynamics of soil nitrogen (N) are highly complex and are subject to variations due to environmental factors that significantly influence the internal N cycle. Precipitation, in particular, plays a crucial role in the internal N cycle through its direct and indirect impacts on N availability and movement, microbial dynamics, and plant N uptake as it alters soil moisture (Cregger *et al.*, 2014; Hess *et al.*, 2020; Lv *et al.*, 2023; Peng *et al.*, 2021). Precipitation influences nitrification, the process of oxidizing $NH_4^+$ to $NO_3^-$ through microbial action (Beeckman *et al.*, 2018) as illustrated by the negative relationship between cumulative rainfall and soil moisture content on $NH_4^+$-N across all depths. Indeed, precipitation-driven soil moisture variations enhance the substrate availability of both ammonium and oxygen through diffusion for microbes, thus indirectly impacting nitrification, especially autotrophic nitrification. This underscores the significant role precipitation plays in soil N transformation.

Furthermore, the average precipitation received between consecutive sampling periods positively influenced soil $NO_3^-$-N concentration in the surface layer. Additionally, increased $NO_3^-$-N content in the deeper layers (20 – 40 cm and 40 – 60 cm) correlated positively with increased precipitation, potentially facilitating the vertical movement of

$NO_3^-$. Similarly, soil temperature variables also affected soil N dynamics, showing a positive interaction with $NO_3^-$-N and a negative correlation with $NH_4^+$-N. This is consistent with other studies that have also reported increased nitrification with rising soil temperature (Bai *et al*., 2013; Elrys *et al*., 2021; Li *et al*., 2020).

**5.4 Grain yield, dry matter biomass, N uptake and harvest index**

The economic importance of using synthetic N fertilizers in crop production lies in their ability to boost harvestable yields. Globally, around 50% of elevated yields across different ecosystems is attributed to increased fertiliser use. In this study, increasing N application rates to 125 kg significantly improved grain yield ($p < 0.05$) to 5.4 t $ha^{-1}$. This supports other similar studies that found grain production rises substantially with N application rates (Aramburu-Merlos *et al*., 2024). However, the highest grain yield in this study was lower (5.4 t $ha^{-1}$) compared to the global average of 5.8 t $ha^{-1}$ (Liu *et al*., 2023). This was likely due to the low kernel number per ear in some plots, resulting from manual pollination, which may have potentially affected ovum fertilization and cob filling. This confirms that grain yield is dependent on the ear and kernel number and their weight (Hütsch & Schubert, 2017), which are further influenced by dry matter accumulation. This relationship was further supported by the positive linear interaction between dry matter accumulation and grain yield **(Figure 15)**.

In this study, dry matter increased with higher N application rates, with yields ranging from 7.23 to 10.85 t $ha^{-1}$. These findings corroborates with reports from other similar studies showing that greater N input promotes maize dry matter accumulation (Bai *et al*., 2020). Increasing N application elevates mineral N availability in the rhizosphere, subsequently leading to improved plant N uptake, as demonstrated in this study. This stimulates leaf growth, enhances carbon assimilation, extends the growing period, delays leaf senescence and ultimately improves dry matter accumulation and grain yield

(Dong *et al*., 2024). In contrast, the control plots recorded the lowest dry matter, likely due to limited N supply, which might have supressed vegetative growth and triggered early senescence (Zakari *et al*., 2021). The observed increase in both grain yield and dry matter may also be partly linked to the relatively long maize growing period (195 days). Liu *et al*. (2023) reported that a long growing period, especially after silking, is crucial for achieving higher grain yield.

Although grain yield and dry matter accumulation increased with the N application rate, the harvest index (HI), which is the ratio of grain yield to the total above-ground dry matter, did not show any significant relationship. Other studies have reported an increased HI with rising grain yield (Liu *et al*., 2023); however, our findings indicate inconsistency. The control, 50 and 125 kg N $ha^{-1}$ treatments exhibited the highest HI of 0.34 kg grain $kg^{-1}$ dry matter; however, this did not differ significantly from the other N application rates. Additionally, the average HI from the present study was considerably lower (0.33 kg grain per kg of dry matter) than the ones reported in other studies (Liu *et al*., 2020; Ruiz *et al*., 2023). For instance, Liu *et al*. (2020) reported on grain HI for five different cultivars, which ranged between 0.46 and 0.54 kg per kg of dry matter. They also conducted a meta-analysis across 40 locations in China, where the average grain HI was 0.51. The low HI could be attributed to the disrupted cob filling process, mentioned in the previous paragraph.

### 4.5 Nitrogen use efficiency

Nitrogen use efficiency (NUE) serves as a crucial indicator in crop production systems and is subject to soil and fertilizer N supply, crop N uptake and losses between the soil-plant system. Therefore, the efficient use of nitrogen fertilizer in crop production is crucial for enhancing yields and mitigating ecosystem degradation, particularly in sub-Saharan Africa (SSA).

$NUE_{grain}$, the fraction of N fertilizer recovered in the grain, reduced linearly with increasing nitrogen application rates, with 25 kg N $ha^{-1}$ exhibiting a ratio of > 1, indicating a potential risk of nitrogen mining in a continuous crop production system. Meanwhile, the lowest $NUE_{crop}$ (0.37) was recorded in the 125 kg N $ha^{-1}$ treatment, reflecting asynchrony between nitrogen supply and uptake by the crop as well as potential oversupply of N, thereby increasing the risk of nitrogen losses from the ecosystem through various pathways. This finding supports the study by Omara *et al*. (2019), who attributed low NUE to high N fertilizer application, as evidenced by values obtained in China and India, which account for the highest consumption of synthetic N fertilizers in their cereal cropping systems. Overall, the average NUE reported in this study fell within the NUE limit target ranges of between 50 and 90%.

Similarly, the partial factor productivity (PFP), ratio of yield to N fertilizer supply, reduced with increasing N application and ranged between 157.07 and 43.2 kg grain $kg^{-1}$ N in the 25 and 125 kg N $ha^{-1}$ N fertilizer levels, respectively. Dobermann (2007) reported that the optimum range for PFP in cereal systems is between 40 and 80 kg $kg^{-1}$ and these findings were within this range, except for the N fertilization level of 25 kg N $ha^{-1}$. However, the high value exhibited by applying 25 kg N $ha^{-1}$ is not an indicator of a well-managed or efficient system, but rather a low N supply and inefficient N exploitation (Dobermann, 2007). By contrast, the documented PFP for SSA is 122 kg $kg^{-1}$, while the global average is 44 kg $kg^{-1}$ (closer to the one demonstrated while applying 125 kg N $ha^{-1}$).

The highest grain yield increase per additional kg N was in the 100 kg N $ha^{-1}$, 13.70 kg grain $kg^{-1}$ N, while the average was 11.78 kg grain $kg^{-1}$ N. This value was considerably lower compared to those reported in the region (Ichami *et al*., 2019; Sileshi *et al*., 2019; Winnie *et al*., 2022); however, they were within the acceptable range of between 10 and 30 kg grain per kg N (Dobermann, 2007). A meta-analysis by Ichami *et al*. (2019) on fertilizer response and NUE in African smallholder maize farms reported an agronomic N efficiency (AE) of 18 and 42 kg grain increase $kg^{-1}$ N for SSA and Kenya, respectively. Furthermore, Sileshi *et al*. (2019) reported an AE of 23.7 kg grain $kg^{-1}$ N from inorganic fertilizers. On the contrary, Winnie *et al*. (2022) observed markedly higher AE values of between 81.7 and 118.7 kg grain $kg^{-1}$ N and 45.4 and 154.3 kg grain $kg^{-1}$ N across two sites in the Lake Victoria basin. However, the high values were attributed to low N supply, which was unable to optimise the AE.

# CHAPTER SIX

# CONCLUSION AND RECOMMENDATION

## 6.1 Conclusion

1. Increasing N fertilizer application raised soil N levels, especially on the surface horizon. The overall $NO_3^-$ and $NH_4^+$ concentrations across the three depths and monitoring period followed the order of 0-20 > 20-40 > 40-60 cm. Additionally, applying N fertilizer at 125 kg $ha^{-1}$ significantly boosted $NO_3^-$ and $NH_4^+$ levels early in the crop's growing season compared to other N rates. This heightened the risk of N leaching, and higher $NO_3^-$ levels were observed in the subsequent depth (20 – 40 cm) at 42 DAP. However, similar $NO_3^-$ concentrations at the lower depths in both fertilized and non-fertilized plots as the crop developed indicated minimal N loss down the soil profile.
2. Increasing N fertilizer use will also result in more $N_2O$ emissions. Fortunately, the level of fertilizer-related $N_2O$ emissions was lower than what has been observed in other intensified agroecosystems globally. Further, the emission factors (EFs) reported in this study were significantly lower than the default IPCC EF of 1%, and the yield-scaled emissions were also low, attributed to the improved yields.
3. Increasing N application rates improved maize grain yield considerably but reduced the overall NUE. Furthermore, applying N fertilizer at 125 kg $ha^{-1}$ increased the risk of N loss to the ecosystem, indicated by the low $NUE_{crop}$ value. The optimum $NUE_{crop}$, physiological efficiency and partial-factor productivity were realised when N was supplied at 75 kg N $ha^{-1}$.

4. Therefore, matching crop demands through judicious N use will be critical to ensure efficient use of N-fertiliser and reduce losses. This study established that N-fertilizer increments to 75 would improve grain yield and also optimise NUE.

## 6.2 Recommendations

Based on the findings, this study recommends:

1. Further research should be undertaken on Nmin concentration in pore water and leachate across different depths in agricultural systems across SSA, as the Nmin measured in the current study was bound within soil colloids, making it hard to distinguish between that which is available and unavailable for plant uptake.
2. Future studies should use $^{15}N$-labeled fertilizer to distinguish between fertilizer supplied by N fertilizers and soil organic N during the crop-growing period, to identify N mining and N oversupply in agricultural systems.

# REFERENCES

Abodi, M. A., Obare, G. A., & Kariuki, I. M. (2021). Supply and demand responsiveness to maize price changes in Kenya: An application of error correction autoregressive distributed lag approach. *Cogent Food & Agriculture*, *7*(1), 1957318. https://doi.org/10.1080/23311932.2021.1957318

Adalibieke, W., Cui, X., Cai, H., You, L., & Zhou, F. (2023). Global crop-specific nitrogen fertilization dataset in 1961–2020. *Scientific Data*, *10*(1), 617. https://doi.org/10.1038/s41597-023-02526-z

AFO. (2018). Review of fertilizer useby crop and by product in Kenya. https://api.hub.ifdc.org/server/api/core/bitstreams/cb2720dc-d0f2-444a-9472-7dbd9e3763e9/content

Agriculture and Food Authority. (2021). Wheat value chain survey report. http://food.agricultureauthority.go.ke/index.php/statistics/reports?download=68:wheat-value-chain-survey-report-feb-march-2023

Albanito, F., Lebender, U., Cornulier, T., Sapkota, T. B., Brentrup, F., Stirling, C., & Hillier, J. (2017). Direct Nitrous Oxide Emissions From Tropical And Sub-Tropical Agricultural Systems—A Review And Modelling Of Emission Factors. *Scientific Reports*, *7*(1), Article 1. https://doi.org/10.1038/srep44235

Alimagham, S., van Loon, M. P., Ramirez-Villegas, J., Adjei-Nsiah, S., Baijukya, F., Bala, A., Chikowo, R., Silva, J. V., Soulé, A. M., Taulya, G., Tenorio, F. A., Tesfaye, K., & van Ittersum, M. K. (2024). Climate change impact and adaptation of rainfed cereal crops in sub-Saharan Africa. *European Journal of Agronomy*, *155*, 127137. https://doi.org/10.1016/j.eja.2024.127137

Anas, M., Liao, F., Verma, K. K., Sarwar, M. A., Mahmood, A., Chen, Z.-L., Li, Q., Zeng, X.-P., Liu, Y., & Li, Y.-R. (2020). Fate of nitrogen in agriculture and environment: Agronomic, eco-physiological and molecular approaches to improve nitrogen use efficiency. *Biological Research*, *53*(1), 47. https://doi.org/10.1186/s40659-020-00312-4

Aramburu-Merlos, F., Tenorio, F. A. M., Mashingaidze, N., Sananka, A., Aston, S., Ojeda, J. J., & Grassini, P. (2024). Adopting yield-improving practices to meet maize demand in Sub-Saharan Africa without cropland expansion. *Nature Communications*, *15*(1), 4492. https://doi.org/10.1038/s41467-024-48859-0

Ayiti, O. E., & Babalola, O. O. (2022). Factors Influencing Soil Nitrification Process and the Effect on Environment and Health. *Frontiers in Sustainable Food Systems*, *6*. https://doi.org/10.3389/fsufs.2022.821994

Bai, E., Li, S., Xu, W., Li, W., Dai, W., & Jiang, P. (2013). A meta-analysis of experimental warming effects on terrestrial nitrogen pools and dynamics. *New Phytologist*, *199*(2), 441–451. https://doi.org/10.1111/nph.12252

Bai, L., Lu, Z., Zhang, X., Wang, Y., Zhang, D., Wang, Y., & Wang, T. (2020). Influence of Different Nitrogen Application Levels on Dry Matter Accumulation and Distribution of Silage Corn. *IOP Conference Series: Earth and Environmental Science*, *615*(1), 012086. https://doi.org/10.1088/1755-1315/615/1/012086

Bates, D., Mächler, M., Bolker, B., & Walker, S. (2015). Fitting Linear Mixed-Effects Models Using **lme4**. *Journal of Statistical Software*, *67*(1). https://doi.org/10.18637/jss.v067.i01

Battye, W., Aneja, V. P., & Schlesinger, W. H. (2017). Is nitrogen the next carbon? *Earth's Future*, *5*(9), 894–904. https://doi.org/10.1002/2017EF000592

Beeckman, F., Motte, H., & Beeckman, T. (2018). Nitrification in agricultural soils: Impact, actors and mitigation. *Current Opinion in Biotechnology*, *50*, 166–173. https://doi.org/10.1016/j.copbio.2018.01.014

Bigaignon, L., Delon, C., Ndiaye, O., Galy-Lacaux, C., Serça, D., Guérin, F., Tallec, T., Merbold, L., Tagesson, T., Fensholt, R., André, S., & Galliau, S. (2020). Understanding N2O Emissions in African Ecosystems: Assessments from a Semi-Arid Savanna Grassland in Senegal and Sub-Tropical Agricultural Fields in Kenya. *Sustainability*, *12*(21), 8875. https://doi.org/10.3390/su12218875

Bijay-Singh, & Craswell, E. (2021). Fertilizers and nitrate pollution of surface and ground water: An increasingly pervasive global problem. *SN Applied Sciences*, *3*(4), 518. https://doi.org/10.1007/s42452-021-04521-8

Bougma, P. C., Bondé, L., Yaro, V. S. O., Dicko, I., Zongo, A. F. R., Gebremichael, A. W., Mohamed, M., Malz, C., Matschullat, J., Linstädter, A., & Ouédraogo, O. (2025). Greenhouse Gas Emissions from Fertilization Practices in Maize Cropping in Sub-Saharan Africa: Toward Climate-Smart Agriculture. *Environments*, *12*(7), 211. https://doi.org/10.3390/environments12070211

Bouwman, A. F., Boumans, L. J. M., & Batjes, N. H. (2002). Emissions of N2O and NO from fertilized fields: Summary of available measurement data. *Global Biogeochemical Cycles*, *16*(4), 6-1-6–13. https://doi.org/10.1029/2001GB001811

Boy-Roura, M., Cameron, K. C., & Di, H. J. (2016). Identification of nitrate leaching loss indicators through regression methods based on a meta-analysis of lysimeter studies. *Environmental Science and Pollution Research*, *23*(4), 3671–3680. https://doi.org/10.1007/s11356-015-5529-9

Breure, M. S., Njoroge, S., Pasley, H. R., & Hoffland, E. (2023). Exploring options for increasing maize yields and grain Zn concentrations in sub-Saharan Africa. *Plant and Soil*, *488*(1–2), 625–636. https://doi.org/10.1007/s11104-023-05998-5

Burton, D. L., Zebarth, B. J., Gillam, K. M., & MacLeod, J. A. (2008). Effect of split application of fertilizer nitrogen on $N_2$ O emissions from potatoes. *Canadian Journal of Soil Science*, *88*(2), 229–239. https://doi.org/10.4141/CJSS06007

Butterbach-Bahl, K., Baggs, E. M., Dannenmann, M., Kiese, R., & Zechmeister-Boltenstern, S. (2013). Nitrous oxide emissions from soils: How well do we understand the processes and their controls? *Philosophical Transactions of the Royal Society B: Biological Sciences*, *368*(1621), 20130122. https://doi.org/10.1098/rstb.2013.0122

Cameron, K. c., Di, H. j., & Moir, J. l. (2013). Nitrogen losses from the soil/plant system: A review. *Annals of Applied Biology*, *162*(2), 145–173. https://doi.org/10.1111/aab.12014

Clark, I. M., Fu, Q., Abadie, M., Dixon, E. R., Blaud, A., & Hirsch, P. R. (2020). Edaphic factors and plants influence denitrification in soils from a long-term arable experiment. *Scientific Reports*, *10*(1), 16053. https://doi.org/10.1038/s41598-020-72679-z

Clough, T. J., Rochette, P., Thomas, S. M., Pihlatie, M., Christiansen, J. R., & Thorman, R. E. (2020). Global Research Alliance N2O chamber methodology guidelines: Design considerations. *Journal of Environmental Quality*, *49*(5), 1081–1091. https://doi.org/10.1002/jeq2.20117

Congreves, K. A., Otchere, O., Ferland, D., Farzadfar, S., Williams, S., & Arcand, M. M. (2021). Nitrogen Use Efficiency Definitions of Today and Tomorrow.

*Frontiers in Plant Science*, *12*. https://www.frontiersin.org/articles/10.3389/fpls.2021.637108

Cregger, M. A., McDowell, N. G., Pangle, R. E., Pockman, W. T., & Classen, A. T. (2014). The impact of precipitation change on nitrogen cycling in a semi-arid ecosystem. *Functional Ecology*, *28*(6), 1534–1544. https://doi.org/10.1111/1365-2435.12282

das Graças Costa, E., & de Souza, P. M. (2023). Introduction to Cereals. In M. A. Shah, K. Valiyapeediyekkal Sunooj, & S. A. Mir (Eds.), *Cereal-Based Food Products* (pp. 1–24). Springer International Publishing. https://doi.org/10.1007/978-3-031-40308-8_1

de Klein, C. A. M., Alfaro, M. A., Giltrap, D., Topp, C. F. E., Simon, P. L., Noble, A. D. L., & van der Weerden, T. J. (2020). Global Research Alliance N2O chamber methodology guidelines: Statistical considerations, emission factor calculation, and data reporting. *Journal of Environmental Quality*, *49*(5), 1156–1167. https://doi.org/10.1002/jeq2.20127

de Sousa, T., & Bhosle, S. (2012). Microbial Denitrification and Its Ecological Implications in the Marine System. In T. Satyanarayana & B. N. Johri (Eds.), *Microorganisms in Environmental Management: Microbes and Environment* (pp. 683–700). Springer Netherlands. https://doi.org/10.1007/978-94-007-2229-3_30

De Vries, W. (2021). Impacts of nitrogen emissions on ecosystems and human health: A mini review. *Current Opinion in Environmental Science & Health*, *21*, 100249. https://doi.org/10.1016/j.coesh.2021.100249

Dimkpa, C., Adzawla, W., Pandey, R., Atakora, W. K., Kouame, A. K., Jemo, M., & Bindraban, P. S. (2023). Fertilizers for food and nutrition security in sub-Saharan Africa: An overview of soil health implications. *Frontiers in Soil Science*, *3*. https://www.frontiersin.org/articles/10.3389/fsoil.2023.1123931

Dobermann, A. (2005). Nitrogen Use Efficiency – State of the Art.

Dobermann, A. (2007). Nutrient use efficiency – measurement and management. https://digitalcommons.unl.edu/agronomyfacpub/1442

Dong, X., Ren, Y., Shi, L., Bao, S., Chai, X., Li, Q., & Liao, L. (2024). Relationship between dry matter accumulation and maize yield in Southwest China. *Food and Energy Security*, *13*(4), e566. https://doi.org/10.1002/fes3.566

Donzelli, G., & Suarez-Varela, M. M. (2024). Tropospheric Ozone: A Critical Review of the Literature on Emissions, Exposure, and Health Effects. *Atmosphere*, *15*(7), Article 7. https://doi.org/10.3390/atmos15070779

Edmonds, D. E., Abreu, S. L., West, A., Caasi, D. R., Conley, T. O., Daft, M. C., Desta, B., England, B. B., Farris, C. D., Nobles, T. J., Patel, N. K., Rounds, E. W., Sanders, B. H., Shawaqfeh, S. S., Lakmini, Lokuralalage, Manandhar, R., & Raun, W. R. (2009). Cereal Nitrogen Use Efficiency in Sub Saharan Africa. *Journal of Plant Nutrition*, *32*(12), 2107–2122. https://doi.org/10.1080/01904160903308184

Elrys, A. S., Desoky, E.-S. M., Alnaimy, M. A., Zhang, H., Zhang, J., Cai, Z., & Cheng, Y. (2021). The food nitrogen footprint for African countries under fertilized and unfertilized farms. *Journal of Environmental Management*, *279*, 111599. https://doi.org/10.1016/j.jenvman.2020.111599

Elrys, A. S., Wang, J., Metwally, M. A. S., Cheng, Y., Zhang, J., Cai, Z., Chang, S. X., & Müller, C. (2021). Global gross nitrification rates are dominantly driven by soil carbon-to-nitrogen stoichiometry and total nitrogen. *Global Change Biology*, *27*(24), 6512–6524. https://doi.org/10.1111/gcb.15883

Erisman, J. W., Galloway, J. N., Seitzinger, S., Bleeker, A., Dise, N. B., Petrescu, A. M. R., Leach, A. M., & de Vries, W. (2013). Consequences of human modification of the global nitrogen cycle. *Philosophical Transactions of the Royal Society B: Biological Sciences*, *368*(1621), 20130116. https://doi.org/10.1098/rstb.2013.0116

Eysholdt, M., Kunkel, R., Rösemann, C., Wendland, F., Wolters, T., Zinnbauer, M., & Fuß, R. (2022). A model-based estimate of nitrate leaching in Germany for GHG reporting. *Journal of Plant Nutrition and Soil Science*, *185*(6), 850–863. https://doi.org/10.1002/jpln.202200119

Ezeh, A., Kissling, F., & Singer, P. (2020). Why sub-Saharan Africa might exceed its projected population size by 2100. *The Lancet*, *396*(10258), 1131–1133. https://doi.org/10.1016/S0140-6736(20)31522-1

Ezui, G., Haugen-Kozyra, K., Heaney, D., Nirjan, L., Graham, C., Njoroge, S., Zingore, S., & Bruulsema, T. (2022). *Can 4R Practices Limit the Nitrous Oxide Emissions from Increasing Fertilizer Use in Sub-Sahara Africa?*

Fageria, N. K., & Baligar, V. C. (2005). Enhancing Nitrogen Use Efficiency in Crop Plants. In *Advances in Agronomy* (Vol. 88, pp. 97–185). Academic Press. https://doi.org/10.1016/S0065-2113(05)88004-6

FAO. (1996). *Rome Declaration and Plan of Action*. https://www.fao.org/4/w3613e/w3613e00.htm

FAO. (2021). *World Food and Agriculture – Statistical Yearbook 2021*. FAO. https://doi.org/10.4060/cb4477en

FAO. (2023). *FAO Climate Info Tool*. https://aquastat.fao.org/climate-information-tool/climate-data?lat=0.5142774999999999&lon=35.2697802&filterParams=%7B%22fromDate%22:1660465443562,%22toDate%22:%222022-12-31T20:59:59.999Z%22%7D

FAO. (2024). *World Food and Agriculture – Statistical Yearbook 2024*. FAO. https://doi.org/10.4060/cd2971en

FAO, IFAD, UNICEF, WFP, & WHO. (2025). *The State of Food Security and Nutrition in the World 2025*. FAO; IFAD; UNICEF; WFP; WHO; https://doi.org/10.4060/cd6008en

FAOSTAT. (2024). *Crops and livestock products*. Food and Agriculture Organization of the United Nations. https://www.fao.org/faostat/en/#data/QCL

Ferraz-Almeida, R. (2024). Balance of Nitrate and Ammonium in Tropical Soil Conditions: Soil Factors Analyzed by Machine Learning. *Nitrogen*, *5*(3), Article 3. https://doi.org/10.3390/nitrogen5030048

Fowler, D., Coyle, M., Skiba, U., Sutton, M. A., Cape, J. N., Reis, S., Sheppard, L. J., Jenkins, A., Grizzetti, B., Galloway, J. N., Vitousek, P., Leach, A., Bouwman, A. F., Butterbach-Bahl, K., Dentener, F., Stevenson, D., Amann, M., & Voss, M. (2013). The global nitrogen cycle in the twenty-first century. *Philosophical Transactions of the Royal Society B: Biological Sciences*, *368*(1621), 20130164. https://doi.org/10.1098/rstb.2013.0164

Freney, J. R., Simpson, J. R., & Denmead, O. T. (1981). Ammonia Volatilization. *Ecological Bulletins*, *33*, 291–302.

Gentile, R., Vanlauwe, B., Van Kessel, C., & Six, J. (2009). Managing N availability and losses by combining fertilizer-N with different quality residues in Kenya. *Agriculture, Ecosystems & Environment*, *131*(3–4), 308–314. https://doi.org/10.1016/j.agee.2009.02.003

Giller, K. E. (2020). The Food Security Conundrum of sub-Saharan Africa. *Global Food Security*, *26*, 100431. https://doi.org/10.1016/j.gfs.2020.100431

Githongo, M. W., Musafiri, C. M., Macharia, J. M., Kiboi, M. N., Fliessbach, A., Muriuki, A., & Ngetich, F. K. (2022). Greenhouse Gas Fluxes from Selected Soil Fertility Management Practices in Humic Nitisols of Upper Eastern Kenya. *Sustainability*, *14*(3), Article 3. https://doi.org/10.3390/su14031938

Gong, C., Tian, H., Liao, H., Pan, N., Pan, S., Ito, A., Jain, A. K., Kou-Giesbrecht, S., Joos, F., Sun, Q., Shi, H., Vuichard, N., Zhu, Q., Peng, C., Maggi, F., Tang, F. H. M., & Zaehle, S. (2024). Global net climate effects of anthropogenic reactive nitrogen. *Nature*, 1–7. https://doi.org/10.1038/s41586-024-07714-4

Govindasamy, P., Muthusamy, S. K., Bagavathiannan, M., Mowrer, J., Jagannadham, P. T. K., Maity, A., Halli, H. M., G. K., S., Vadivel, R., T. K., D., Raj, R., Pooniya, V., Babu, S., Rathore, S. S., L., M., & Tiwari, G. (2023). Nitrogen use efficiency—A key to enhance crop productivity under a changing climate. *Frontiers in Plant Science*, *14*, 1121073. https://doi.org/10.3389/fpls.2023.1121073

Grace, P., Shcherbak, I., Macdonald, B., Scheer, C., & Rowlings, D. (2016). Emission factors for estimating fertiliser-induced nitrous oxide emissions from clay soils in Australia's irrigated cotton industry. *Soil Research*, *54*(5), 598. https://doi.org/10.1071/SR16091

Gyanchandani, V. (2016). *UNFCCC Nationally Determined Contributions: Climate Change and Trade*.

Hanif, M. N. (2023). Factors Affecting Nitrogen Use Efficiency (NUE): Meta Analysis. *Türkiye Tarımsal Araştırmalar Dergisi*, *10*(2), 231–242. https://doi.org/10.19159/tutad.1260531

Harmand, J.-M., Ávila, H., Oliver, R., Saint-André, L., & Dambrine, E. (2010). The impact of kaolinite and oxi-hydroxides on nitrate adsorption in deep layers of a Costarican Acrisol under coffee cultivation. *Geoderma*, *158*(3), 216–224. https://doi.org/10.1016/j.geoderma.2010.04.032

Hayashi, K., Tokida, T., & Hasegawa, T. (2011). Potential ammonia emission from flag leaves of paddy rice (*Oryza sativa* L. cv. Koshihikari). *Agriculture, Ecosystems & Environment*, *144*(1), 117–123. https://doi.org/10.1016/j.agee.2011.07.012

Herrera, J., Rubio, G., Häner, L., Delgado, J., Lucho-Constantino, C., Islas-Valdez, S., & Pellet, D. (2016). Emerging and Established Technologies to Increase Nitrogen Use Efficiency of Cereals. *Agronomy*, *6*(2), 25. https://doi.org/10.3390/agronomy6020025

Hess, L. J. T., Hinckley, E.-L. S., Robertson, G. P., & Matson, P. A. (2020). Rainfall intensification increases nitrate leaching from tilled but not no-till cropping systems in the U.S. Midwest. *Agriculture, Ecosystems & Environment*, *290*, 106747. https://doi.org/10.1016/j.agee.2019.106747

Hickman, J. E., Havlikova, M., Kroeze, C., & Palm, C. A. (2011). Current and future nitrous oxide emissions from African agriculture. *Current Opinion in Environmental Sustainability*, *3*(5), 370–378. https://doi.org/10.1016/j.cosust.2011.08.001

Hickman, J. E., Scholes, R. J., Rosenstock, T. S., Garcia-Pando, C. P., & Nyamangara, J. (2014). Assessing non-CO2 climate-forcing emissions and mitigation in sub-Saharan Africa. *Current Opinion in Environmental Sustainability*, *9*, 65–72. https://doi.org/10.1016/j.cosust.2014.07.010

Hickman, J. E., Tully, K. L., Groffman, P. M., Diru, W., & Palm, C. A. (2015). A potential tipping point in tropical agriculture: Avoiding rapid increases in nitrous oxide fluxes from agricultural intensification in Kenya. *Journal of Geophysical Research: Biogeosciences*, *120*(5), 938–951. https://doi.org/10.1002/2015JG002913

Hickman, J., Havlikova Grecequet, M., Kroeze, C., & Palm, C. (2011). Current and future nitrous oxide emissions from African agriculture. *Current Opinion in Environmental Sustainability*, *3*, 370–378. https://doi.org/10.1016/j.cosust.2011.08.001

Hickman, J., Palm, C., Mutuo, P., Melillo, J., & Tang, J. (2014). Nitrous oxide (N2O) emissions in response to increasing fertilizer addition in maize (Zea mays L.) agriculture in western Kenya. *Nutrient Cycling in Agroecosystems*, *100*. https://doi.org/10.1007/s10705-014-9636-7

Hofstra, N., & Bouwman, A. F. (2005). Denitrification in Agricultural Soils: Summarizing Published Data and Estimating Global Annual Rates. *Nutrient Cycling in Agroecosystems*, *72*(3), 267–278. https://doi.org/10.1007/s10705-005-3109-y

Hong, M., Zhang, Y., Braun, R. C., & Bremer, D. J. (2023). Simulations of nitrous oxide emissions and global warming potential in a C4 turfgrass system using process-based models. *European Journal of Agronomy*, *142*, 126668. https://doi.org/10.1016/j.eja.2022.126668

Huddell, A. M., Galford, G. L., Tully, K. L., Crowley, C., Palm, C. A., Neill, C., Hickman, J. E., & Menge, D. N. L. (2020). Meta-analysis on the potential for increasing nitrogen losses from intensifying tropical agriculture. *Global Change Biology*, *26*(3), 1668–1680. https://doi.org/10.1111/gcb.14951

Hurtado, J., Velázquez, E., Lassaletta, L., Guardia, G., Aguilera, E., & Sanz-Cobena, A. (2024). Drivers of ammonia volatilization in Mediterranean climate cropping systems. *Environmental Pollution*, *341*, 122814. https://doi.org/10.1016/j.envpol.2023.122814

Hütsch, B. W., & Schubert, S. (2017). Harvest Index of Maize (*Zea mays* L.): Are There Possibilities for Improvement? In D. L. Sparks (Ed.), *Advances in Agronomy* (Vol. 146, pp. 37–82). Academic Press. https://doi.org/10.1016/bs.agron.2017.07.004

Ichami, S. M., Shepherd, K. D., Sila, A. M., Stoorvogel, J. J., & Hoffland, E. (2019). Fertilizer response and nitrogen use efficiency in African smallholder maize farms. *Nutrient Cycling in Agroecosystems*, *113*(1), 1–19. https://doi.org/10.1007/s10705-018-9958-y

IUSS Working Group WRB. (2022). World Reference Base for Soil Resources. International soil classification system for naming soils and creating legends for soil maps (4th ed.). International Union of Soil Sciences (IUSS). https://www.isric.org/sites/default/files/WRB_fourth_edition_2022-12-18.pdf

Jaetzold, R., & Schmidt, H. (1983). Farm Management Handbook of Kenya Vol. II: Natural Conditions and Farm Management Information (Part A: West Kenya, Part B: Central Kenya, Part C: East Kenya). *Nairobi: Ministry of Agriculture*.

Jayne, T. S., Mason, N. M., Burke, W. J., & Ariga, J. (2018). Review: Taking stock of Africa's second-generation agricultural input subsidy programs. *Food Policy*, *75*, 1–14. https://doi.org/10.1016/j.foodpol.2018.01.003

Jena, P. R., De Groote, H., Nayak, B. P., & Hittmeyer, A. (2021). Evolution of Fertiliser Use and its Impact on Maize Productivity in Kenya: Evidence from Multiple Surveys. *Food Security*, *13*(1), 95–111. https://doi.org/10.1007/s12571-020-01105-z

Kenya National Bureau of Statistics. (2023). Maize Production by County 2012—2020. *National Information Platform for Food Security and Nutrition*. https://nipfn.knbs.or.ke/download/maize-production-by-county-2012-2020/

Kibet, E., Musafiri, C. M., Kiboi, M., Macharia, J., Ng'etich, O. K., Kosgei, D. K., Mulianga, B., Okoti, M., Zeila, A., & Ngetich, F. K. (2022). Soil greenhouse gas emissions from different land utilization types in Western Kenya. *Frontiers in Soil Science*, *2*, 956634. https://doi.org/10.3389/fsoil.2022.956634

Kim, D.-G., Thomas, A. D., Pelster, D., Rosenstock, T. S., & Sanz-Cobena, A. (2016). Greenhouse gas emissions from natural ecosystems and agricultural lands in sub-Saharan Africa: Synthesis of available data and suggestions for further research. *Biogeosciences*, *13*(16), 4789–4809. https://doi.org/10.5194/bg-13-4789-2016

Kuypers, M. M. M., Marchant, H. K., & Kartal, B. (2018). The microbial nitrogen-cycling network. *Nature Reviews Microbiology*, *16*(5), 263–276. https://doi.org/10.1038/nrmicro.2018.9

Ladha, J. K., Jat, M. L., Stirling, C. M., Chakraborty, D., Pradhan, P., Krupnik, T. J., Sapkota, T. B., Pathak, H., Rana, D. S., Tesfaye, K., & Gerard, B. (2020). Chapter Two - Achieving the sustainable development goals in agriculture: The crucial role of nitrogen in cereal-based systems. In D. L. Sparks (Ed.), *Advances in Agronomy* (Vol. 163, pp. 39–116). Academic Press. https://doi.org/10.1016/bs.agron.2020.05.006

Lassaletta, L., Billen, G., Grizzetti, B., Anglade, J., & Garnier, J. (2014). 50 year trends in nitrogen use efficiency of world cropping systems: The relationship between yield and nitrogen input to cropland. *Environmental Research Letters*, *9*(10), 105011. https://doi.org/10.1088/1748-9326/9/10/105011

Leitner, S., Pelster, D. E., Werner, C., Merbold, L., Baggs, E. M., Mapanda, F., & Butterbach-Bahl, K. (2020). Closing maize yield gaps in sub-Saharan Africa will boost soil N2O emissions. *Current Opinion in Environmental Sustainability*, *47*, 95–105. https://doi.org/10.1016/j.cosust.2020.08.018

Lemarpe, S. E., Musafiri, C. M., Macharia, J. M., Kiboi, M. N., Ng'etich, O. K., Shisanya, C. A., Okeyo, J., Okwuosa, E. A., & Ngetich, F. K. (2021). Nitrous Oxide Emissions from Smallholders' Cropping Systems in Sub-Saharan Africa. *Advances in Agriculture*, *2021*, e4800527. https://doi.org/10.1155/2021/4800527

Li, X., Lu, M., Wu, J., Chen, L., Zhang, Z., Wang, X., Zhou, J., Jensen, K., Zhang, X., & Dou, X. (2025). Global change pattern of sedimentary nitrogen isotope during the Anthropocene epoch. *Communications Earth & Environment*, *6*(1), 809. https://doi.org/10.1038/s43247-025-02773-5

Li, Z., Zeng, Z., Tian, D., Wang, J., Fu, Z., Zhang, F., Zhang, R., Chen, W., Luo, Y., & Niu, S. (2020). Global patterns and controlling factors of soil nitrification rate. *Global Change Biology*, *26*(7), 4147–4157. https://doi.org/10.1111/gcb.15119

Lin, B.-L., Sakoda, A., Shibasaki, R., & Suzuki, M. (2001). A Modelling Approach to Global Nitrate Leaching Caused by Anthropogenic Fertilisation. *Water Research*, *35*(8), 1961–1968. https://doi.org/10.1016/S0043-1354(00)00484-X

Liu, G., Yang, Y., Guo, X., Liu, W., Xie, R., Ming, B., Xue, J., Wang, K., Li, S., & Hou, P. (2023). A global analysis of dry matter accumulation and allocation for maize yield breakthrough from 1.0 to 25.0 Mg ha−1. *Resources, Conservation and Recycling*, *188*, 106656. https://doi.org/10.1016/j.resconrec.2022.106656

Liu, W., Hou, P., Liu, G., Yang, Y., Guo, X., Ming, B., Xie, R., Wang, K., Liu, Y., & Li, S. (2020). Contribution of total dry matter and harvest index to maize grain yield—A multisource data analysis. *Food and Energy Security*, *9*(4), e256. https://doi.org/10.1002/fes3.256

Luo, J., Tillman, R. W., & Ball, P. R. (1999). Factors regulating denitrification in a soil under pasture. *Soil Biology and Biochemistry*, *31*(6), 913–927. https://doi.org/10.1016/S0038-0717(99)00013-9

Lv, P., Sun, S., Zhao, X., Li, Y., Zhao, S., Zhang, J., Hu, Y., Guo, A., Yue, P., & Zuo, X. (2023). Effects of altered precipitation patterns on soil nitrogen transformation in different landscape types during the growing season in northern China. *CATENA*, *222*, 106813. https://doi.org/10.1016/j.catena.2022.106813

Macharia, J. M., Pelster, D. E., Ngetich, F. K., Shisanya, C. A., Mucheru-Muna, M., & Mugendi, D. N. (2020). Soil Greenhouse Gas Fluxes From Maize Production Under Different Soil Fertility Management Practices in East Africa. *Journal of Geophysical Research: Biogeosciences*, *125*(7), e2019JG005427. https://doi.org/10.1029/2019JG005427

Maheswari, M., Murthy, A. N. G., & Shanker, A. K. (2017). 12—Nitrogen Nutrition in Crops and Its Importance in Crop Quality. In Y. P. Abrol, T. K. Adhya, V. P. Aneja, N. Raghuram, H. Pathak, U. Kulshrestha, C. Sharma, & B. Singh (Eds.), *The Indian Nitrogen Assessment* (pp. 175–186). Elsevier. https://doi.org/10.1016/B978-0-12-811836-8.00012-4

Mapanda, F., Wuta, M., Nyamangara, J., & Rees, R. M. (2011). Effects of organic and mineral fertilizer nitrogen on greenhouse gas emissions and plant-captured carbon under maize cropping in Zimbabwe. *Plant and Soil*, *343*(1–2), 67–81. https://doi.org/10.1007/s11104-011-0753-7

Motasim, A. M., Samsuri, Abd. W., Nabayi, A., Akter, A., Haque, M. A., Abdul Sukor, A. S., & Adibah, A. Mohd. (2024). Urea application in soil: Processes, losses, and alternatives—a review. *Discover Agriculture*, *2*(1), 42. https://doi.org/10.1007/s44279-024-00060-z

Mucheru-Muna, M., Mugendi, D., Mugwe, J., Kung'u, J., Merckx, R., & Vanlauwe, B. (2009). *Soil Mineral N Dynamics in a Maize Crop Following Different Soil Fertility Amendments in Different Soil Fertility Status in Sub-humid and Semi-arid Regions in Central Kenya*.

Mugwe, J., Mugendi, D. N., Mucheru-Muna, M., & Kung'u, J. B. (2011). Soil Inorganic N and N Uptake by Maize Following Application of Legume Biomass, Tithonia, Manure and Mineral Fertilizer in Central Kenya. In A. Bationo, B. Waswa, J. M. Okeyo, F. Maina, & J. M. Kihara (Eds.), *Innovations as Key to the Green Revolution in Africa* (pp. 605–616). Springer Netherlands. https://doi.org/10.1007/978-90-481-2543-2_62

Murrell, T., & Chivenge, P. (2023). Measurement of maize grain yield and aboveground biomass at maturity by crop cut at plot level, *v1. Standard Operating Procedure 008. In: Saito K, Johnson J-M, Hauser S, Corbeels M, Devkota M and Casimero M. Guideline for measuring agronomic gain key performance indicators in on- farm trials, v. 1. Excellence in Agronomy for Sustainable Intensification and Climate Change Adaptation Initiative.*

Musafiri, C. M., Macharia, J. M., Kiboi, M. N., Ng'etich, O. K., Shisanya, C. A., Okeyo, J. M., Mugendi, D. N., Okwuosa, E. A., & Ngetich, F. K. (2020). Soil greenhouse gas fluxes from maize cropping system under different soil fertility management technologies in Kenya. *Agriculture, Ecosystems & Environment*, *301*, 107064. https://doi.org/10.1016/j.agee.2020.107064

Mutegi, E. M., Kung'u, J. B., Muna, M., Pieter, P., & Mugendi, D. N. (2012). Complementary effects of organic and mineral fertilizers on maize production in the smallholder farms of Meru South District, Kenya. *Agricultural Sciences*, *03*(02), 221–229. https://doi.org/10.4236/as.2012.32026

Ngeno, V. (2024). Profit efficiency among kenyan maize farmers. *Heliyon*, *10*, e24657. https://doi.org/10.1016/j.heliyon.2024.e24657

Nguyen, L., Russ, J., & Triyana, M. (2023). *The Effect of Agricultural Input Subsidies on Productivity: A Meta-Analysis*.

Nhlengethwa, S., Thangata, P., Muthini, D., Djido, A., & Njiwa, D. (2023). Review of Agricultural Subsidy Programmes in Sub Saharan Africa*: The Impact of the Russia – Ukraine War*.

Njeru, F., Wambua, A., Muge, E., Haesaert, G., Gettemans, J., & Misinzo, G. (2023). Major biotic stresses affecting maize production in Kenya and their implications for food security. *PeerJ*, *11*, e15685. https://doi.org/10.7717/peerj.15685

Ntinyari, W., & Gweyi-Onyango, J. P. (2021). Greenhouse Gases Emissions in Agricultural Systems and Climate Change Effects in sub-Saharan Africa. In W. Leal Filho, N. Oguge, D. Ayal, L. Adeleke, & I. Da Silva (Eds.), *African Handbook of Climate Change Adaptation* (pp. 1–25). Springer International Publishing. https://doi.org/10.1007/978-3-030-42091-8_43-1

Ogle, S. M., Buendia, L., Butterbach-Bahl, K., Breidt, F. J., Hartman, M., Yagi, K., Nayamuth, R., Spencer, S., Wirth, T., & Smith, P. (2013). Advancing national greenhouse gas inventories for agriculture in developing countries: Improving activity data, emission factors and software technology. *Environmental Research Letters*, *8*(1), 015030. https://doi.org/10.1088/1748-9326/8/1/015030

Okalebo, J. R., Gathua, K. W., & Woomer, P. L. (2002). Laboratory Methods of Soil and Plant Analysis: A Working Manual. *Laboratory Methods of Soil and Plant Analysis: A Working Manual*.

Omara, P., Aula, L., Oyebiyi, F., & Raun, W. R. (2019). World Cereal Nitrogen Use Efficiency Trends: Review and Current Knowledge. *Agrosystems, Geosciences & Environment*, *2*(1), 180045. https://doi.org/10.2134/age2018.10.0045

Ouma, J. O., & De Groote, H. (2011). *Determinants of improved maize seed and fertilizer adoption in Kenya*.

Padilla, F. M., Gallardo, M., & Manzano-Agugliaro, F. (2018). Global trends in nitrate leaching research in the 1960–2017 period. *Science of The Total Environment*, *643*, 400–413. https://doi.org/10.1016/j.scitotenv.2018.06.215

Pan, B., Lam, S. K., Mosier, A., Luo, Y., & Chen, D. (2016). Ammonia volatilization from synthetic fertilizers and its mitigation strategies: A global synthesis. *Agriculture, Ecosystems & Environment*, *232*, 283–289. https://doi.org/10.1016/j.agee.2016.08.019

Pan, B., Xia, L., Lam, S. K., Wang, E., Zhang, Y., Mosier, A., & Chen, D. (2022). A global synthesis of soil denitrification: Driving factors and mitigation strategies. *Agriculture, Ecosystems & Environment*, *327*, 107850. https://doi.org/10.1016/j.agee.2021.107850

Pasley, H. R., Camberato, J. J., Cairns, J. E., Zaman-Allah, M., Das, B., & Vyn, T. J. (2020). Nitrogen rate impacts on tropical maize nitrogen use efficiency and soil nitrogen depletion in eastern and southern Africa. *Nutrient Cycling in Agroecosystems*, *116*(3), 397–408. https://doi.org/10.1007/s10705-020-10049-x

Pelster, D., Rufino, M., Rosenstock, T., Mango, J., Saiz, G., Diaz-Pines, E., Baldi, G., & Butterbach-Bahl, K. (2017). Smallholder farms in eastern African tropical highlands have low soil greenhouse gas fluxes. *Biogeosciences*, *14*(1), 187–202. https://doi.org/10.5194/bg-14-187-2017

Peng, B., Sun, J., Liu, J., Xia, Z., & Dai, W. (2021). Relative contributions of different substrates to soil N2O emission and their responses to N addition in a temperate forest. *Science of The Total Environment*, *767*, 144126. https://doi.org/10.1016/j.scitotenv.2020.144126

R Core Team. (2025). *R: A Language and Environment for Statistical Computing* [Computer software]. R Foundation for Statistical Computing. https://www.R-project.org/

Ramalingappa, P. L., Shrivastava, M., Dhar, S., Bandyopadhyay, K., Prasad, S., Langyan, S., Tomer, R., Khandelwal, A., Darjee, S., & Singh, R. (2023). Reducing options of ammonia volatilization and improving nitrogen use efficiency*via*organic and inorganic amendments in wheat (*Triticum aestivum*L.). *PeerJ*, *11*, e14965. https://doi.org/10.7717/peerj.14965

Rashmi, I., Shirale, A., Kartikha, K. S., Shinogi, K. C., Meena, B. P., & Kala, S. (2017). Leaching of Plant Nutrients from Agricultural Lands. In M. Naeem, A. A.

Ansari, & S. S. Gill (Eds.), *Essential Plant Nutrients* (pp. 465–489). Springer International Publishing. https://doi.org/10.1007/978-3-319-58841-4_19

Razon, L. F. (2018). Reactive nitrogen: A perspective on its global impact and prospects for its sustainable production. *Sustainable Production and Consumption*, *15*, 35–48. https://doi.org/10.1016/j.spc.2018.04.003

Richards, M., van Ittersum, M., Mamo, T., Stirling, C., Vanlauwe, B., & Zougmore, R. (2016). *Fertilizers and low emission development in sub-Saharan Africa*. www.ccafs.cgiar.org

Ricker-Gilbert, J., Mather, D. L., Maredia, M. K., Olwande, J., & Khaled, N. B. (2024). *Evaluating Kenya's National Fertilizer Subsidy Program: Implementation, Crowding-out, and Benefit-Cost Analysis*.

Rockström, J., Gupta, J., Qin, D., Lade, S. J., Abrams, J. F., Andersen, L. S., Armstrong McKay, D. I., Bai, X., Bala, G., Bunn, S. E., Ciobanu, D., DeClerck, F., Ebi, K., Gifford, L., Gordon, C., Hasan, S., Kanie, N., Lenton, T. M., Loriani, S., … Zhang, X. (2023). Safe and just Earth system boundaries. *Nature*, *619*(7968), 102–111. https://doi.org/10.1038/s41586-023-06083-8

Rosenstock, T. S., & Wilkes, A. (2021). Reorienting emissions research to catalyse African agricultural development. *Nature Climate Change*, *11*(6), 463–465. https://doi.org/10.1038/s41558-021-01055-0

Ruiz, A., Trifunovic, S., Eudy, D. M., Sciarresi, C. S., Baum, M., Danalatos, G. J. N., Elli, E. F., Kalogeropoulos, G., King, K., dos Santos, C., Thies, A., Pico, L. O., Castellano, M. J., Schnable, P. S., Topp, C., Graham, M., Lamkey, K. R., Vyn, T. J., & Archontoulis, S. V. (2023). Harvest index has increased over the last 50 years of maize breeding. *Field Crops Research*, *300*, 108991. https://doi.org/10.1016/j.fcr.2023.108991

Russo, T. A., Tully, K., Palm, C., & Neill, C. (2017). Leaching losses from Kenyan maize cropland receiving different rates of nitrogen fertilizer. *Nutrient Cycling in Agroecosystems*, *108*(2), 195–209. https://doi.org/10.1007/s10705-017-9852-z

Scheer, C., Rowlings, D. W., Antille, D. L., De Antoni Migliorati, M., Fuchs, K., & Grace, P. R. (2023). Improving nitrogen use efficiency in irrigated cotton production. *Nutrient Cycling in Agroecosystems*, *125*(2), 95–106. https://doi.org/10.1007/s10705-022-10204-6

Schoninger, E. L., González-Villalba, H. A., Bendassolli, J. A., & Ocheuze Trivelin, P. C. (2018). Fertilizer Nitrogen and Corn Plants: Not all Volatilized Ammonia is Lost. *Agronomy Journal*, *110*(3), 1111–1118. https://doi.org/10.2134/agronj2017.07.0372

Schwenke, G. D., Herridge, D. F., Scheer, C., Rowlings, D. W., Haigh, B. M., & McMullen, K. G. (2016). Greenhouse gas (N2O and CH4) fluxes under nitrogen-fertilised dryland wheat and barley on subtropical Vertosols: Risk, rainfall and alternatives. *Soil Research*, *54*(5), 634. https://doi.org/10.1071/SR15338

Signor, D., & Cerri, C. E. P. (2013). Nitrous oxide emissions in agricultural soils: A review. *Pesquisa Agropecuária Tropical*, *43*, 322–338. https://doi.org/10.1590/S1983-40632013000300014

Sileshi, G. W., Jama, B., Vanlauwe, B., Negassa, W., Harawa, R., Kiwia, A., & Kimani, D. (2019). Nutrient use efficiency and crop yield response to the combined application of cattle manure and inorganic fertilizer in sub-Saharan Africa. *Nutrient Cycling in Agroecosystems*, *113*(2), 181–199. https://doi.org/10.1007/s10705-019-09974-3

Sinclair, T. R., & Rufty, T. W. (2012). Nitrogen and water resources commonly limit crop yield increases, not necessarily plant genetics. *Global Food Security*, *1*(2), 94–98. https://doi.org/10.1016/j.gfs.2012.07.001

Smith, K. A., McTaggart, I. P., & Tsuruta, H. (1997). Emissions of N2O and NO associated with nitrogen fertilization in intensive agriculture, and the potential for mitigation. *Soil Use and Management*, *13*(s4), 296–304. https://doi.org/10.1111/j.1475-2743.1997.tb00601.x

Soilueang, P., Jaikrasen, K., Chromkaew, Y., Buachun, S., Yimyam, N., Sanjunthong, W., Kullachonphuri, S., Wicharuck, S., Mawan, N., & Khongdee, N. (2023). Dynamics of soil nitrogen availability following conversion of natural forests to various coffee cropping systems in northern Thailand. *Heliyon*, *9*(12), e22988. https://doi.org/10.1016/j.heliyon.2023.e22988

Sommer, R., Mukalama, J., Kihara, J., Koala, S., Winowiecki, L., & Bossio, D. (2015). Nitrogen dynamics and nitrous oxide emissions in a long-term trial on integrated soil fertility management in Western Kenya. *Nutrient Cycling in Agroecosystems*, *105*. https://doi.org/10.1007/s10705-015-9693-6

Steffen, W., Richardson, K., Rockström, J., Cornell, S. E., Fetzer, I., Bennett, E. M., Biggs, R., Carpenter, S. R., De Vries, W., De Wit, C. A., Folke, C., Gerten, D., Heinke, J., Mace, G. M., Persson, L. M., Ramanathan, V., Reyers, B., & Sörlin, S. (2015). Planetary boundaries: Guiding human development on a changing planet. *Science*, *347*(6223). https://doi.org/10.1126/science.1259855

Strenge, E., Zoboli, O., Mehdi-Schulz, B., Parajka, J., Schönhart, M., Krampe, J., & Zessner, M. (2023). Regional nitrogen budgets of agricultural production systems in Austria constrained by natural boundary conditions. *Journal of Environmental Management*, *347*, 119023. https://doi.org/10.1016/j.jenvman.2023.119023

ten Berge, H. F. M., Hijbeek, R., van Loon, M. P., Rurinda, J., Tesfaye, K., Zingore, S., Craufurd, P., van Heerwaarden, J., Brentrup, F., Schröder, J. J., Boogaard, H. L., de Groot, H. L. E., & van Ittersum, M. K. (2019). Maize crop nutrient input requirements for food security in sub-Saharan Africa. *Global Food Security*, *23*, 9–21. https://doi.org/10.1016/j.gfs.2019.02.001

Tesfaye, K., Takele, R., Sapkota, T. B., Khatri-Chhetri, A., Solomon, D., Stirling, C., & Albanito, F. (2021a). Model comparison and quantification of nitrous oxide emission and mitigation potential from maize and wheat fields at a global scale. *Science of The Total Environment*, *782*, 146696. https://doi.org/10.1016/j.scitotenv.2021.146696

Tesfaye, K., Takele, R., Sapkota, T. B., Khatri-Chhetri, A., Solomon, D., Stirling, C., & Albanito, F. (2021b). Model comparison and quantification of nitrous oxide emission and mitigation potential from maize and wheat fields at a global scale. *Science of The Total Environment*, *782*, 146696. https://doi.org/10.1016/j.scitotenv.2021.146696

Tian, H., Xu, R., Canadell, J. G., Thompson, R. L., Winiwarter, W., Suntharalingam, P., Davidson, E. A., Ciais, P., Jackson, R. B., Janssens-Maenhout, G., Prather, M. J., Regnier, P., Pan, N., Pan, S., Peters, G. P., Shi, H., Tubiello, F. N., Zaehle, S., Zhou, F., … Yao, Y. (2020). A comprehensive quantification of global nitrous oxide sources and sinks. *Nature*, *586*(7828), 248–256. https://doi.org/10.1038/s41586-020-2780-0

Tully, K. L., Hickman, J. E., Russo, T. A., Neill, C., Matata, P., Nyadzi, G., Mutuo, P., & Palm, C. A. (2023). The Fate of Nitrogen During Agricultural Intensification in East Africa: Nitrogen Budgets in Contrasting Agroecosystems. *Journal of Geophysical Research: Biogeosciences*, *128*(7), e2022JG007128. https://doi.org/10.1029/2022JG007128

Tully, K. L., Hickman, J., McKenna, M., Neill, C., & Palm, C. A. (2016). Effects of fertilizer on inorganic soil N in East Africa maize systems: Vertical distributions and temporal dynamics. *Ecological Applications*, *26*(6), 1907–1919. https://doi.org/10.1890/15-1518.1

Van Ittersum, M. K., Alimagham, S., Silva, J. V., Adjei-Nsiah, S., Baijukya, F. P., Bala, A., Chikowo, R., Grassini, P., De Groot, H. L. E., Nshizirungu, A., Mahamane Soulé, A., Sulser, T. B., Taulya, G., Amor Tenorio, F., Tesfaye, K., Yuan, S., & Van Loon, M. P. (2025). Prospects for cereal self-sufficiency in sub-Saharan Africa. *Proceedings of the National Academy of Sciences*, *122*(24). https://doi.org/10.1073/pnas.2423669122

van Loon, M. P., Hijbeek, R., ten Berge, H. F. M., De Sy, V., ten Broeke, G. A., Solomon, D., & van Ittersum, M. K. (2019). Impacts of intensifying or expanding cereal cropping in sub-Saharan Africa on greenhouse gas emissions and food security. *Global Change Biology*, *25*(11), 3720–3730. https://doi.org/10.1111/gcb.14783

Van Loon, M. P., Hijbeek, R., Ten Berge, H. F. M., De Sy, V., Ten Broeke, G. A., Solomon, D., & Van Ittersum, M. K. (2019). Impacts of intensifying or expanding cereal cropping in sub-Saharan Africa on greenhouse gas emissions and food security. *Global Change Biology*, *25*(11), 3720–3730. https://doi.org/10.1111/gcb.14783

Wachiye, S., Merbold, L., Vesala, T., Rinne, J., Räsänen, M., Leitner, S., & Pellikka, P. (2020). Soil greenhouse gas emissions under different land-use types in savanna ecosystems of Kenya. *Biogeosciences*, *17*(8), 2149–2167. https://doi.org/10.5194/bg-17-2149-2020

Wang, H., Guo, Z., Shi, Y., Zhang, Y., & Yu, Z. (2015). Impact of tillage practices on nitrogen accumulation and translocation in wheat and soil nitrate-nitrogen leaching in drylands. *Soil and Tillage Research*, *153*, 20–27. https://doi.org/10.1016/j.still.2015.03.006

Wang, J., Chadwick, D. R., Cheng, Y., & Yan, X. (2018). Global analysis of agricultural soil denitrification in response to fertilizer nitrogen. *Science of The Total Environment*, *616–617*, 908–917. https://doi.org/10.1016/j.scitotenv.2017.10.229

Wang, Q., Li, S., Li, J., & Huang, D. (2024). The Utilization and Roles of Nitrogen in Plants. *Forests*, *15*(7), Article 7. https://doi.org/10.3390/f15071191

Wang, X., Zou, C., Gao, X., Guan, X., Zhang, Y., Shi, X., & Chen, X. (2018). Nitrate leaching from open-field and greenhouse vegetable systems in China: A meta-analysis. *Environmental Science and Pollution Research*, *25*(31), 31007–31016. https://doi.org/10.1007/s11356-018-3082-z

Wang, Y., Ying, H., Yin, Y., Zheng, H., & Cui, Z. (2019). Estimating soil nitrate leaching of nitrogen fertilizer from global meta-analysis. *Science of The Total Environment*, *657*, 96–102. https://doi.org/10.1016/j.scitotenv.2018.12.029

Wey, H., Hunkeler, D., Bischoff, W.-A., & Bünemann, E. K. (2021). Field-scale monitoring of nitrate leaching in agriculture: Assessment of three methods. *Environmental Monitoring and Assessment*, *194*(1), 4. https://doi.org/10.1007/s10661-021-09605-x

Winnie, N., Giweta, M., Gweyi-Onyango, J., Mochoge, B., Mutegi, J., Nziguheba, G., & Masso, C. (2022). Assessment of the 2006 Abuja Fertilizer Declaration With Emphasis on Nitrogen Use Efficiency to Reduce Yield Gaps in Maize Production. *Frontiers in Sustainable Food Systems*, *5*, 758724. https://doi.org/10.3389/fsufs.2021.758724

Wu, D., Zhang, Y., Dong, G., Du, Z., Wu, W., Chadwick, D., & Bol, R. (2021). The importance of ammonia volatilization in estimating the efficacy of nitrification inhibitors to reduce N2O emissions: A global meta-analysis. *Environmental Pollution*, *271*, 116365. https://doi.org/10.1016/j.envpol.2020.116365

Yao, Z., Pelster, D. E., Liu, C., Zheng, X., & Butterbach-Bahl, K. (2020). Soil N intensity as a measure to estimate annual N2O and NO fluxes from natural and managed ecosystems. *Current Opinion in Environmental Sustainability*, *47*, 1–6. https://doi.org/10.1016/j.cosust.2020.03.008

Zakari, S. A., Zaidi, S. H. R., Sunusi, M., & Dauda, K. D. (2021). Nitrogen deficiency regulates premature senescence by modulating flag leaf function, ROS homeostasis, and intercellular sugar concentration in rice during grain filling. *Journal of Genetic Engineering and Biotechnology*, *19*(1), 177. https://doi.org/10.1186/s43141-021-00275-3

Zayed, O., Hewedy, O. A., Abdelmoteleb, A., Ali, M., Youssef, M. S., Roumia, A. F., Seymour, D., & Yuan, Z.-C. (2023). Nitrogen Journey in Plants: From Uptake to Metabolism, Stress Response, and Microbe Interaction. *Biomolecules*, *13*(10), 1443. https://doi.org/10.3390/biom13101443

Zebarth, B. J., Snowdon, E., Burton, D. L., Goyer, C., & Dowbenko, R. (2012). Controlled release fertilizer product effects on potato crop response and nitrous oxide emissions under rain-fed production on a medium-textured soil. *Canadian Journal of Soil Science*, *92*(5), 759–769. https://doi.org/10.4141/cjss2012-008

Zhao, G., Werku, B. C., & Bulto, T. W. (2025). Impact of agricultural emissions on goal 13 of the sustainable development agenda: In East African strategy for climate action. *Environmental Sciences Europe*, *37*(1), 35. https://doi.org/10.1186/s12302-025-01056-2

Zhao, H., Lakshmanan, P., Wang, X., Xiong, H., Yang, L., Liu, B., Shi, X., Chen, X., Wang, J., Zhang, Y., & Zhang, F. (2022). Global reactive nitrogen loss in orchard systems: A review. *Science of The Total Environment*, *821*, 153462. https://doi.org/10.1016/j.scitotenv.2022.153462

Zheng, J., Qu, Y., Kilasara, M. M., Mmari, W. N., & Funakawa, S. (2019a). Soil-atmosphere exchange of nitrous oxide in two Tanzanian croplands: Effects of nitrogen and stover management. *Agricultural and Forest Meteorology*, *275*, 24–36. https://doi.org/10.1016/j.agrformet.2019.05.009

Zheng, J., Qu, Y., Kilasara, M. M., Mmari, W. N., & Funakawa, S. (2019b). Soil-atmosphere exchange of nitrous oxide in two Tanzanian croplands: Effects of nitrogen and stover management. *Agricultural and Forest Meteorology*, *275*, 24–36. https://doi.org/10.1016/j.agrformet.2019.05.009

Zhou, M., & Butterbach-Bahl, K. (2014). Assessment of nitrate leaching loss on a yield-scaled basis from maize and wheat cropping systems. *Plant and Soil*, *374*(1–2), 977–991. https://doi.org/10.1007/s11104-013-1876-9

Zhou, M., Zhu, B., Butterbach-Bahl, K., Wang, T., Bergmann, J., Brüggemann, N., Wang, Z., Li, T., & Kuang, F. (2012). Nitrate leaching, direct and indirect nitrous oxide fluxes from sloping cropland in the purple soil area, southwestern China. *Environmental Pollution*, *162*, 361–368. https://doi.org/10.1016/j.envpol.2011.12.001

Zou, C., Pearce, R. C., Grove, J. H., Li, Y., Hu, X., Chen, J., Li, J., Jin, Y., Zou, C., Pearce, R. C., Grove, J. H., Li, Y., Hu, X., Chen, J., Li, J., & Jin, Y. (2018). Relationship of Agronomic Practices to Soil Nitrogen Dynamics. In *Soil Productivity Enhancement*. IntechOpen. https://doi.org/10.5772/intechopen.77229

# APPENDICES

**Appendix I: ANOVA results for the effect of N application rates on Nitrate concentration at three different depths**

| Source of Variation | NumDF | DenDF | F-value | P-value |
|---|---|---|---|---|
| Treatment | 5 | 790 | 17.5554 | <0.0001 |
| Depth | 2 | 790 | 41.5709 | <0.0001 |
| Treatment*Depth | 10 | 790 | 1.8749 | 0.0453 |
| **Total** | **17** | | | |

**Appendix II: ANOVA results for the effect of N application rates on Ammonium concentration at three different depths**

| Source of Variation | NumDF | DenDF | F-value | P-value |
|---|---|---|---|---|
| Treatment | 5 | 790 | 8.43858 | <0.0001 |
| Depth | 2 | 790 | 1.96848 | 0.1404 |
| Treatment*Depth | 10 | 790 | 4.31014 | <0.0001 |
| **Total** | **17** | | | |

**Appendix III: An overall summary of Nitrate concentration as influenced by N rates**

| | Depth (cm) | | | |
|---|---|---|---|---|
| **N application rate** | **0-20** | **20-40** | **40-60** | **Mean** |
| 0 kg N $ha^{-1}$ | $10.05^{abcd}$ | $8.16^{ab}$ | $10.06^{abcde}$ | **9.42** |
| 25 kg N $ha^{-1}$ | $11.57^{bcde}$ | $8.60^{abc}$ | $7.23^{a}$ | **9.13** |
| 50 kg N $ha^{-1}$ | $13.09^{defg}$ | $9.21^{abc}$ | $7.73^{ab}$ | **10.01** |
| 75 kg N $ha^{-1}$ | $14.18^{efg}$ | $10.66^{abcde}$ | $8.53^{abc}$ | **11.12** |
| 100 kg N $ha^{-1}$ | $15.66^{fg}$ | $12.29^{cdef}$ | $9.96^{abcd}$ | **12.64** |
| 125 kg N $ha^{-1}$ | $16.47^{g}$ | $13.78^{defg}$ | $10.89^{abcde}$ | **13.71** |
| **Mean** | **13.5** | **10.45** | **9.07** | **11.01** |
| **SE** | 0.894 | 0.978 | 1.1 | |

**Appendix IV: An overall summary of Ammonium concentration as influenced by N rates**

| | Depth (cm) | | | |
|---|---|---|---|---|
| **N application rate** | **0-20** | **20-40** | **40-60** | **Mean** |
| 0 kg N $ha^{-1}$ | $6.60^{a}$ | $7.20^{a}$ | $8.45^{ab}$ | **7.41** |
| 25 kg N $ha^{-1}$ | $6.80^{a}$ | $5.97^{a}$ | $6.08^{a}$ | **6.28** |
| 50 kg N $ha^{-1}$ | $7.87^{a}$ | $8.48^{ab}$ | $8.38^{ab}$ | **8.24** |
| 75 kg N $ha^{-1}$ | $6.55^{a}$ | $7.81^{a}$ | $6.11^{a}$ | **6.82** |
| 100 kg N $ha^{-1}$ | $8.19^{a}$ | $7.13^{a}$ | $6.52^{a}$ | **7.28** |
| 125 kg N $ha^{-1}$ | $10.80^{b}$ | $7.15^{a}$ | $7.74^{a}$ | **8.56** |
| **Mean** | **7.8** | **7.29** | **7.21** | **7.43** |
| **SE** | 0.652 | 0.703 | 0.779 | |

**Appendix V: The chronological sequence of activities carried out through the monitoring period. a) land preparation, b) experimental site after the secondary tillage and levelling, c) planting of maize seeds and application of fertilizer, d) plant count 14 DAP, e) weeding, f) subsequent soil sampling, g) maize crop at vegetative growth stage, h) spraying of pesticides to control aphids and fall armyworm, i) maize crop at physiological maturity, j) maize harvesting, k) biomass estimation, l) laboratory analysis**

**Appendix VI: $N_2O$ flux measurement regime, where each block consisted of two chambers from different treatments. While both chambers within a block would close at the same time, only one was sampled at any time of measurement. When the current set of chambers open, the next set closes and the sampling sequence begin and the cycle continues**

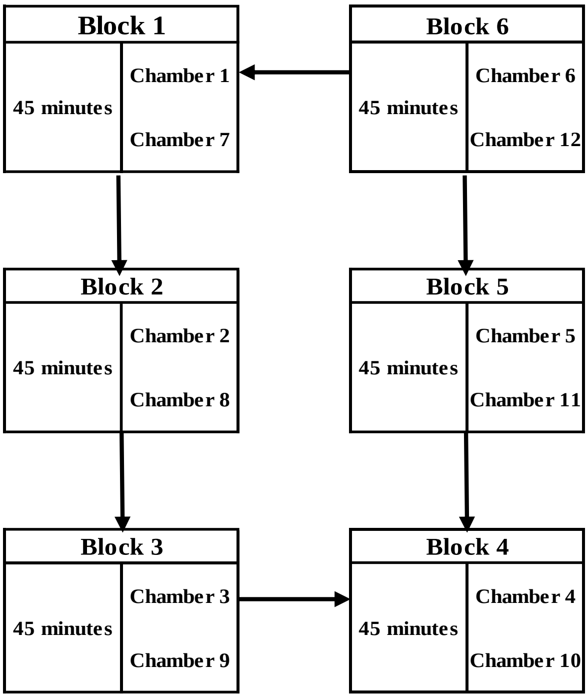


**Appendix VII: Chamber deployment in the flux measurement plots and a close-up of a chamber**

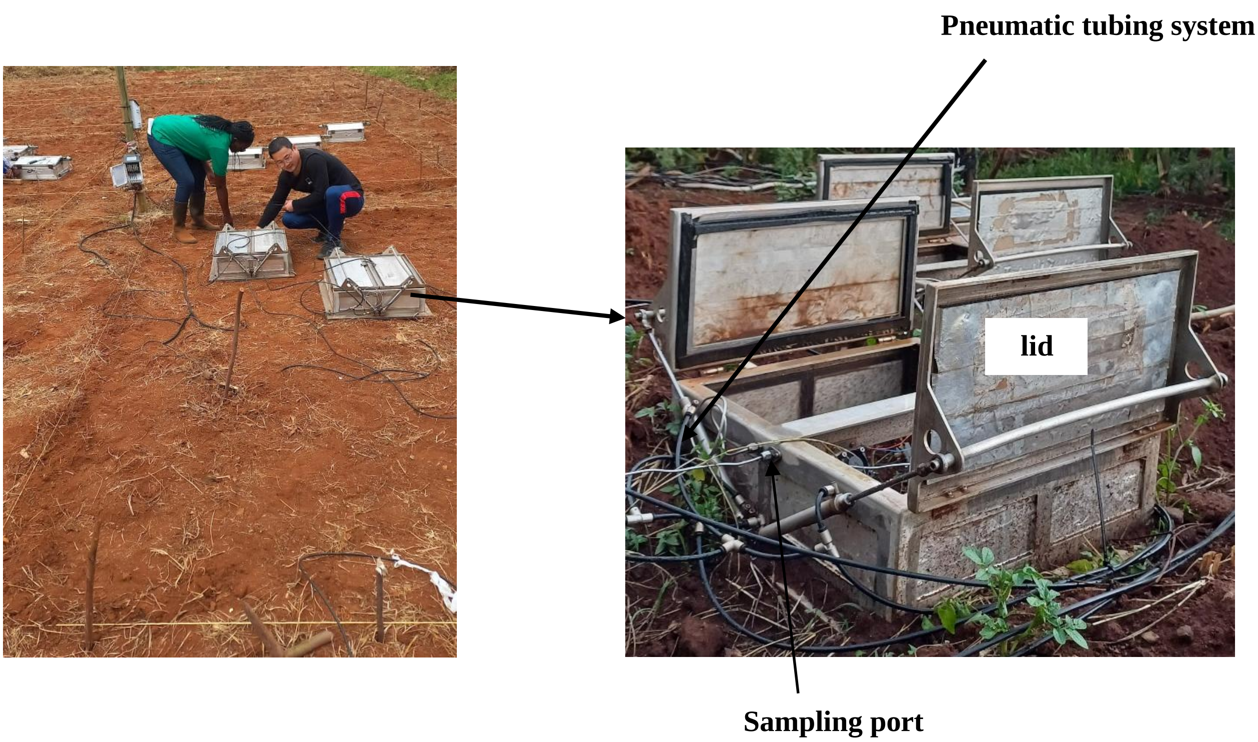

**Appendix VIII: P-values from Pearson correlation analysis among soil and precipitation variables in the 0-20 cm depth**

| | Nitrate | Ammonium | pH | Organic_C | Total_N | CN_ratio | SMC | Cum_Prep | Avg_Prep | Soil_Temp | Avg_Soil_Temp | Avg_SMC |
|---|---|---|---|---|---|---|---|---|---|---|---|---|
| **Nitrate** | 0 | 0.192 | <0.05 | 0.002 | <0.05 | <0.05 | 0.909 | 0.927 | 0.261 | <0.05 | <0.05 | 0.495 |
| **Ammonium** | 0.192 | 0 | 0.310 | 0.000 | 0.122 | 0.942 | 0.480 | 0.920 | 0.143 | 0.021 | 0.429 | 0.179 |
| **pH** | <0.05 | 0.310 | 0 | 0.057 | 0.015 | 0.076 | 0.903 | 0.589 | 0.285 | 0.186 | 0.762 | 0.143 |
| **Organic_C** | 0.002 | 0.000 | 0.057 | 0 | 0.076 | 0.720 | 0.622 | 0.740 | 0.489 | <0.05 | 0.209 | 0.842 |
| **Total_N** | <0.05 | 0.122 | 0.015 | 0.076 | 0 | <0.05 | 0.407 | <0.05 | <0.05 | <0.05 | <0.05 | <0.05 |
| **CN_ratio** | 0.001 | 0.942 | 0.076 | 0.720 | 0.000 | 0 | 0.223 | <0.05 | <0.05 | <0.05 | <0.05 | <0.05 |
| **SMC** | 0.909 | 0.480 | 0.903 | 0.622 | 0.407 | 0.223 | 0 | <0.05 | 0.469 | 0.060 | 0.178 | 0.930 |
| **Cum_Prep** | 0.927 | 0.920 | 0.589 | 0.740 | <0.05 | <0.05 | <0.05 | 0 | <0.05 | <0.05 | 0.408 | <0.05 |
| **Avg_Prep** | 0.261 | 0.143 | 0.285 | 0.489 | <0.05 | <0.05 | 0.469 | <0.05 | 0 | <0.05 | 0.329 | <0.05 |
| **Soil_Temp** | <0.05 | 0.021 | 0.186 | 0.003 | <0.05 | <0.05 | 0.060 | <0.05 | <0.05 | 0 | <0.05 | <0.05 |
| **Avg_Soil_Temp** | <0.05 | 0.429 | 0.762 | 0.209 | <0.05 | <0.05 | 0.178 | 0.408 | 0.33 | <0.05 | 0 | 0.880 |
| **Avg_SMC** | 0.495 | 0.179 | 0.143 | 0.842 | <0.05 | <0.05 | 0.930 | <0.05 | <0.05 | 0.000 | 0.880 | 0 |

**Appendix IX: P-values from Pearson correlation analysis among soil and precipitation variables in the 20-40 cm depth**

| | Nitrate | Ammonium | pH | Organic_C | SMC | CN_ratio | Total_N | Cum_Prep | Avg_Prep |
|---|---|---|---|---|---|---|---|---|---|
| **Nitrate** | 0 | 0.708 | 0.159 | 0.831 | 0.007 | <0.05 | <0.05 | 0.320 | 0.006 |
| **Ammonium** | 0.708 | 0 | 0.027 | 0.043 | 0.014 | 0.402 | 0.479 | 0.800 | 0.388 |
| **pH** | 0.159 | 0.027 | 0 | 0.225 | 0.672 | 0.087 | 0.457 | 0.382 | 0.006 |
| **Organic_C** | 0.831 | 0.043 | 0.225 | 0 | 0.358 | 0.121 | 0.027 | <0.05 | 0.009 |
| **SMC** | 0.007 | 0.014 | 0.672 | 0.358 | 0 | 0.001 | 0.001 | 0.002 | 0.040 |
| **CN_ratio** | <0.05 | 0.402 | 0.087 | 0.121 | 0.001 | 0 | 0.000 | 0.433 | 0.008 |
| **Total_N** | <0.05 | 0.479 | 0.457 | 0.027 | 0.001 | <0.05 | 0 | 0.003 | <0.05 |
| **Cum_Prep** | 0.320 | 0.800 | 0.382 | <0.05 | 0.002 | 0.433 | 0.003 | 0 | <0.05 |
| **Avg_Prep** | 0.006 | 0.388 | 0.006 | 0.009 | 0.040 | 0.008 | 1.6E-06 | <0.05 | 0 |

**Appendix X: P-values from Pearson correlation analysis among soil and precipitation variables in the 40 – 60 cm depth**

| | Nitrate | Ammonium | pH | Organic_C | SMC | Total_N | CN_ratio | Cum_Prep | AvgPrep |
|---|---|---|---|---|---|---|---|---|---|
| **Nitrate** | 0 | 0.444 | 0.050 | 0.351 | 0.034 | 0.834 | 0.194 | 0.838 | 0.012 |
| **Ammonium** | 0.444 | 0 | 0.015 | 0.241 | 0.000 | 0.022 | 0.612 | 0.893 | 0.008 |
| **pH** | 0.050 | 0.015 | 0 | 0.004 | 0.136 | 0.005 | 0.213 | 0.046 | 0.258 |
| **Organic_C** | 0.351 | 0.241 | 0.004 | 0 | 0.958 | <0.05 | <0.05 | <0.05 | 0.222 |
| **SMC** | 0.034 | <0.05 | 0.136 | 0.958 | 0 | 0.025 | 0.060 | 0.762 | 0.000 |
| **Total_N** | 0.834 | 0.022 | 0.005 | <0.05 | 0.025 | 0 | 0.765 | 0.000 | 0.025 |
| **CN_ratio** | 0.194 | 0.612 | 0.213 | <0.05 | 0.060 | 0.765 | 0 | <0.05 | 0.768 |
| **Cum_Prep** | 0.838 | 0.893 | 0.046 | <0.05 | 0.762 | <0.05 | 0.05< | 0 | 0.097 |
| **AvgPrep** | 0.012 | 0.008 | 0.258 | 0.222 | <0.05 | 0.025 | 0.768 | 0.097 | 0 |

## Appendix XI: Temporal dynamics of $NO_3^-/NH_4^+$ ratio observed during the monitoring period

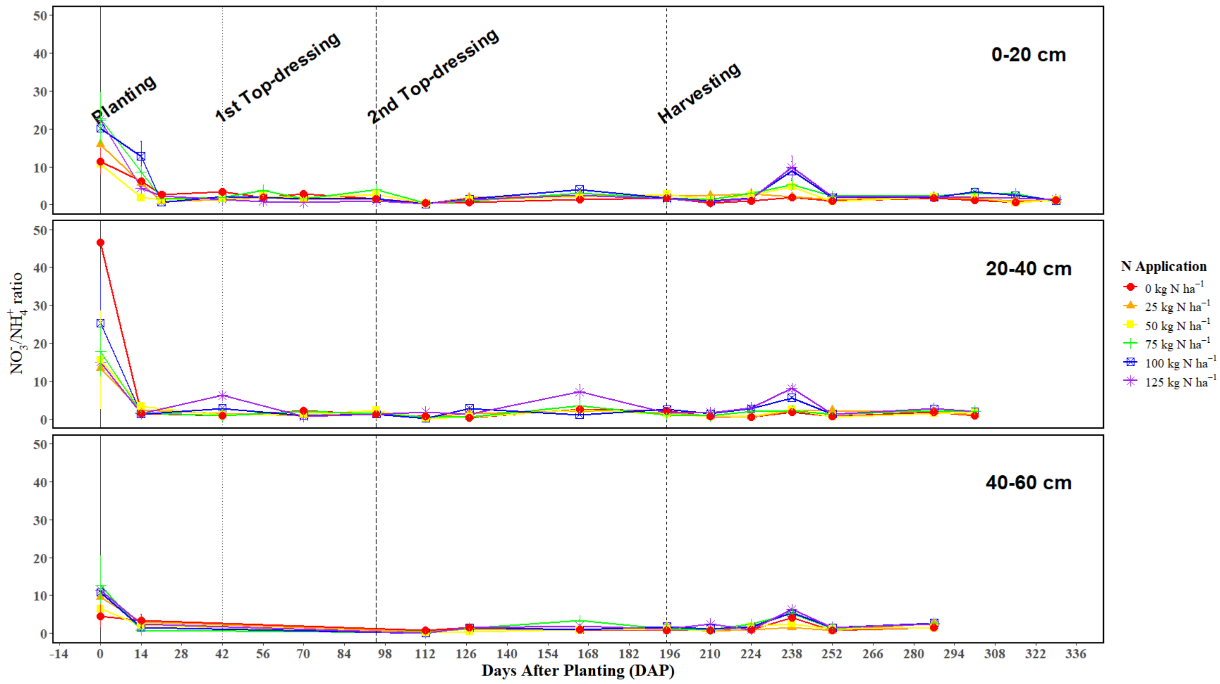


## Appendix XII: Vertical distribution of soil pH throughout the monitoring period

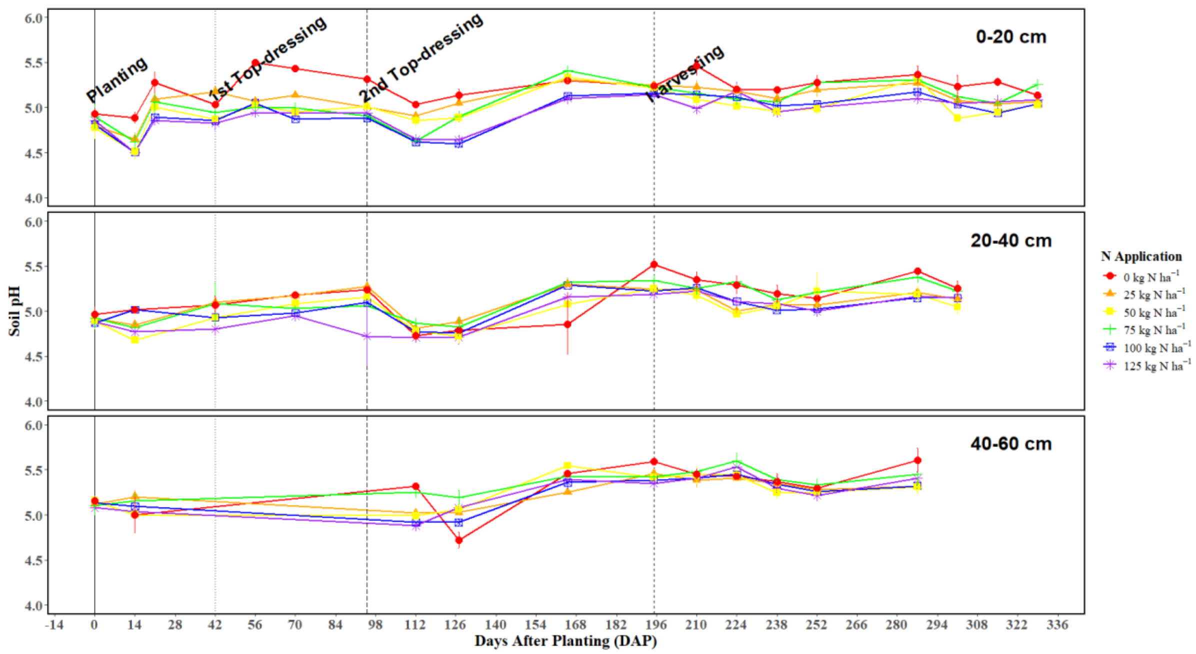

## Appendix XIII: Vertical distribution of soil organic carbon throughout the monitoring period

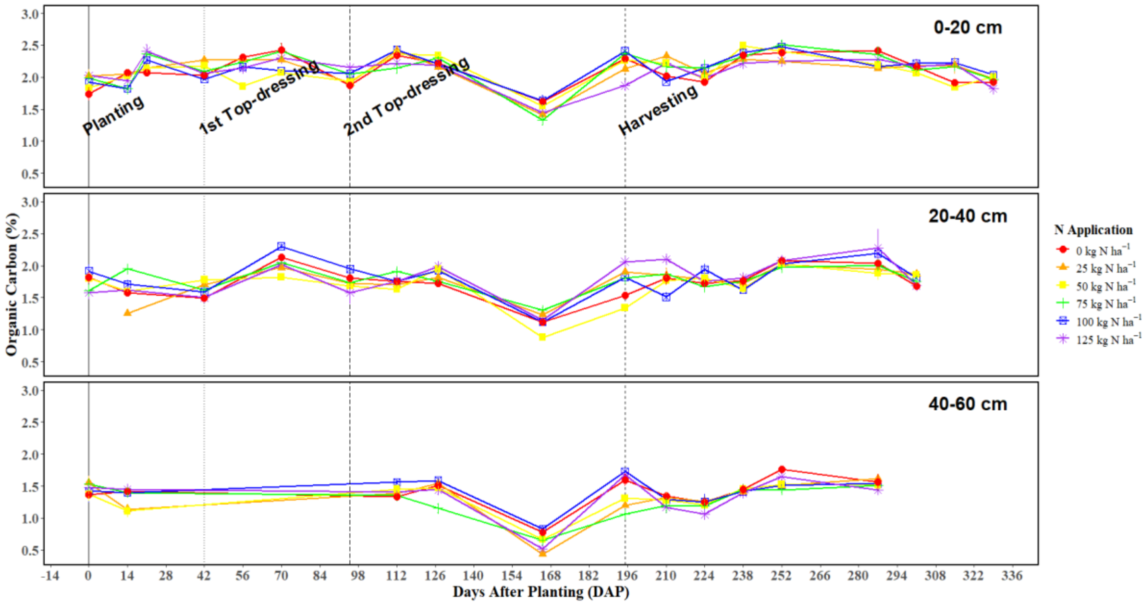


## Appendix XIV: Vertical distribution of soil total N throughout the monitoring period

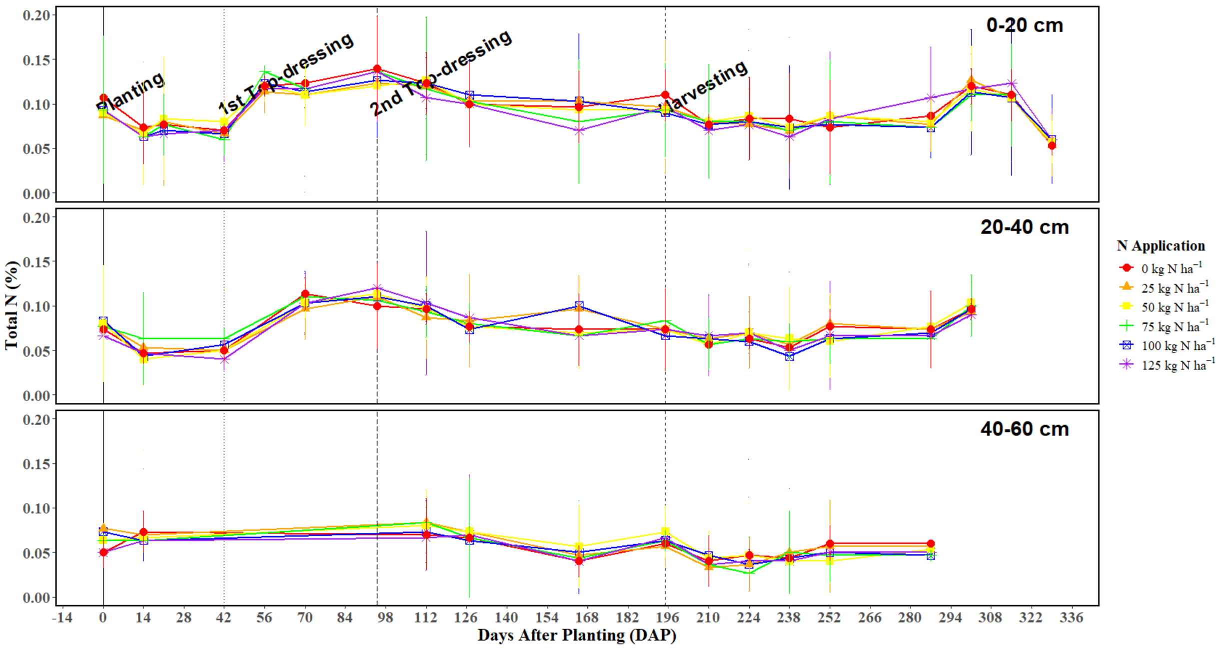

# Appendix XVI: Performance analysis of the random forest model in predicting $N_2O$ fluxes in the 0 kg N ha$^{-1}$ plot

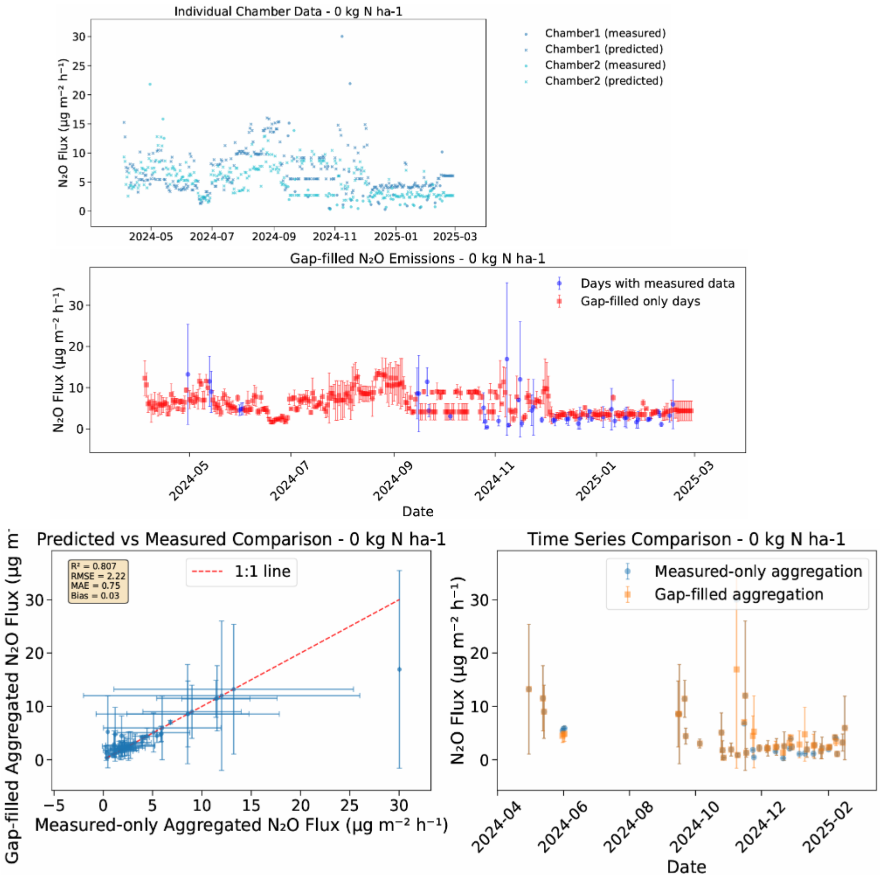


# Appendix XVII: Performance analysis of the random forest model in predicting $N_2O$ fluxes in the 25 kg N ha$^{-1}$ plot

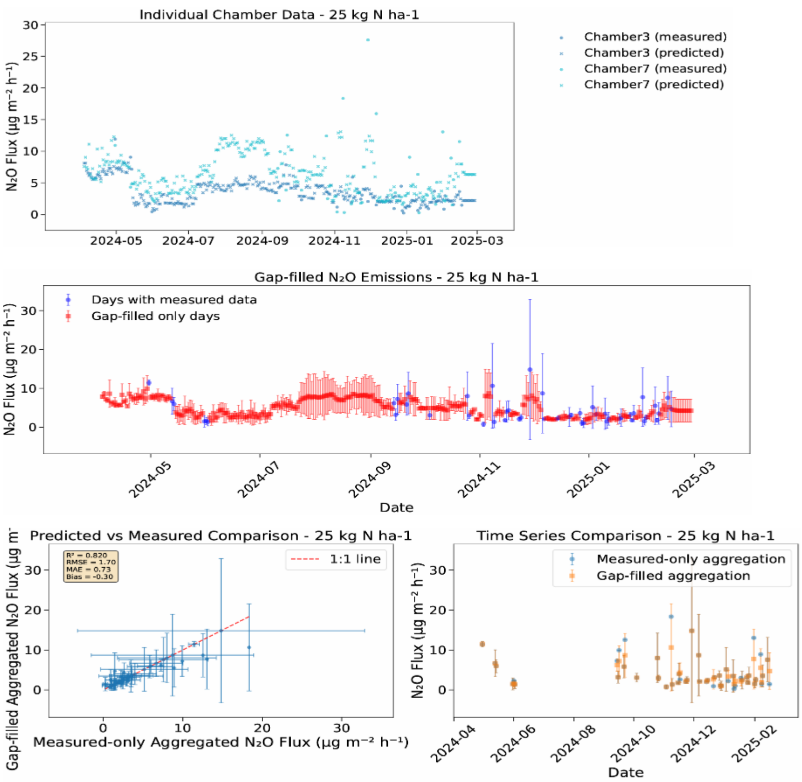

## Appendix XVIII: Performance analysis of the random forest model in predicting $N_2O$ fluxes in the 50 kg N ha$^{-1}$ plot

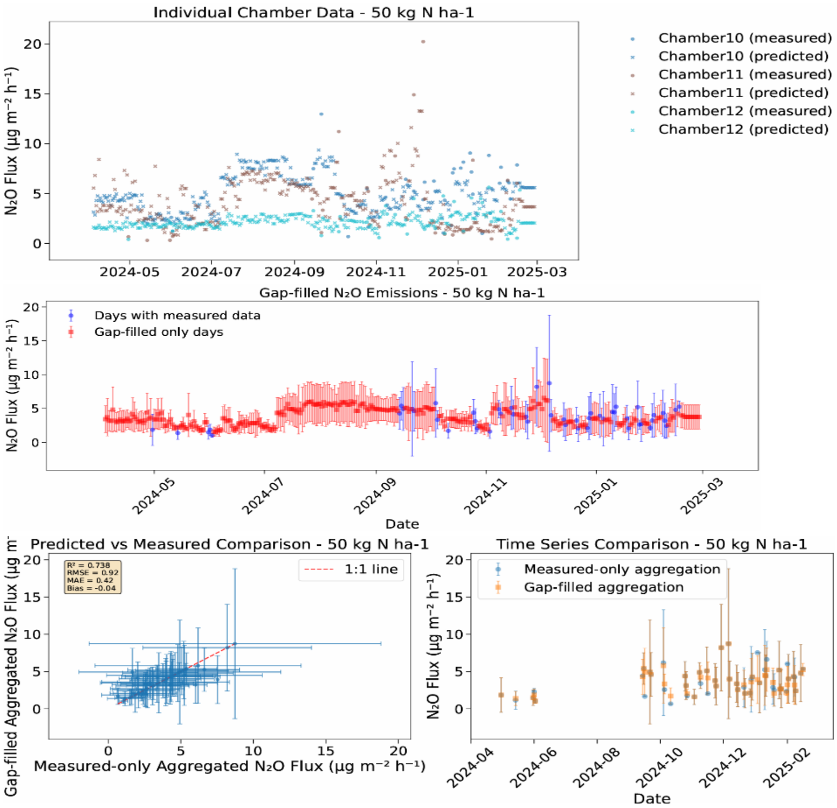


## Appendix XIX: Performance analysis of the random forest model in predicting $N_2O$ fluxes in the 0 kg N ha$^{-1}$ plot

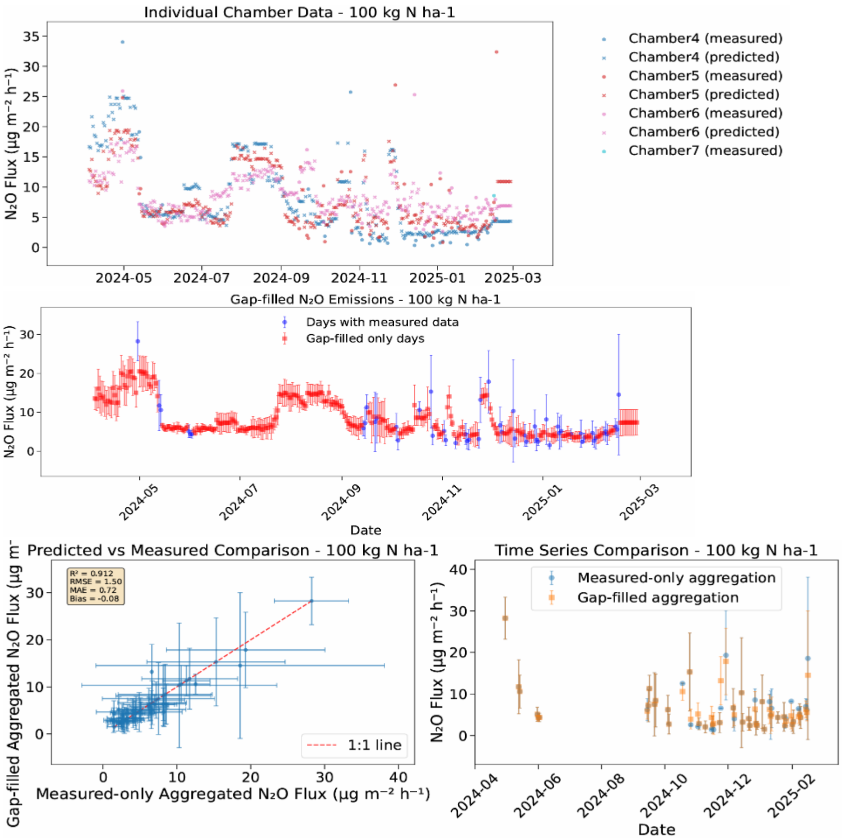

# Appendix XX: Performance analysis of the random forest model in predicting $N_2O$ fluxes in the 125 kg N $ha^{-1}$ plot

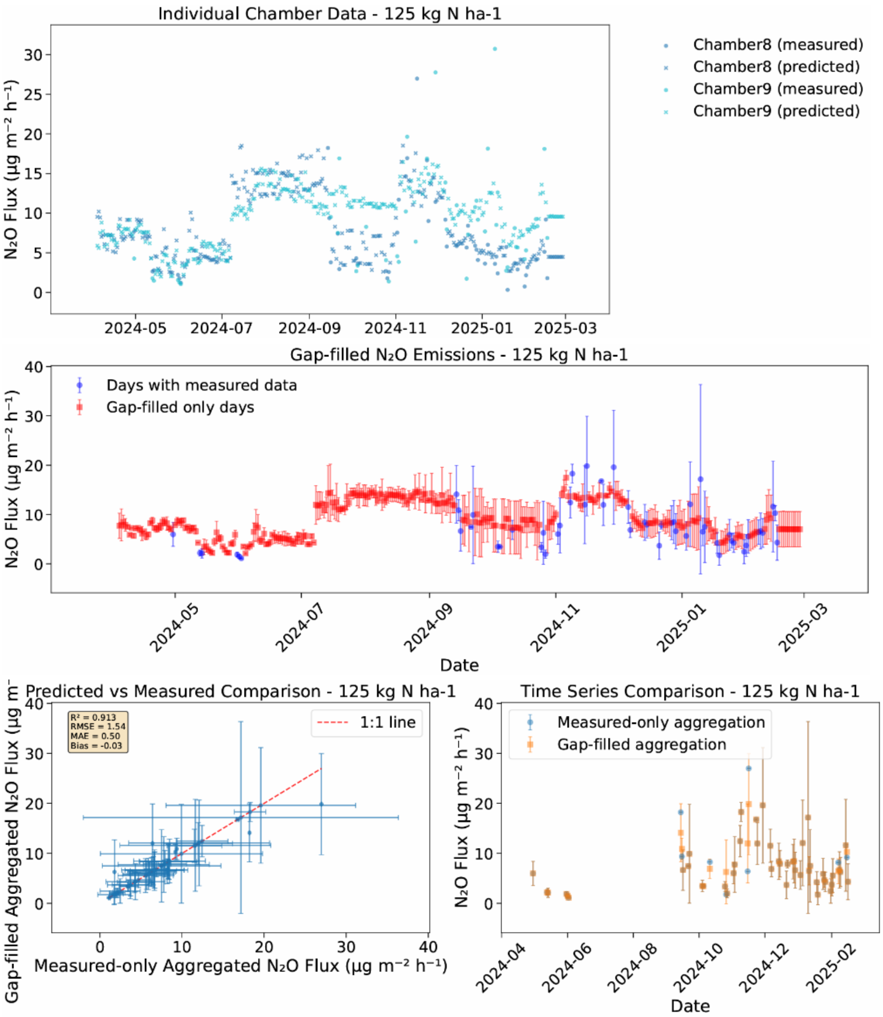

**Appendix XXI: Similarity Report**

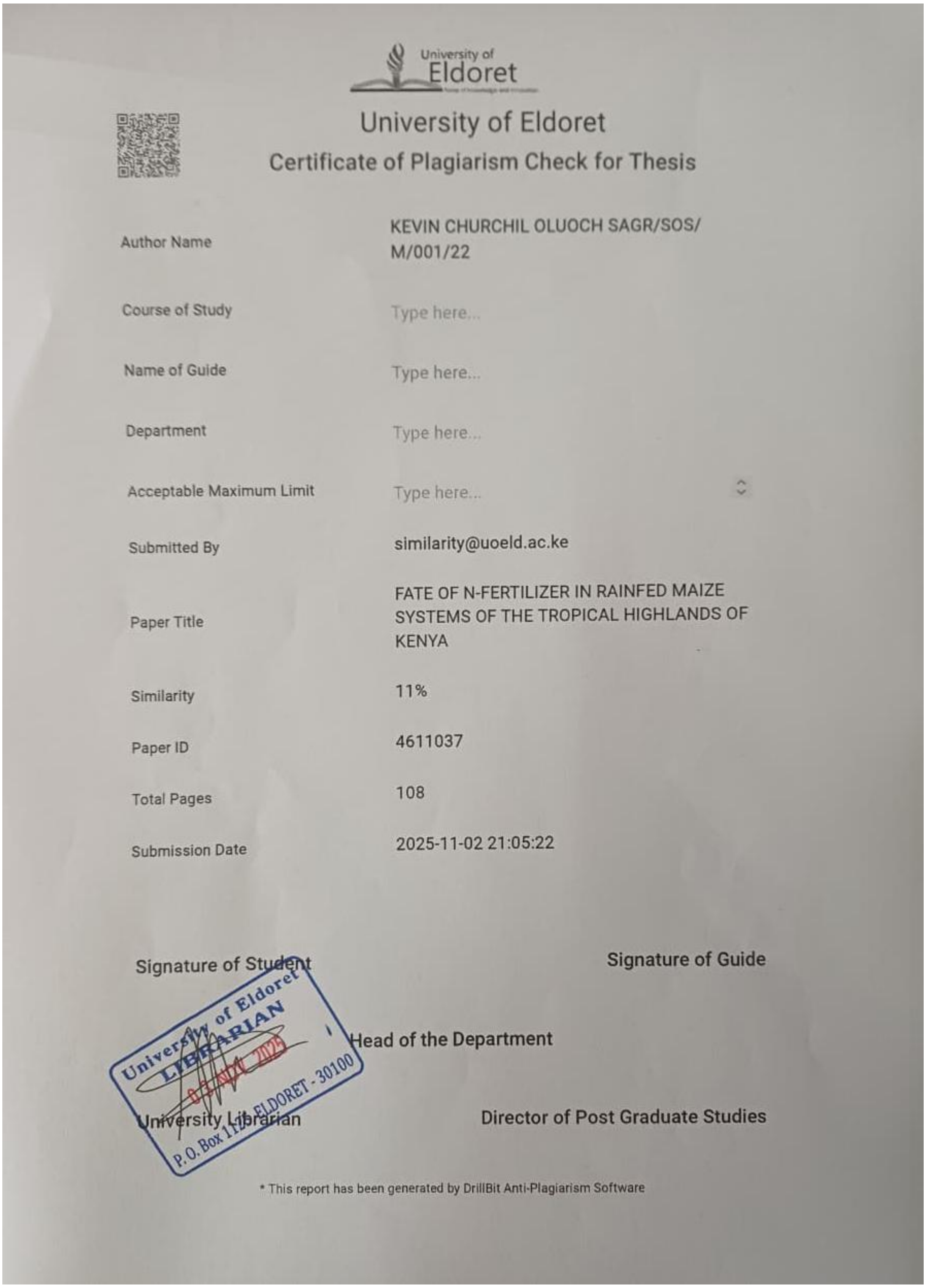

University of Eldoret

## University of Eldoret

### Certificate of Plagiarism Check for Thesis

| | |
|---|---|
| Author Name | KEVIN CHURCHIL OLUOCH SAGR/SOS/M/001/22 |
| Course of Study | Type here... |
| Name of Guide | Type here... |
| Department | Type here... |
| Acceptable Maximum Limit | Type here... |
| Submitted By | similarity@uoeld.ac.ke |
| Paper Title | FATE OF N-FERTILIZER IN RAINFED MAIZE SYSTEMS OF THE TROPICAL HIGHLANDS OF KENYA |
| Similarity | 11% |
| Paper ID | 4611037 |
| Total Pages | 108 |
| Submission Date | 2025-11-02 21:05:22 |

Signature of Student

Signature of Guide

Head of the Department

University Librarian

Director of Post Graduate Studies



* This report has been generated by DrillBit Anti-Plagiarism Software